Using GIS and Remote Sensing Techniques for Solar Panel Installation Site Selection

by

Dongrong Li

A thesis
presented to the University of Waterloo
in fulfillment of the
thesis requirement for the degree of
Master of Science
in
Geography

Waterloo, Ontario, Canada, 2013

Author's Declaration

I hereby declare that I am the sole author of this thesis. This is a true copy of the thesis, including any required final revisions, as accepted by my examiners. I understand that my thesis may be made electronically available to the public.

Abstract

Solar energy replacing conventional non-renewable energy has been widely implemented around the world. Currently, one of the most challenging problems is how to improve the efficiency of producing solar energy. Before installing solar panels, assessing where solar panels should be placed can significantly benefit panel performance. This study aims to conduct a site selection analysis for solar panel installation using Geographical Information Systems (GIS). The University of Waterloo main campus and the City of Waterloo were selected as study areas for micro-scale and macro-scale, respectively. The focus of the micro-scale analysis is on building rooftop installations, while the macro-scale analysis considers ground-mounted installation at the city-level.

Knowledge about solar gains incident on different land cover types (e.g., urban and farmland) is useful for assessing potential solar energy installation sites in a local area. In this study, Light Detection and Ranging (LIDAR) data were applied to automatically derive accumulated solar radiation energy under clear-sky and overcast conditions at the micro-scale level from which ideal sites for solar panel placement on building rooftops were determined. Macro-scale solar radiation maps were based on Digital Elevation Model (DEM) data using ArcGIS software. Optimal ground-mounted solar panel installation sites were determined using a multi-criteria analysis approach that considered various environmental and socioeconomic factors. A questionnaire survey was distributed to select solar power companies in Southern Ontario to assess current solar panel installation practices, which were then used to better inform and modify the GIS multi-criteria approach. Finally, a feasibility assessment was performed with ground truth information to verify selected sites.

Acknowledgements

First of all, I would like to express my sincerest appreciation to my dear supervisor, Dr. Su-Yin Tan, for all of her support, encouragement and patience. Without her guidance and help, this work could not have been accomplished. Throughout my master study, she has always been there to guide me and provide insightful advice. Her support has been invaluable on both an academic and a personal level, for which I am extremely grateful.

Next, I want to acknowledge Mike Lackner, James McCarthy and Scott MacFarlane in MAD help desk, and all of them showed their great patience and have provided me some technical assistance. I also want to thank Jonathan Morgan in the University Map Library for helping me to obtain most of the data used in this study. Without their kindness and assistance, I could not even carry out this research.

I would also like to thank my committee member Dr. Paul Parker, and readers Dr. Peter Deadman and Dr. Geoff Lewis for reading my thesis and providing me valuable feedback.

Many thanks go to my lovely friends and colleagues for their support and encouragement.

Last but not least, I would like to express my special thank to my dear mother and father. I could not be where I am today without their love and unequivocal support, for which my mere expression of gratitude does not suffice.

Table of Contents

List of Figures

List of Tables

Chapter 1. Introduction

In recent times, the nature and magnitude of global energy demands have changed and increased in an unprecedented manner, especially with today's rapid population growth and modernization (Foster et al., 2010; Sen, 2008). Since the Industrial Revolution from the 18th to the 19th century, conventional fossil fuels have been largely consumed (Sen, 2008) and consequently, various greenhouse gases (e.g., CO_2, CH_4, etc.) have been emitted into the atmosphere. This has led to an abnormal increase in the Earth's average atmospheric temperature and other environmental concerns (Kalogrou, 2009; Sen, 2008). Renewable or green forms of energy have been proposed as substitute a primary energy resources, and are now generally believed to be capable of meeting much of the growing energy demand (Kalogrou, 2009). In Canada, sources of renewable electricity (i.e., water, wind, solar, geothermal and biomass) accounted for approximately 64% of national electricity generation in 2005 (Natural Resources Canada, 2009). Among the renewable energy sources, solar energy is unique in that it can provide a local source of electricity for people living in rural areas without direct access to the electric grid (Foster et al., 2010). From 2005 to 2010, global solar PV capacity grew by 49% per year (Kadowaki, 2012).

Solar energy is transmitted to the Earth in the form of electromagnetic radiation, which is comprised of photons (Foster et al., 2010; The German Solar Society, 2005). The amount of irradiance reaching a location on the Earth's surface over a specific time period varies depending on global, local, spatial, temporal and meteorological factors (Redweik, et al., 2011). Generally, large quantities of solar energy manifest in diverse forms when reaching the Earth, such as direct sunlight for plant photosynthesis, heated air masses causing wind, and evaporation of the oceans, which result in rain that in turn, supplies rivers and provides hydropower (Foster et al., 2010). Achieving an accurate estimation of daily, monthly or yearly global solar radiation reaching the Earth's surface is of great importance when developing solar energy resources, especially when determining the optimal location for placing photovoltaics (Rehman and Ghori, 2000). As shown in Figure 1.1, identifying appropriate sites for solar panel placement is beneficial not only ecologically by considering environmentally sensitive areas and land

accessibility, but also economically by analyzing energy production potential, existing transmission system, and the solar power market (Gastli and Charabi, 2010a).

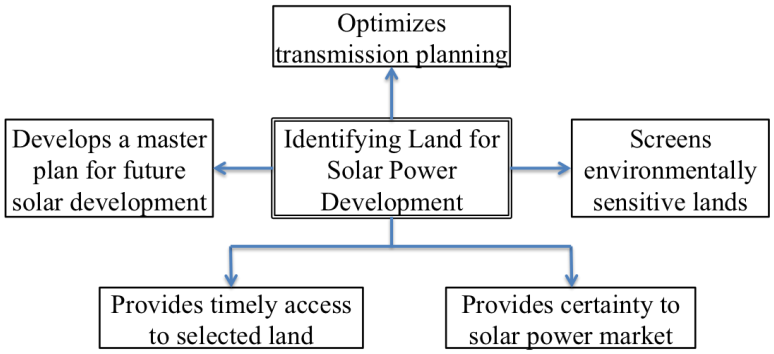

Figure 1.1 - Benefits of identifying land for solar power development (Gastli and Charabi, 2010a)

In order to identify potential sites for solar panel installation, availability of solar radiation should be considered first. Based on different data sources, such as weather station data and elevation data, solar radiation can be estimated using different approaches. For example, solar radiation can be obtained by weather station surveillance, which measures irradiance for a specific location. Solar radiation data are gathered in the form of dispersed observation points (e.g., Stoffel, 2005), and interpolation techniques can be used to estimate unknown radiation data in intervening areas (e.g., Sen and Sahin, 2001). Multivariate statistical methods are another approach for estimating solar radiation and are based on multiple variables, such as latitude and sunshine ratio (e.g., Sfetsos and Coonick, 2000). Additionally, Light Detection And Ranging (LiDAR) data or high-resolution Digital Elevation Model (DEM) data have been implemented to estimate radiation at the small scale or regional level, typically for a subdivision in an urban area or individual fields (e.g., Jochem et al., 2009; Mulherin, 2011). Other optical imagery has also been applied to detect solar radiation at the macro level. The thermal band of optical imagery with detected surface temperature information can also be used to calculate solar irradiation (e.g., Fluri, 2009). This thesis will focus on using topographic information derived from LiDAR points and DEM for estimating solar radiation.

Locating potential sites for PV panels should also take into account other factors based on the scale and types of installation involved. More specifically, for rooftop solar panel installation, shadow effects due to surrounding obstacles and roof structure are

important factors to consider. Regarding ground-mounted solar panel installatios, environmental and economic concerns, and energy generation potential should be taken into account during the site selection process. For example, installation sites should be located away from forest areas and environmental sensitive land. Proximity to existing transmission facilities is desirable for reducing transmission loss. In some regions with abundant dust, effects of dust accumulation on the performance of solar panels are important. In order to consider these factors and to identify potential sites for solar panel installation, a Multicriteria Analysis (MCA) is undertaken in this study. This paper will examine the potential benefits of using spatial analytical techniques for identifying optimal sites for roof-mounted solar panels at the micro-scale level and ground-mounted solar panels at the macro-scale level. This thesis consists of six chapters in total. The remaining chapters are outlined as follows.

Chapter 2 – Literature Review: introduces electricity usage in Ontario, Canada. Types of solar energy technologies and their impacts are introduced. Factors and methods considered for solar panel site selection are also discussed. Finally, several case studies of solar energy applications on the University of Waterloo campus are presented.

Chapter 3 – Research Design: describes the main goal and objectives of the present study. The study areas and data sources are discussed.

Chapter 4 – Methodology: introduces methods being used for solar radiation estimation and solar panel site selection at the micro- and macro- scales. Questionnaire survey design and implementation are detailed.

Chapter 5 – Results and Analysis: begins by displaying results generated from the micro-scale and macro-scale analyses. Following this, feasibility assessment results are described.

Chapter 6 – Discussion and Conclusion: presents a discussion on the final findings of this study and its implications. The recognized limitations of the study are discussed, along with suggestions for potential further work. This chapter concludes with reviewing the potential contribution of this research.

Chapter 2. Literature Review

A considerable amount of literature has been published on what factors should be considered in photovoltaic (PV) panel site selection. This chapter provides a review of energy usage and renewable energy promotion policies in Ontario. Next, background information about PV systems is introduced. Factors usually considered in the solar panel site selection process are reviewed. In particular, the relationship between energy demand and supply, and methods applied for solar radiation estimation are discussed. Following this, a detailed description of other physical factors (e.g., tilt) affecting solar power system performance is provided. In the third part of this chapter, site selection implementation methods are introduced and compared. The final part of this chapter shows two case studies about solar panel installation on the campus of University of Waterloo (UW).

2.1. Research Background

2.1.1. Ontario's Electricity Supply and Demand

Ontario's energy supply is composed of diverse sources, which are in the process of incorporating increasing amounts of renewable energy (IESO, 2012a). Table 2.1 shows Ontario's energy supply in 2000, 2005, 2010 and 2012. According to this table, energy supply from coal has decreased from 29% in 2000 to 2.8% in 2012. At the same time, wind power and other renewable energy sources have gradually increased their proportion from 1% in 2000 to 3.8% in 2012 in energy supply. To meet most of the base-load demand, Ontario takes advantage of the uniform and reliable electricity-producing rate of nuclear and large hydroelectric stations (IESO, 2012a). From Table 2.1, more than half of the electrical power came from nuclear sources in 2010 and 2012. In 2012, hydro and natural gas, generating approximately 22.3% and 14.6% respectively, account for a remarkably large proportion. In the same year, wind energy with 3% of electricity supply surpassed 2.8% of electricity supply from coal. Other energy sources, such as solar energy account for 0.8%. A recent report by Navigant Consulting Inc. (2012) states that

289 MW_{DC} of solar PV capacity were installed in Canada in 2011 with Ontario accounting for 91%.

Table 2.1 - Ontario's electricity supply mix change (2000: Ontario Ministry of Energy, 2002; 2005: Ontario Ministry of Energy, 20005; 2010: Ontario Ministry of Energy, 2010; 2012: IESO, 2012a)

Year	Nuclear	Hydro	Gas/oil	Wind	Coal	Other
2000	37%	26%	7%	N/A	29%	1%
2005	41%	23%	15%	N/A	19%	2%
2010	52%	19%	15%	2%	8%	1%
2012	56.40%	22.30%	14.60%	3%	2.80%	0.80%

In general, energy demand is affected by a combination of the state of the global economy, conservation initiatives, increased energy generation capacity and time-of-use rates (IESO, 2012b). It is primarily influenced by hours of daylight, business hours, weather, etc., in Ontario (IESO, 2012c). As a result, electricity demand in Ontario shows a seasonal variation trend, from which future peak energy demand can be forecast. Table 2.2 shows the Independent Electricity System Operator's (IESO) 18-month forecast. Comparing the peak demand in summer and winter, it is apparent that more power is required during the summer period. In this case, installation of solar PV systems on the roofs of homes and businesses is an ideal energy option to reduce the spikes in demand for grid-supplied electricity in summer when solar energy is at its strongest (Ontario Clean Air Alliance, 2012).

Table 2.2 - Peak electricity demand forecasts for periods from 2013 summer to 2014 summer (IESO, 2012c)

Season	Seasonal Normal Weather Peak (MW)	Extreme Weather Peak (MW)
Summer 2013	23,275	25,430
Winter 2013-2014	22,128	23,361
Summer 2014	22,700	24,717

2.1.2. Ontario's Green Energy Act

It has been well established by numerous scientific bodies that natural and anthropogenic climate change has potentially significant impacts on numerous ecosystems and human systems (IPCC, 2007). To mitigate and address climate change, the Ontario Power

Authority (OPA) developed a plan in 2006 for provincial replacement of coal-fired generation with renewable and green alternatives. This plan indicated the importance of renewable energy for meeting the needs of future generations with a proposed increase of 7,863 MW in capacity by 2025. In response to this, the Ontario's Green Energy Act (GEA) was passed in 2009 with objectives of expanding renewable energy generation, encouraging energy conservation, and promoting the creation of clean energy jobs in Ontario.

The centerpiece of the Act is a schedule of subsidized electricity purchase contracts called Feed-in-Tariff (FIT) that provides incentives for individuals and businesses to adopt renewable energy technologies. According to a review by Solangi et al. (2001) on global solar energy policy, FITs have proven to be the most effective government incentive program, and in fact, half of the world's PV installations are due to FIT programs. The FIT program is divided into two streams depending on electricity generation capacity. The FIT program is available for renewable energy projects greater than 10 kilowatts, and the microFIT program is for renewable energy projects of 10 kilowatts or less. Technologies supported include on-shore wind, waterpower, bioenergy (i.e., biogas, biomass, and landfill gas), and ground-mounted and rooftop solar photovoltaic (PV). 99% of microFIT program applications are for solar PV projects (OPA, 2013a). The program has seen a great deal of interest at the FIT and MicroFIT levels, and about 1,600 total applications and contracts of rooftop PV and over 600 of ground-mounted PV have been executed as of March 2013 (OPA, 2013b).

2.1.3. Photovoltaic Systems

PV systems consist of PV solar panels installed on rooftops or mounted on posts in the ground. These systems operate by sunlight/photons striking a PV cell, and an electric current being produced by stimulating electrons (negative charges) in a layer in the cell designed to give up electrons easily. The existing electric field in the solar cell pulls these electrons to another layer. By connecting the cell to an external load, this movement of charges can then be used to power the load (EPA and NREL, 2013). Usually, a PV system (shown in Figure 2.1) is comprised of a series of collector panels, batteries wires,

and devices that convert electricity into its alternating current (AC) form that can be used for powering household appliances and lights (REEP, 2013).

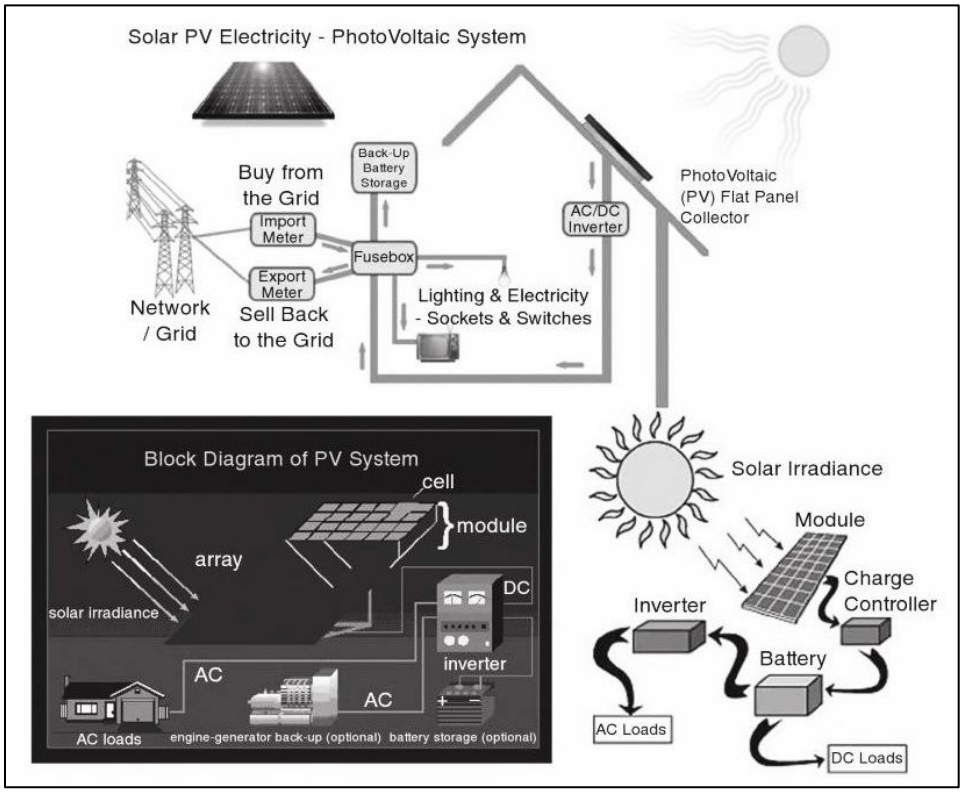

Figure 2.1 - Examples of basic PV power systems (Strauch et al., 2010)

PV technology has been shown to offer numerous advantages over conventional energy converters (Dornan, 2011; Svantesson and Linder, 2012), which are summarized in Table 2.3. First, PV cells are solid-state devices with no moving parts; therefore, nearly no maintenance is required for their simple and robust design (Foster et al., 2010; Svantesson and Linder, 2012). Second, PV panels do not require an additional energy source, such as fuel to operate, meaning that less transport is required (Svantesson and Linder, 2012). Since the demand for transportation of fuel and technicians is low, PV technology is exceptionally useful in remote areas. PV systems also have the uniqueness of being totally scalable, giving the possibility of expanding the system, once demand increases and enough space is available. Furthermore, the life cycle cost is generally lower than for other conventional lighting sources in developing regions and remote areas (Svantesson and Linder, 2012). Therefore, PV power is a sustainable energy alternative that offers substantial advantages over conventional sources of energy.

Nevertheless, different PV systems also have various drawbacks (summarized in Table 2.3). The service cost and lifetime of off-grid and on-grid PV systems are diverse. In particular, batteries needed in an off-grid system are a recurring problem (Mala et al., 2009). The batteries themselves can be expensive, inefficient and not environmentally friendly. For example, electrolyte in lead batteries without extra protection may evaporate in hot climates (Svantesson and Linder, 2012). Faulty usage or maintenance may also lead to unnecessarily shortening of a battery's lifetime (Svantesson and Linder, 2012). In remote areas, there is a risk of batteries ending up in the backyard, where they may pollute the ambient environment (Svantesson and Linder, 2012). Therefore, the best way of making use of a PV system is to utilize the electricity immediately when it is generated.

In addition, physical conditions of the installation location may further impact on the service cost and lifetime of the system (Svantesson and Linder, 2012). For example, operation and maintenance may account for half of the service cost in areas with hot and humid conditions. Another potential drawback is the construction process of a PV system may lead to environmental damage to the surrounding landscape. Finally, PV arrays may cause visualization or aesthetics issues to the local residential community (e.g., Aydin, 2009).

Table 2.3 - Summary of the pros and cons of PV technology

Advantages	Disadvantages
Less maintenance required	Large upfront costs
No need for external operating support	Maintenance issues for battery systems
Ideal for remote areas	Potential construction contamination
Scalable to required expansion	Visual impact
Less life cycle cost	
Sustainable and clean	

PV systems can be used for a wide variety of applications, from small stand-alone systems to large utility grid-connected systems (Foster et al., 2010). Stand-alone systems (or off-grid systems) are usually used in remote areas that are not easily accessible to an electric grid (Kalogirou, 2009). Energy produced by such systems is normally stored in batteries. Typically, a stand-alone system consists of a PV module or modules, a charge controller, and batteries (shown in Figure 2.2). The charge controller regulates the power

from PV modules and delivers direct current (DC) electricity for storage. An inverter is included to convert DC electricity to AC form that is required by normal appliances (Kalogirou, 2009). This type of application provides cost-effective, modest levels of power for fans, lighting, communication, water pumping, and so on (Foster et al., 2010).

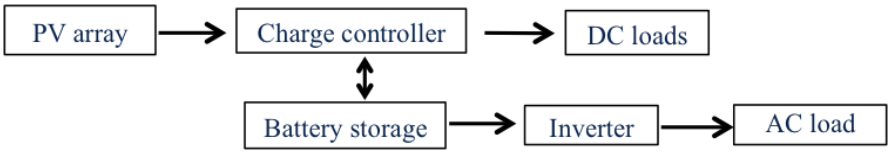

Figure 2.2 - Schematic diagram of a stand-alone PV application (Kalogirou, 2009)

Since solar power can be generated only during the daytime when sunshine is available, battery storage is a significant component for this type of system, especially during the winter season. Hence, in places where winters allow for very limited hours of sunshine, the stand-alone system is bridged with a hybrid system (Kalogirou, 2009). In Canada, the total market share of the off-grid market is projected to continually decrease as the grid-connected market rapidly expands over the coming years (Navigant Consulting Inc., 2012).

The grid-connected systems (or grid-tied systems) are designed for decentralized applications. During the daytime, DC electricity generated by the system is converted to AC by the inverter and fed into a power distribution system (Foster et al., 2010). The electricity can either be utilized immediately or be transmitted and sold to an electricity supplier. In the evening, when solar power cannot be generated, power can be bought back from the network (Foster et al., 2010; Kalogirou, 2009). This system does not include battery storage, since the grid acts as an energy storage system (Kalogirou, 2009). A schematic diagram of a grid-connected PV system is shown in Figure 2.3.

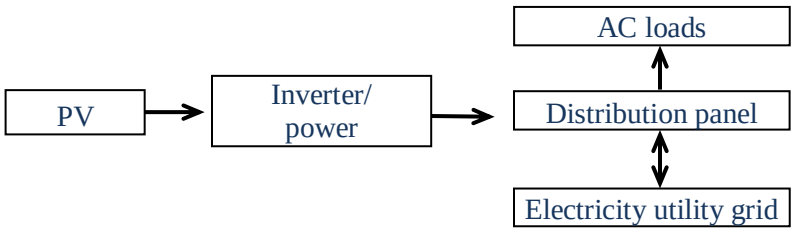

Figure 2.3 - Schematic diagram of a grid-connected system (Kalogirou, 2009)

In effect, the cost of bringing utility power via transmission and distribution lines to other areas connecting to the grid is significant, especially for small household electrical loads and villages located at great distances over difficult terrain from the transmission grid (Foster et al., 2010). In addition, the cost of grid extension can be prohibitive, especially for a gully, mountain, or other difficult terrain conditions (Foster et al., 2010). This study examines grid-connected systems; therefore, distances to transmission and distribution lines are important considerations in the PV site selection process.

2.2. Site Selection - Factors

2.2.1. Demand and Supply

Before determining a suitable location for a PV farm, potential energy demand and generation capacity of local areas/regions can be assessed to determine the optimal size of the farm. In 2001, Sorensen adopted GIS techniques to map solar resources on the basis of satellite data and to match it with energy demand modelling based on population density and energy demand intensity. In some studies, energy demand analysis was based solely on gross domestic product (GDP) growth levels. For example, Sambo (2008) analyzed the electricity demand in Nigeria by dividing the energy consumption into four scenarios on a GDP basis: Reference Scenario - 7% GDP Growth; High Growth Scenario - 10% GDP Growth; Optimistic Scenario I - 11.5% GDP Growth; and Optimistic Scenario II - 13% GDP Growth.

Energy demand can also be analyzed based on detailed social and economic factors. For example, the Ethiopian Rural Energy Development and Promotion Center (EREDPC) (2007) investigated the national energy demand based on consumption from households, agriculture, industry, transport, and services sectors. Setting the households sector as an example, the energy demand was determined from usage in cooking, baking, lighting, water heating, space heating, electric appliances, refrigeration, and air conditioning. In order to predict future energy demand, EREDPC made assumptions on the general growth rate for each sector and subsector. Although this method is comprehensive in terms of covering each sector, the prediction nevertheless requires validation with previous energy consumption data.

Similarly, in 2012, the Ontario Power Authority (OPA) provided a provincial electricity demand forecast based on different sectors (residential, commercial, industrial, transportation, and agriculture) and the end use in each sector (e.g., lighting, cooling, etc.). The OPA compared the current demand forecast to forecasts conducted in previous years based on the trends in end uses in each sector. From the reported results, it was determined that current forecasts of energy demand are much lower than previously thought due to predicted increases in electricity prices. Uncertainty in specific sectors, such as transportation exists due to technology development and changes in energy usage (OPA, 2012).

In addition to analyzing the energy demand, it is necessary to also consider changes in potential energy supply. For example, Mulherin (2011) applied GIS techniques to estimate potential energy outputs from rooftop PV panels for homeowners. More specifically, incoming solar radiation for each rooftop was calculated based on LiDAR data without considering chimneys and dormers. Electricity and financial costs of the investment of PV panels were then compared to aid each household in making the decision of PV panel placement. This study suggested that potential energy supply should be considered more realistically, especially at the micro-scale level, since rooftop structure may impact PV system performance and power generation capacity. Since the potential supply of solar energy highly depends on the PV system's performance, other influential factors, such as shading effects and PV panel angle, should be analyzed.

2.2.2. System Performance Factors

Without considering the types/materials of solar panels being used and inverter efficiency, the efficiency of a PV system is affected by multiple external factors. First, the availability of electromagnetic radiation directly determines the energy generation potential of the system. Even though solar radiation is a worldwide energy source, it has distinct patterns in seasonal and daily variability and can be easily obstructed by ambient objects. Third, when solar panels are installed, the optimal tilt angle will differ according to the location and season. Last, energy lost during transmission so distance from the electricity grid of transmission lines should be considered.

2.2.2.1. Amount of Incoming Solar Radiation

Solar installation sites must be able to generate an adequate electricity supply to ensure their long-term viability for supporting energy demands. The most important factor for generation capacity is the average level of sun exposure that a site experiences throughout the year. According to the following research studies, solar radiation striking a specific location on the Earth's surface can be measured or estimated by different methods depending on the types of data available.

a. Application of Geostatistical Techniques

Solar radiation data obtained from dispersed weather stations can be utilized to generate a solar radiation map by geostatistical techniques. For example, Rehman and Ghori (2000) adopted a geostatistical technique to estimate solar radiation in Saudi Arabia. The process consisted of five steps: 1) data collection; 2) univariate analysis; 3) experimental variogram calculations and model fitting; 4) estimation of solar radiation using ordinary kriging; and 5) plotting contour maps. This country has 41 solar radiation measuring stations, where global horizontal solar radiation and sunshine duration values have been recorded since 1972. A total of 492 values of H/H_0, i.e., 12 values for each location, were used in the study by Rehman and Ghori (2000). Here, H is the global solar radiation, and H_0 is the extraterrestrial solar radiation outside the atmosphere. This study applied a spherical model to fit the experimental variogram. After obtaining nugget and lag distance values of variogram parameters, kriged estimation results were generated. According to the results, the seasonal trend, with lower values of H/H_0 in winter months (December to March) and higher in summer months (April to November) were clearly discernible (Rehman and Ghori, 2000).

b. Application of Multivariate Statistical Methods

In addition to geostatistical techniques, several research groups have endorsed the use of artificial neural networks (ANN) and in particular, Radial Basis Function (RBF) networks for estimating solar radiation in locations where collection equipment is not available (Elizondo et al., 1994; Sfetsos and Coonick, 2000). These approaches are based on regression analysis, and feed-forward neural networks are most commonly used to

estimate the daily solar radiation (e.g., Dorvlo et al., 2002). In this estimation, meteorological parameters such as clear sky radiation, precipitation, temperature, day length and day of the year are used as inputs in the ANN. All studies reported that neural network approaches outperformed the traditional linear methods, since training approaches are applied to assist regression analysis of neural network approaches (Elizondo et al., 1994; Williams and Zazueta, 1996).

c. Application of LiDAR Point Cloud Data

Three-dimensional LiDAR point clouds have been successfully used as inputs to solar radiation estimation models, generating accurate estimated results (e.g., Latif et al., 2012; Wehr and Lohr, 1999). These models can be implemented and computed within commercial or open-source GIS solutions, such as SAGA GIS (Agugiaro et al., 2012; Redweik et al., 2011). Well known models include the solar analyst in ArcView, spatial radiation tools in ArcGIS, and GRASS r.sun (e.g., Kryza et al., 2010; Nguyen et al., 2010; Redweik et al., 2011; Charabi and Gastli, 2011).

For example, Jochem et al. (2009) applied a solar radiation model in SAGA GIS to estimate insolation and used part of the City of Feldkirch in the Federal state of Vorarlberg (Austria) to test its viability. More specifically, LiDAR point cloud was obtained by Airborne Laser Scanning (ALS) systems under snow-free conditions. For the point cloud-based solar radiation model, the global radiation was computed as the sum of the direct and diffuse radiation. The position of the sun at any time and its incidence angle on the point of interest were provided using the SOLPOS Code developed by the National Renewable Energy Laboratory (NREL). Data from a nearby meteorological ground station were used to calculate the clear sky index (CSI) to correct the modeled incoming global radiation and to consider atmospheric effects and terrain shadows (i.e., shadows casted by mountains and hills) (Jochem et al., 2009). The CSI was calculated based on the atmospheric longwave irradiance, as well as air temperature and humidity measured at screen level height. Since the meteorological station was affected by shadows cast by the surrounding terrain, these effects were incorporated into the CSI (Jochem et al., 2009). Shadows considered in this solar radiation model involved those of nearby objects and shadows from surrounding terrain.

In 2011, Mulherin proposed a robust approach for modeling solar radiation at the household level by accounting for shadowing effects and topographic variation at particular locations by incorporating LIDAR data. The bare-earth and first-return signals were used as inputs to calculate the spatial distribution of solar radiation. This study also provided solar energy information at the household level and financial costs information to guide homeowners as they made decisions regarding solar PV systems.

In 2011, Liddell and Bishop estimated total rooftop solar electricity potential in Seattle using LiDAR data associated with ArcGIS and LiDAR Analyst. As shown in the estimation workflow in Figure 2.4, LiDAR point cloud data were used as an input for the solar radiation analysis, while NREL helped to determine tool parameters in ArcGIS. LiDAR point clouds were also applied to identify bare earth and buildings for rooftop extraction. In the end, the extract by mask tool was used to identify solar radiation levels of rooftops only. The total rooftop solar electricity potential was thus obtained.

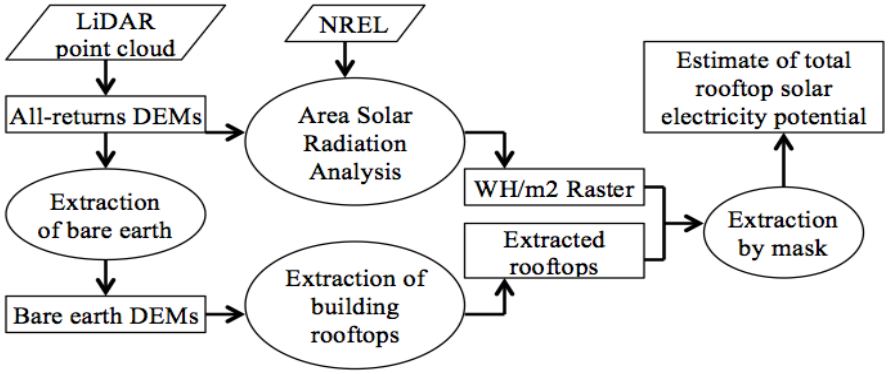

Figure 2.4 - Workflow of estimating PV production potential using LiDAR point cloud (Liddell and Bishop, 2011)

d. Application of Satellite Imagery

Lastly, geostationary satellites, such as METEOSAT 7 and Geostationary Operational Environmental Satellite (GOES), perform continuous and reliable meteorological observations from space; thus, they provide the opportunity to derive information on the solar irradiance for a large area (Broesamle et al., 2001). For example, in Hoyer et al.'s study (2002), METEOSAT 7 imagery were used to obtain a cloud index, and direct normal solar irradiation were computed by considering scattering, absorption and

extinction in the atmosphere. The calculated direct irradiance and global irradiance were then compared to ground data.

2.2.2.2. Shadow Impacts

Physical factors, such as surface orientation, land-surface gradient, and surrounding obstacles have a significant impact on the optimal performance of PV panels by causing shadow effects (Carrion et al., 2007; Wiginton et al., 2010). To determine an appropriate orientation, the relative angular position of the sun throughout the day and year should be considered. Summer in the Northern Hemisphere coincides with the Northern Hemisphere being oriented more towards the sun, which causes solar rays to strike the ground more directly. In the winter the Northern Hemisphere is oriented away from the sun (Mulherin, 2011). Therefore, for installations in the northern hemisphere, a southern exposure is generally optimal for obtaining the strongest intensity of sunlight in general. A northern orientation is preferable in the southern hemisphere (Carrion et al., 2007; Reijenga and Ruoss, 2005).

In 2007, Carrion et al. conducted a study regarding the importance of considering the gradient of land through their analysis of appropriate locations for grid-connected PV stations in Andalusia. Their analysis found that sites containing a slope of more than 2% could cause shadow effects from the panels themselves, while in a similar study conducted by Charabi and Gastli (2011), a 5% graded slope or greater could result in shadow effects. This becomes especially problematic for installations involving multiple rows of panels. Therefore, topographic aspect and gradient must be taken into account to maximize solar exposure potential. In the study carried out by Bravo (2007), a maximum 7% slope was required for southwest and southeast oriented land surfaces, and 2% for other orientations.

Surrounding obstacles can reduce the solar exposure of PV installations. For example, ambient trees may obstruct incoming solar radiation (Reijenga and Ruoss, 2005). Therefore, when determining the suitability of a site, only unshaded areas should be considered when calculating average sun exposure (Wiginton et al., 2010). In Carrion et al.'s study (2007), they suggested that areas with vegetation and crops are not

appropriate for grid-connected PV stations. Voegtle et al. (2005) suggested that topographic shading, structural shading, and vegetative shading should be considered in roof-mounted PV site selection process. Overall, installations on rooftops and grounds may be subject to shadow effects from nearby vegetation, buildings and/or the gradient of land during certain times of the day.

2.2.2.3. Tilt

To improve the efficiency of solar PV generation, panel tilt angle has been widely considered. The optimal tilt angle with the horizontal is related to the local climatic condition, the period of use of solar panels, and the geographic latitude (e.g., Siraki and Pillary, 2012; Tiris and Tiris, 1998). Thus, the tilt angle should be defined according to the specific geographic location and period. Optimum collector tilt angle of a fixed PV array should be equal to the geographic latitude with an azimuth of due south in the northern hemisphere throughout a year (Rowlands et al., 2011).

A considerable number of research studies have applied various simulation software (e.g., TRNSYS, PVSYST) (e.g., Cheng et al., 2009; Hussein et al., 2004), or developed their own mathematical models (e.g., Bakirci, 2012; Tang and Wu, 2004) for determining the optimal tilt angle of solar panels. The simulation procedure essentially considers factors, including the average global and diffuse radiation on horizontal surface, clearness index, surface tilt from horizontal, solar declination, geographic location, and some sun-related parameters (e.g., sunset hour angle) (e.g., Bakirci, 2012; Siraki and Pillary, 2012). According to Morcos (1994), the optimum tilt angle varies day-to-day, but changing the angle to its daily optimal values throughout the year is not practical or realistic. As a result, a fixed tilt angle for each month or even each season for a specific location may be determined based on the average daily optimum tilt angles (Morcos, 1994). For average seasonal performance, the optimum tilt angle can be equated to approximately the latitude angle (φ) ± 15 °(e.g., Gunerhan and Hepbasli, 2007; Pavlović et al., 2010), while the yearly optimal tilt angle is nearly equal to ($0.9 \times \varphi$) (e.g., Chang, 2009; Garg and Gupta, 1978). These findings are supported by previous research focused on specific locations of interest. For example, Calabro (2009) adopted a simulation tool to study the

optimum tilt angle at different latitudes from 36 ° to 46 °. They noticed that the annual optimum tilt angle is (φ - 10 °). Chen et al. (2005) used a genetic algorithm searching technique to find the optimum tilt angle for Chiayi, Taiwan (with latitude of φ = 23.5 °), which was determined to be 20 ° (φ - 3.5 °). Rowlands et al. (2011) used measured and modeled solar radiation data, simulated photovoltaic panel performance, and hourly electricity market data, as well as details regarding pricing regimes from 2003 to 2008 to determine the tilt angle and azimuth for a photovoltaic panel in both Toronto and Ottawa, Ontario. Optimum tilt for Ottawa (φ = 45°N) was found between 36 ° and 38 ° with the desired azimuth between 4 ° west of due south and 6 ° east of due south, and between 32 ° and 35° for Toronto (φ = 44°N) with azimuth between 1 ° west of due south and 2 ° east of due south.

A different finding regarding optimum tilt is from Beringer et al. (2011). They claim that there are few studies considering cell temperature effects and reflection characteristics of the collector surface in their simulation models. As Balenzategui and Chenlo (2005) concluded from their study, different collector surface covers behave differently according to reflection losses. As a result, in Beringer et al.'s study, experimental measurements were conducted using a short circuit current, measuring the open circuit voltage and the temperature of each cell to determine the monthly optimum tilt angle in Hannover, Germany. Collectors in the experiment were mounted at a different tilt angle from 0 ° to 70 ° with a 10 ° interval, and were directed towards a southern direction. From their experimental results, a difference of only 6% between minimum and maximum values was discovered for summer, and a difference of 10% was found over the winter. These results show that differences are much smaller in reality than those obtained from modeled results. A possible reason may be due to the temperature effect or inaccuracies of the experimental model (Beringer et al., 2011).

2.2.2.4. Other System Performance Factors

To improve PV system performance, several other factors have been considered in previous research. For example, Carrion et al. (2007) considered losses of energy during the transmission, and the distance of solar installation to substations and urban areas in

the site selection process. Since energy loss during long-distance transmission directly leads to economic loss, it is often considered to be the most important factor in on-grid PV system site selection. Distances to transmission lines defined in previous studies are quite different based on scope of area of interest. For example, Pletka (2007) adopted 1 mile as the maximum distance for regional-scale projects in Arizona, while Fluri (2009) used 20 km and 10 km in a provincial scale analysis in South Africa. Accessibility to highways is an important factor for cost effectiveness and construction convenience (Charabi and Gastli, 2011; Janke, 2010). On the other hand, proximity to roads or highways can negatively affect energy production efficiency by increasing dust cover on PV panels (Janke, 2010). Vandalism and theft may also occur if PV panels are located close to roads, or publicly accessible areas, but weight added on this concern is almost equal to 0 according to Aragonés-Beltrán et al. (2010).

Snow cover is a concern during winter for many regions. For example, Powers et al. (2010) conducted an experiment to gauge the energy loss of PV panels installed in California near Lake Tahoe due to snow for three common tilt angles (0°, 24°, and 39°). The annual estimation based on the monthly results was that the energy losses for the 39°, 24°, and 0° tilts were 12%, 15%, and 18%, respectively. When Thevenard and Pelland (2013) examined the uncertainty in long-term PV system yield predictions by statistical modeling of a hypothetical 10 MW_{AC}, c-Si photovoltaic system in Toronto, Canada, they found that 1.5% of uncertainties were due to losses caused by snow cover. In addition, dust or soiling can affect PV system performance. According to Thevenard and Pelland (2013), potential sources of dust cover include pollution, bird droppings, the growth of lichen, etc., which are difficult to model or extrapolate from case studies.

2.2.3. Environmental Factors

While PV array installations are generally praised for their negligible environmental impact, the construction process may present significant environmental harm to the selected site or the ambient landscape as previously discussed in Section 2.1.2.2. As a result, environmental restrictions are legal requirements, along with environmental protection laws, such as the right to highway, rivers, and coastal zone access, or the

existence of protected areas (e.g., national parks and nature reserves) (Carrion et al., 2007).

Although solar installations should be located away from water sources and coastal zones to minimize water pollution risk from PV construction contamination, water resources may be required for cleaning or cooling of some solar operation components (e.g., central receiver power plants) (Trieb et al., 1997). Available alternatives for cleaning and cooling include placing the solar panel with a tilt that facilitates self-cleaning during rainfall events and using advanced nanotechnology solutions to provide a non-stick coating that reduces the need for cleaning (Gray, 2012). Dry cooling is a popular alternative for solar panel cooling, especially in areas lacking water. Therefore, proximity to water sources is not essential for PV site selection. Impacts of visualization and construction contamination on the local residential community should be considered as well.

2.2.4. Summary of Factors

It is clear that when developing solar installations, multiple factors must be taken into consideration. Factors can be categorized into environmental, economic, and technical (energy production) concerns. Criteria considered by previous studies for solar panel installation site selection are summarized in Table 2.4. Since information of some factors cannot be obtained directly, LiDAR data, satellite or aerial imagery, and other data can be applied to model variables indirectly. For example, solar potential can be estimated from LiDAR elevation data, while obstruction heights and shadows can be calculated from LiDAR data and three-dimensional models (Yimprayoon and Navvab, 2010). LiDAR data can be applied for deriving slope, hillshade, and aspect information (Vaughan, 2009). Optical satellite or aerial imagery, such as Landsat data, can help to quickly identify land cover characteristics in a region, and visually assist to determine which areas are unsuitable for development.

According to Charabi and Gastli (2011)[1], distance to major roads was given a very low weight of 16.8%, while weight of solar potential was 54.5%, using the analytical hierarchy process (AHP). The rest of the weight (28.7%) was assigned to other constraint factors, including dams, flood area, land use, village boundary, historical and touristic monuments, rivers, sand dunes, roads, and slope, which were treated equally. In another study, Janke (2010) assigned the greatest weight to solar potential, the second highest weight to distance to transmission lines, and the lowest weight to distance to roads. In addition the three criteria, this study also considered distance to cities, population density, and land cover, which were given the same weight as distance to road (Janke, 2010). Overall, distance to transmission lines is deemed to be more desirable than distance to roads from an economic perspective. Solar potential is the most important factor among all concerns involved in the PV potential site selection process.

[1] Research by Charabi and Gastli (2011) did not consider transmission line in the PV site suitability analysis due to data availability.

Table 2.4 - Summary of criteria used for solar panel installation site selection from reviewed literature

Variable/criteria	Description	References
Slope	Gradient of land will affect the receiving radiation. The more flat, the more amount of radiation received	Bravo et al. (2007); Pletka et al. (2007); Broesamle et al. (2001); Charabi and Gastli (2011)
Aspect	Slope direction	Bravo et al. (2007); Janke (2010)
Direct Normal Irradiance or solar potential	Solar radiation data can be obtained or estimated by various approaches. It provides information of solar potential to area of interest	Bravo et al. (2007); Pletka et al. (2007); Fluri (2009); Clifton & Boruff (2010); Dawson & Schlyter (2012); Broesamle et al. (2001); Gastli & Charabi (2010 a & b)
Proximity to roads	Proximity to roads minimizes cost in infrastructure construction and maintenance but may contribute to vandalism, dust and other concerns	Clifton & Boruff (2010); Dawson & Schlyter (2012); Janke (2010);
Distance to transmission/power lines or pipeline	Access to transmission network infrastructure to connect supply with demand	Fluri (2009); Clifton & Boruff (2010); Broesamle et al. (2001); Janke (2010);
Sand/dust risk	Area with abundance of dust, combined with mist and fog, may affect the efficiency (revenue) of PV farms	Charabi & Gastli (2010)
Access to water source	Water source accessibility benefits cooling solar panels	Fluri (2009); Dawson & Schlyter (2012); Broesamle et al. (2001); Clifton & Boruff (2010)
Environmentally sensitive areas (ESA)	To decrease negative environmental impacts from large scale PV farms, ESA should be filtered out in site selection	Dawson & Schlyter (2012); Lehman (2011); Charabi & Gastli (2010); Clifton & Boruff (2010)
Land cover or land use profile (accessibility)	Accessibility to different land use types can vary.	Bravo et al. (2007); Pletka et al. (2007); Broesamle et al. (2001); Charabi & Gastli (2010); Janke (2010);
Supply-demand balance	Based on the local energy demand information, people can determine the size of solar farms so that supply-demand balance can be achieved.	Armstrong (2009); Sambo (2008); EREDPC (2007);
Visual impact	Aesthetic consideration to ambient environment	Dawson & Schlyter (2012);
Weather conditions	Weather conditions in local area of interest reflect annual incoming solar radiation	Dawson & Schlyter (2012);
Configuration of solar panels	Different configurations of solar panels perform with different efficiency.	Broesamle et al. (2001);
Population density	To assist energy demand forecast	Janke (2010)
Flood pathways	PV farms should be kept away from areas with high risk of floods	Charabi & Gastli (2010)
Dam	Same as above	Charabi & Gastli (2010)
Distance to cities	This helps to reduce vandalism	Janke (2010)
Cultural heritage sites	To protect cultural heritage from solar power farms	Clifton & Boruff (2010)

2.3. Site Selection - Methods

During the 1970s, energy planning efforts were directed primarily towards energy models to explore the energy-economy relationships in energy sector (Pohekar and Ramachandran, 2004). In the 1980s, growing environmental awareness has slightly modified the decision framework (Nijcamp and Volwahsen, 1990). The need to incorporate social, technical, political, and environmental considerations in energy planning leads to the increasing application of multicriteria approaches (Pohekar and Ramachandran, 2004; San Cristóbal Mateo, 2012). In recent years, Multicriteria Analysis (MCA) (or Multicriteria Decision Making (MCDM)) methods have been widely used for PV panel installation site selection (e.g., Ben Salah et al., 2008; Kahraman et al., 2009). These methods have been of interest to decision makers for years by providing a means to identify explicit, rational and efficient choices (Haurant et al., 2011). These methods deal with the process of making decisions in the presence of multiple objectives or limitations. Usually the objectives are conflicting, and thus, the solution depends highly on the preferences of the decision maker or stakeholders (Pohekar and Ramachandran, 2004). These techniques are usually based on weighted averages, priority setting, and outranking to achieve an agreeable outcome (Aydin, 2009; Wang et al., 2009).

The first step of an MCA process is to formulate problems of project, and to establish a set of criteria that will form a basis for the project requirements (San Cristóbal Mateo, 2012). The next step is to determine priorities of criteria by assigning weights that show the relative importance of criteria in MCA (Wang et al., 2009). After this, a multicriteria method is selected and applied to rank alternatives, and then finally propose optimal solution based on the best ranked alternative (Wang et al., 2009). This framework makes its contributions through decision-aiding science, formulating recommendations, while decision makers maintain their freedom to make choices. The final decision belongs to the decision makers regarding how to interpret the scientific conclusions (Haurant et al., 2011).

Different rules can be applied during the MCA decision-making process. The weighted product method (WPM), weighted sum method (WSM), fuzzy set method, and

analytical hierarchy process (AHP) are the commonly used approaches (e.g., Gastli and Charabi, 2010a; Wang et al., 2009). In particular, AHP is used to combine the priority for all levels of the hierarchical structure (Gastli and Charabi, 2010b). According to Pohekar and Ramachandran (2004) and Wang et al. (2009), AHP is the most popular method for prioritizing the alternatives for its understandability in theory and the simplicity in application.

In addition, outranking techniques PROMETHEE and ELECTRE have also been widely used. For example, Haurant et al. (2011) considered criteria of energy, geo-economic, ecological, visual impact, territorial use, and financial effect in an ELECTRE multicriteria model to determine optimal sites on farming fields for photovoltaic plants on Corsica Island, France. The ELECTRE outranking approach is a mathematical tool that tests comparisons between different alternatives according to several criteria that are often controversial (e.g., Roy, 1996; Figuera et al., 2005). This method has a clear view of alternatives by eliminating less favorable ones, especially convenient when encountering a few criteria with a large number of alternatives in a decision-making problem (Pohekar and Ramachandran, 2004).

2.4. Case Studies on UW campus

In 2004, STEP (Sustainable Technology Education Project) volunteers successfully installed the first ever student-designed PV array in Canada (STEP, 2013). These panels are located at Federation (FED) Hall of University of Waterloo (UW). A report prepared by Finamore et al. (2002) examined the feasibility of implementing a PV system at FED Hall technologically, economically, environmentally and socially. The study evaluated the solar panel installation based on literature review, field trips and key informant interviews. They consulted several professionals from both within and outside the UW community.

According to the review results, panels placed at a 60° angle with south-facing orientation were considered to be optimal (Finamore et al., 2002). DeLoyde (2002) also indicated that FED hall roofs have a 45°-tilt angle. The south face of the building, it was not shaded by trees or buildings and had enough space for panels. The reason for not

selecting the flat/parapet rooftop of FED Hall was because the flat roof required a higher weight bearing capacity than sloped roofs due to snow and rain accumulation (Finamore et al., 2002). This project did not provide a quantitative assessment of solar power potential. Hence, a more reliable evaluation, including incoming solar radiation estimation is required. A photo of the installed solar array on FED Hall is shown in Figure 2.5. Unfortunately, after the solar panel installation, monitoring and evaluation of the performance and reliability of the panels was not implemented and a lack of documentation exists.

Figure 2.5 - Solar panels on the FED Hall rooftop

Another study addressing feasibility of solar array implementation on UW campus' buildings was undertaken by Buttery et al. (2004), who prepared a report for Environment 2 (EV2) of the UW campus. This study applied RETScreen software to calculate the energy production of solar panels prior to the installation. Buttery et al. (2004) examined different kinds of PV arrays to evaluate the cost and benefits. Similarly, they adopted expert interviews to obtain information regarding positioning, and installation techniques. In order to maximize quantity of solar energy, Buttery et al. (2004) discussed panel tilt based on the location of the study area and the seasonal sun path. In the summer time, the ideal panel angle was determined to be 35 °, whereas the tilt angle increases to 60 °in winter. In spring and fall, solar panel should be placed at appropriately 45 °.

Buttery et al. (2004) indicated that the structure of EV2 roof was designed as an inverted roof, meaning that the roof membrane was covered by a layer of sheathing,

insulation and ballast (Figure 2.6). This design ensures the security and stabilization of solar panels during adverse weather conditions (Buttery et al., 2004). Although this study provided a comprehensive report regarding feasibility of PV array installation on the EV2 rooftop, it did not identify the optimal sites for solar panel placement.

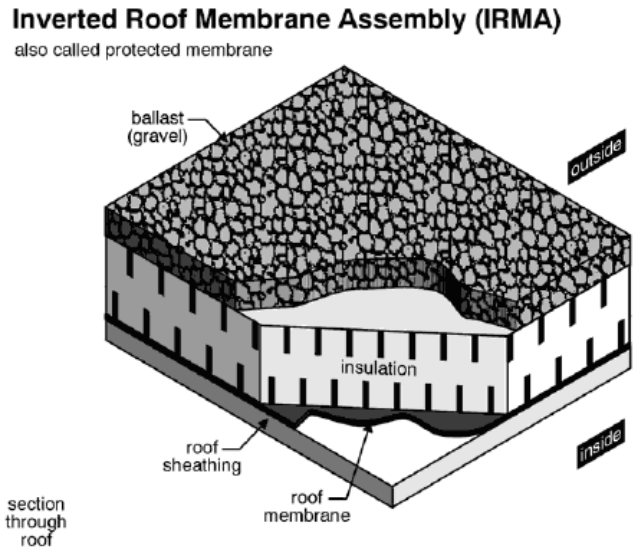

Figure 2.6 - Structural design of an inverted roof (Buttery et al., 2004)

2.5. Chapter Summary

Solar energy has a competitive advantage over traditional sources of energy, since it provides a sustainable energy supply (Huld et al., 2003). As a result of increasing interest in renewable energy sources, determining optimal solar PV installation sites is an essential requirement. This chapter reviewed various factors that can be considered during the site selection process, as well as quantitative methods for solar panel site evaluation and selection. Several factors were compared and their relative importance was discussed by presenting previous case studies.

The relationship between local energy demand and generation capacity provides a reference for the size of a PV system. In order to acquire energy-demand information, several studies have applied GDP or energy consumption assessments in households, industry, transportation, etc., to estimate the demand for energy. PV power is one of the energy sources that can help meet energy demand requirements. However, energy

generation capacity relies on the PV system's performance, which is ultimately determined by the PV array, inverter and transmission efficiency. PV panel performance also depends on the type of PV panel and materials, amount of solar radiation, shadow impacts, tilt angle, and orientation.

The amount of incoming solar irradiance can be estimated using a variety of techniques. For example, solar radiation from dispersed observation points can be interpolated to generate a continuous solar map by geostatistical techniques that estimate solar radiation levels via a variogram or semivariogram associated with interpolation methods, such as kriging. Airborne LiDAR point cloud or DEM data with land surface elevation information are also commonly used, while considering shadow effects and obstacles. In addition, multivariate statistical methods can estimate solar radiation by accounting for multiple variables affecting the radiation in artificial intelligence models. For the application of geostationary satellite imagery, meteorological factors from specific bands, such as visible and infrared bands, can be used to estimate the radiation under various sky conditions.

To minimize shading effects caused by ambient objects or topographic features, ground-mounted PV panels should be placed on flat open spaces, whereas rooftop PV panels should be oriented between southwest and southeast in the northern hemisphere. Tilt placement can be altered seasonally, and optimal tilt angles are location specific. In general, tilt angle equated to approximately the latitude angle (φ) $\pm \leq 15°$ is suggested to maximize solar electricity production.

The complex and costly process of solar PV site selection involves not only technical, economic, and generation considerations, but also environmental factors. From an energy generation point of view, the viability of generating electricity at a given site needs to be taken into account. Environmental impact of solar energy installations is an important concern, since the construction processes can have a significant impact on the surrounding environment. Since a variety of factors should be considered in the solar site selection process, multicritera analysis (MCA) is a suitable approach for aiding the decision-making process.

Chapter 3. Research Design

3.1. Research Goal and Objectives

The main purpose of the present study is to demonstrate the potential benefits of applying spatial analytical techniques to remote sensing data for determining the optimal sites for solar panel installation at both micro- and macro-scales. The micro-scale analysis considers solar panel installations on building roofs, whereas the macro scale analysis considers ground-mounted installations within a municipality region. In the micro-scale analysis, optimal location determination is primarily based on the spatial variation of incoming solar radiation on a building rooftop surface. Appropriate installation site analysis for ground-mounted solar panels will be carried out by multicriteria analysis associated with environmental, economic, and system efficiency factors (e.g., proximity to transmission lines, land surface slope). In order to evaluate the real-world implementation of the proposed methodology, a survey was administered to explore commonly used approaches and datasets currently applied by solar companies in Ontario. A detailed workflow of the present study is shown in Figure 3.1.

The objectives of the present study are as follows:

i. To examine the spatial distribution and amount of solar radiation under both clear-sky and overcast conditions;

ii. To generate a shadow mask and to identify the optimal area for micro-scale site selection for rooftop-mounted solar panels;

iii. To determine optimal sites based on multiple criteria (e.g., restrictions due to environmentally friendly regulations) for ground-mounted solar panels and to perform an on-site feasibility assessment of potential sites;

iv. To conduct a questionnaire survey of solar power companies and their representatives to collect information regarding current solar panel installation practices.

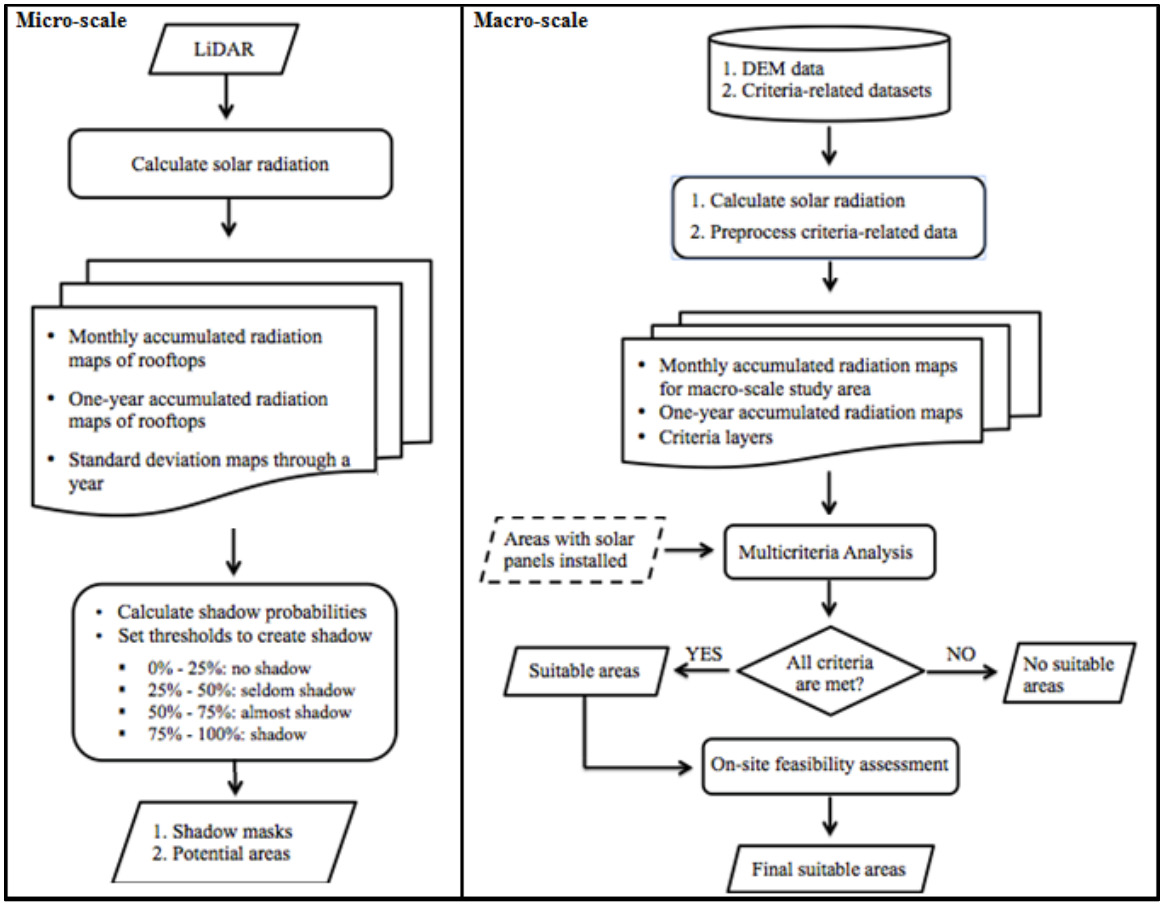

Figure 3.1 - Workflow of micro-scale and macro-scale site selection analysis

3.2. Study Areas

Site selection in this research study was implemented at both the micro- and macro-scales of analysis. For the micro-scale analysis, five buildings on the University of Waterloo campus were selected as case studies, including the Physical Activities Complex (PAC), Dana Porter (DP) Library, Environment (EV) buildings, FED Hall, and Student Village (V) 1. The EV buildings are comprised of EV1 and EV2. EV1 is located on the southwest side of campus, while EV2 is connected to the southwest of EV1. V1 is comprised of a group of chained buildings located at the northwest side of the campus. These five buildings selected for this study have different types of rooftops and building heights. For example, the PAC is a building with clean flat rooftops with different heights, except that its southern rooftop has an approximately 10 ° of gradient. The FED Hall has a main building with four tilted edges. The EV buildings and the DP Library differ by having complex rooftop structures. For example, EV1 has a pyramidal glass roof on one side and

a rooftop construction on the other side (Figure 3.3). In terms of the building height, the DP Library has ten stories and is the tallest building on the UW campus, as shown in Picture B in Figure 3.3.

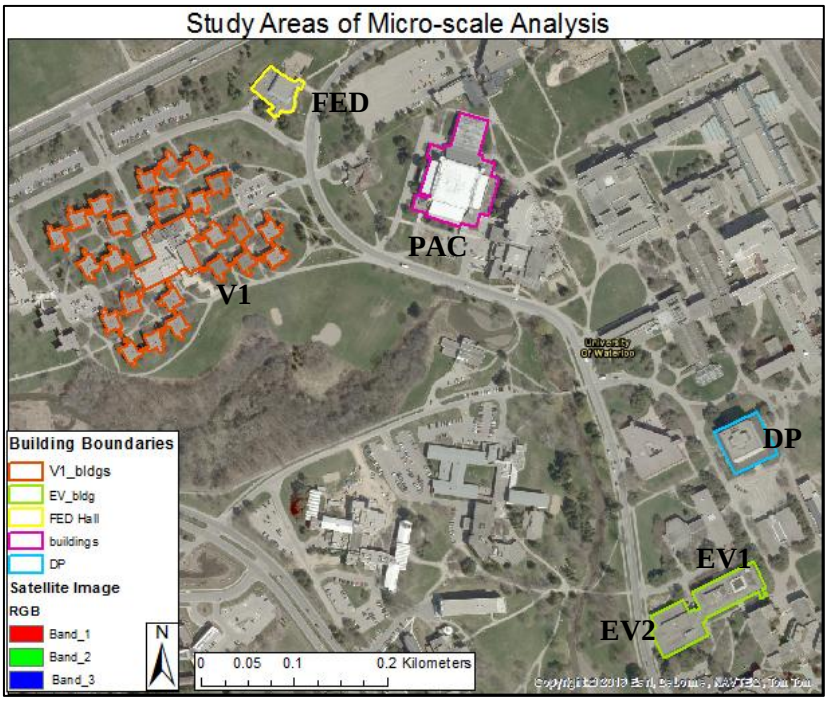

Figure 3.2 - Five selected buildings on the UW campus for the micro-scale analysis

Figure 3.3 - Pictures of the EV1 and DP Library roofs

For the macro-scale analysis, the City of Waterloo was the selected case study, encompassing approximately 65 km^2. The city boundary is marked in Figure 3.4. Land use types within the study area include residential, industrial, commercial, agricultural, and green areas, as well as open spaces. Natural land cover types consist of lakes, ponds, and woodlots among others. In the center of the city, residential buildings and commercial stores are highly concentrated, associated with buildings of two university campuses. Around the city boundary, land use is primarily comprised of industrial, agricultural and residential areas. In terms of city topography, elevation decreases from southwest to northeast (Appendix A).

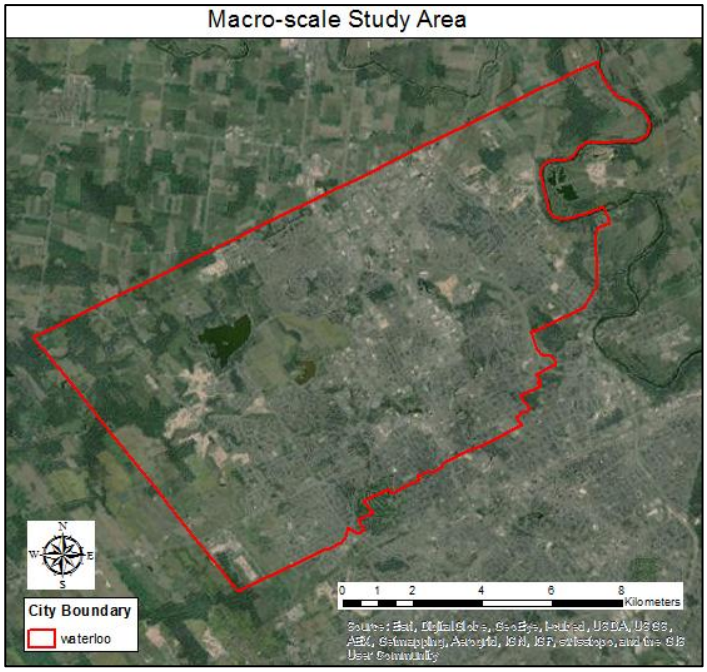

Figure 3.4 - Study area for macro-scale analysis - City of Waterloo.

The City of Waterloo region has a humid continental climate, with warm summers and no dry season (Vector Magic, Inc., n.d.). The temperature typically varies from -10 ℃ to 26 ℃ over the course of a year. The sky is usually cloudiest in the winter and clearest in the summer. Wind speeds of this area vary from 0 m/s to 8 m/s, representing a calm to moderate breeze, respectively (Vector Magic, Inc., n.d.). The wind speed has a similar seasonal pattern to temperature and cloud cover in the city throughout the year. The highest average wind speed occurs in winter, whereas the lowest average is in

summer. Precipitation in Waterloo is usually in the form of light snow, light rain, and moderate rain over the entire year. During the warm season (May 28 - September 20), there is a greater chance that precipitation will be observed than in the cold season (December 3 - March 10). When precipitation occurs, it is most often in the form of light rain, moderate rain, thunderstorms, and heavy rain during the warm season, while it is most often in the form of light snow during the cold season (Vector Magic, Inc., n.d.). Snowfall in Waterloo usually starts in the middle of October, reaching the highest rates around January and February, and ending in April (Vector Magic, Inc., n.d.). As a result of its long duration, snow cover may be a challenging issue for maintaining solar panels in this area during wintertime.

3.3. Data

Datasets used in the present study are summarized in Table 3.1. These include LiDAR point cloud and DEM data for solar radiation estimation, high-resolution aerial imagery for visual comprehension, and Waterloo zoning data for land cover reference. Other datasets include road networks, transmission network, ESA, soil types, pit and quarry sites, and water sources as criteria for input into the multi-criteria analysis (MCA) for solar panel site selection.

The 1064 nm LiDAR 3-dimentional point cloud data was collected on March 11th, 2006 by Optech Incorporated. This dataset was collected with an Airborne Laser Terrain Mapper (ALTM) instrument based on a specified flightline altitude, aircraft speed, scan angle, scan frequency and pulse repetition frequency (PRF). The point cloud has a high point density of 1.5 point/m^2. Since LiDAR data are not widely available for the City of Waterloo, DEM data with 10 m spatial resolution obtained from the Grand River Conservation Authority (GRCA) (Appendix A) were utilized for solar radiation calculations at the macro-scale or regional level. In order to identify buildings and other land features, a high-resolution 10 cm orthoimage was used, collected by Northways under contract from the Regional Municipality of Waterloo in 2006. Land use and land cover information was derived from Waterloo zoning by-law data from 2011, which includes information about land use regulations and restrictions, the primary use, location,

height and bulk of buildings and infrastructure, and the occupancy of lots within the City of Waterloo (Restricted Area Zoning By-Law for the City of Waterloo, 2012). Ontario road networks from 2010, transmission network and water source data from 2012 were obtained from DMTI Spatial Inc. Environmentally Sensitive Areas (ESA) data were considered for environmental protection criteria and obtained from the City of Waterloo Municipal Data. To include a proxy of dust risk in the analysis, data about soil type and pit/quarry site were acquired from the Ontario Ministry of Agriculture, Food and Rural Affairs and the Ministry of Natural Resources (MNR).

Table 3.1- Summary of datasets used in the research study

	Data	Date Production	Scale	Source	Data Type
1	LiDAR	2006	1.5 pt/m^2	MAD Helpdesk	LAS
2	DEM	2010	10 m	GRCA	Raster
3	High-resolution orthoimage	2006	10 cm	Regional Municipality of Waterloo	Raster
4	City boundary	2011	N/A	The City of Waterloo Municipal Data	Feature class
5	Waterloo zoning	2011	N/A	The City of Waterloo Municipal Data	Feature class
6	Road networks	2010	N/A	DMTI Spatial	Feature class
7	Transmission network	2012	N/A	DMTI Spatial	Feature class
8	Environmentally sensitive areas	2008	N/A	The City of Waterloo Municipal Data	Feature class
9	Soil Type	2007	N/A	Ontario Ministry of Agriculture, Food and Rural Affairs	Feature class
10	Pit and quarry site	2010	N/A	MNR	Feature class
11	Water source	2012	N/A	DMTI Spatial	Feature class

Chapter 4. Methodology

To develop a process for solar panel placement site selection, different methods were applied for micro- and macro-scale levels of the study. The micro-scale area analysis was carried out for building rooftops only, while the macro-scale analysis focused on ground-mounted solar panel installations on vacant lands or lands earmarked for retrofitting. First, data preprocessing, such as solar radiation estimation and re-projecting, was conducted. Monthly- and yearly-accumulated solar radiation maps were generated to assist site selection at both micro and macro scales. A multicriteria analysis (MCA) approach was adopted at the macro-scale level. The present study also administered a questionnaire survey to collect information about current solar panel installation practices in solar power companies in Ontario. Details about the adopted methodology for this thesis are further described in the following sections.

4.1. Data Processing

Incoming solar radiation amounts, considering shadow effects, provide the main indicator of solar energy supply or inputs in the present study. The output products at both micro- and macro-scales of the study were monthly- and yearly-accumulated radiation maps that could be subsequently used for site selection for solar panel installation. At the macro-scale level, technical, economical, and environmental constraints were considered in the analysis. However, before applying the MCA methodology, it was necessary to select, process, and scale the criteria datasets in order to compare them using a GIS.

4.1.1. Solar Radiation Maps

The spatial variability of solar radiation at the regional or landscape scale is mainly determined by the topography characteristics of the surface (Gastli et al., 2010). In contrast at the building rooftop scale, the spatial variability is primarily due to surface objects and building structure. In both cases, solar radiation analysis tools in ArcGIS software enable solar radiation in a geographic area to be mapped for specific time periods using high- resolution elevation data (Gastli et al., 2010). The generated solar map takes into account alterations in the azimuth and position of the sun, as well as

shading effects due to surface objects or topography in the input elevation data (Chaves and Bahill, 2010). In general, the path of incoming solar radiation is modified while travelling through the atmosphere and further affected by the Earth's surface, classified as scattered (reflected), diffuse and/or direct radiation (e.g., Gastli et al., 2010; Sen, 2008; Suri and Hofierka, 2004). The sum of these three components forms the global radiation balance (e.g., Gastli et al., 2010; Suri and Hofierka, 2004). Specifically, direct radiation is the principal component of total radiation, whereas reflected radiation is the smallest component (e.g., Suri and Hofierka, 2004). The solar radiation analyst tools in ArcGIS exclude reflected radiation from the total radiation calculation (Gastli et al., 2010). Therefore, the total radiation is obtained as the sum of the direct and diffuse radiation.

For the micro-scale analysis, elevation information from LiDAR point clouds were used to model irradiance. The first-return LiDAR points were interpolated with a spatial resolution of 0.5 meters based on linear interpolation using the ENVI software package. Compared to the bare-earth surface elevation, which is typically represented by digital terrain models (DTMs), the elevation of the first-return data includes features above the bare earth. Therefore, using first-return data to derive incoming solar radiation information will include effects of land surface features. For the macro-scale area, considering the availability of LiDAR points and data processing efficiency, a 10 m resolution DEM was used for the irradiance calculation. This DEM accounts for the elevation of the bare earth. Both annual and monthly global solar radiation was calculated for the areas of interest in this study.

The radiation model in ArcGIS calculates "insolation across a landscape or for specific locations, based on methods from the hemispherical viewshed algorithm developed by Rich et al. (Rich 1990, Rich et al. 1994) and further developed by Fu and Rich (2000, 2002)" (ESRI, 2012a, par. 1). Specifically, the model first calculates an upward-looking hemispherical viewshed based on topography from an input DEM. The viewshed represents the entire sky that is visible and/or obstructed by surrounding surface features and topography when looking up in all direction from a particular location. Figure 4.1 (B) is an upward-looking hemispherical photograph. It provides a view of the visible sky (depicted in white in Figure 4.1 (A)) and the sky directions obstructed by the

surrounding surface features and topography (depicted in grey in Figure 4.1 (A)). The viewshed calculation is implemented by "searching in a specified number of directions around a location of interest and determining the maximum angle of sky obstruction, or horizon angle" (ESRI, 2012b, par. 6). Interpolation of horizon angles is then undertaken for all other unsearched directions. After this, horizon angles are converted to a hemispherical coordinate system.

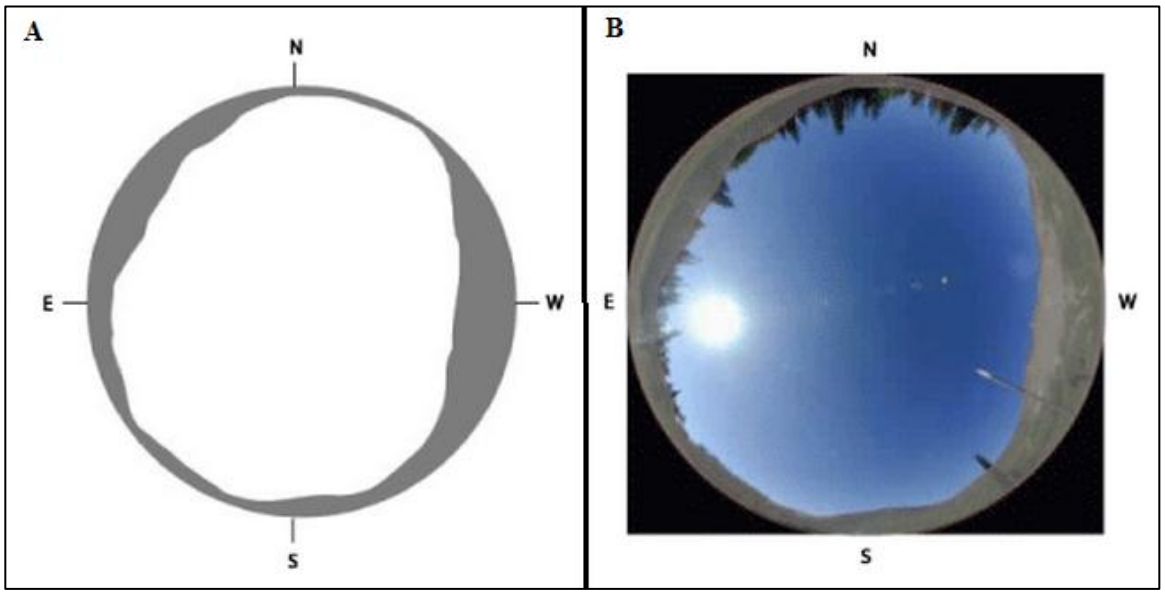

Figure 4.1 - A: Viewshed map with white for the view of visible sky and grey for the obstructed sky direction; **B:** An upward-looking hemispherical photograph (ESRI, 2012b)

A sun map representing solar positions (or sun tracks) for particular time periods, and a sky map showing a hemispherical view of the entire sky are then calculated. The sun map is composed of discrete sun map sectors defined by the sun's position at particular intervals during specific time periods. Figure 4.2 (A) shows a sun map for 39 ºN latitude calculated from the winter solstice (December 21) to summer solstice (June 21). Each sun sector (colored box) represents the sun's position with 0.5-hour intervals through the day and monthly intervals through the year (Fu and Rich, 2000). For each sun sector, the associated time duration, the azimuth and zenith at its centroid are calculated.

As a result of atmospheric scattering, diffuse radiation originates from all sky directions. To calculate diffuse radiation for a particular location, a sky map is created with a series of sky sectors defined by zenith and azimuth angles to show a hemispherical

view of the entire sky (ESRI, 2012b). Figure 4.2 (B) shows a sky map with sky sectors defined by 16 zenith divisions and 16 azimuth divisions. Each color represents a sky sector, from which diffuse radiation originates (Fu and Rich, 2000).

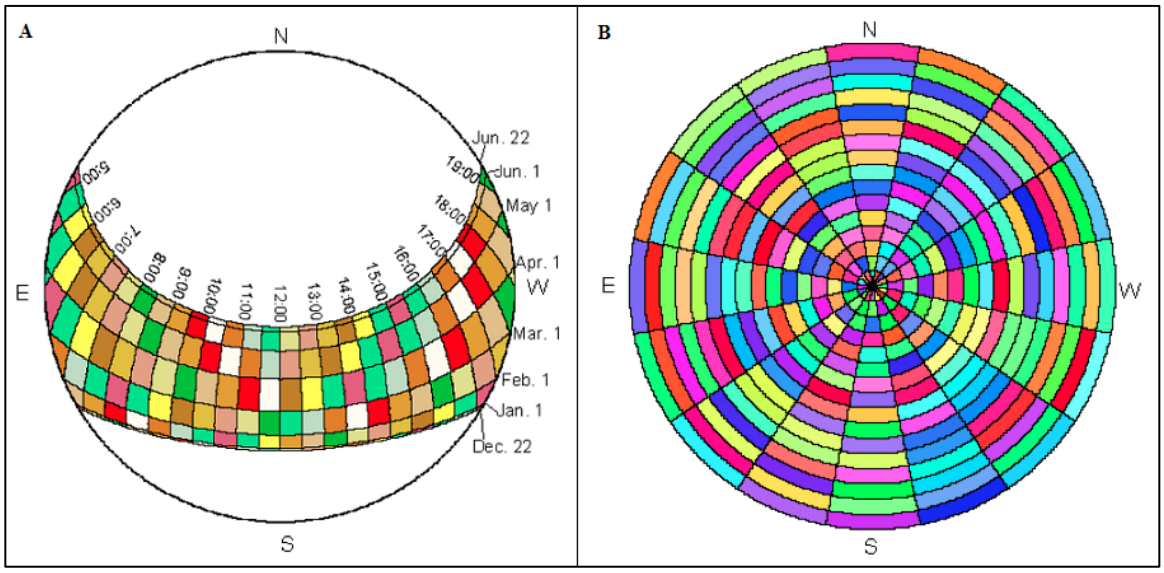

Figure 4.2 - A: Sun map for Winter Solstice to Summer Solstice**; B:** A skymap with sky sectors defined by 16 zenith divisions and 16 azimuth divisions (Fu and Rich, 2000).

This model calculates global solar radiation (R_{Glo}) by adding direct (R_{dir}) and diffuse (R_{dif}) radiation. The direct radiation and diffuse radiation are then calculated by overlaying the viewshed on the direct sun maps and the sky maps respectively for each sky direction. This process is iterated for every location of interest to produce the final insolation map. The steps for using a DEM data to calculate solar radiation using ArcGIS are summarized in the following workflow (Figure 4.3).

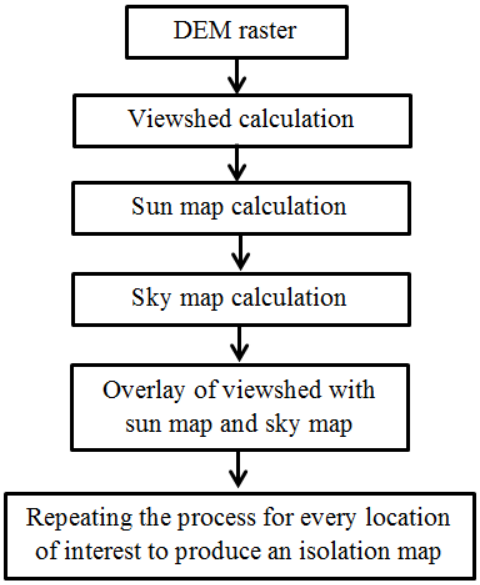

Figure 4.3 - Steps of solar radiation calculation on a DEM in ArcGIS (Gastli and Charabi, 2010a)

The total direct solar radiation for a given location can be obtained by the summation of the direct insolation (I_{dir}) from all sun map sectors. This radiation can be mathematically calculated by:

$$R_{dir} = \sum I_{dir} = \sum S_{const} * \beta^{m(\theta)} * T_{\theta,\alpha} * Gap_{\theta,\alpha} * \cos(I_{\theta,\alpha}) \quad (1)$$

where S_{const} is the solar flux outside the atmosphere at the mean earth-sun distance known as the solar constant. Its value used in the analysis is 1,367 W/m^2, which is consistent with the World Radiation Center solar constant. β is the average transmissivity of the atmosphere over all wavelengths for the shortest path. m(θ) is the relative optical path length (see equation (2)). $T_{\theta,\alpha}$ is the time duration represented by the sky sector and equal to the day interval multiplied by the hour interval, while for near the horizon sector, the duration is obtained using spherical geometry. $Gap_{\theta,\alpha}$ is the gap fraction for the sun map sector, and $I_{\theta,\alpha}$ is the angle of incidence between the centroid of the sky sector and axis normal to the surface (see equation (3)) (ESRI, 2012a). When the solar zenith angle θ is less than 80^o, the relative optical path length m(θ) can be determined by:

$$m(\theta) = EXP(-0.000118 * H - 1.638*10\text{-}9 * H^2) / \cos(\theta) \quad (2)$$

where H is the elevation above sea level in meters. The effect of surface orientation is considered by multiplying by the cosine of the angle of incidence (ESRI, 2012a). The angle of incidence ($I_{\theta,\alpha}$) is calculated using the following equation:

$$I_{\theta,\alpha} = \text{acos}(\cos(\theta) * \cos(G_z) + \sin(\theta) * \sin(G_z) * \cos(\alpha - G_a)) \quad (3)$$

where G_z is the surface zenith angle and G_a is the surface azimuth angle.

Total diffuse solar radiation for the location (R_{dif}) is calculated as the sum of the diffuse solar radiation (I_{dif}), which is integrated over the time interval, and corrected by the gap fraction and angle of incidence using the following equation:

$$R_{dif} = \sum I_{dif} = R_{glb} * P_{dif} * T_{dur} * SkyGap_{\theta,\alpha} * W_{\theta,\alpha} * \cos(I_{\theta,\alpha}) \quad (4)$$

where R_{glb} is the global normal radiation (see equation 6 below), P_{dif} is the proportion of global normal radiation flux that is diffused. Typically, it is approximately 0.2 for very clear sky conditions, 0.3 for generally clear sky conditions, and 0.7 for very cloudy sky conditions (Fu and Rich, 2000). T_{dur} is the time interval for analysis. $SkyGap_{\theta,\alpha}$ is the gap fraction (proportion of visible sky) for the sky sector, and $W_{\theta,\alpha}$ is the proportion of diffuse radiation originating in a given sky sector relative to all sectors (see equations 6 and 7 below). $I_{\theta,\alpha}$ is the angle of incidence between the centroid of the sky sector and the intercepting surface (equation (3)) (ESRI, 2012a). The global normal radiation (R_{glb}) can be achieved by adding the direct radiation from every sky sector without correction for angle of incidence, and then correcting for proportion of direct radiation (ESRI, 2012a). It can be obtained by:

$$R_{glb} = (S_{Const} \Sigma(\beta m(\theta))) / (1 - P_{dif}) \quad (5)$$

For the uniform sky diffuse model, $W_{\theta,\alpha}$ is calculated as follows:

$$W_{\theta,\alpha} = (\cos\theta_2 - \cos\theta_1) / D_{azi} \quad (6)$$

where θ_1 and θ_2 are the bounding zenith angles of the sky sector, and D_{azi} is the number of azimuthal divisions in the sky map. For the standard overcast sky model, $W_{\theta,\alpha}$ is calculated as follows:

$$W_{\theta,\alpha} = (2\cos\theta_2 + \cos 2\theta_2 - 2\cos\theta_1 - \cos 2\theta_1) / 4 * D_{azi} \quad (7)$$

Solar radiation maps of the present study under clear-sky and overcast conditions were generated from the first-return LiDAR data (micro-scale) or georeferenced DEM (macro-scale) specifying Waterloo's latitude of 43 º by using the solar radiation calculation tool. Since the amount of solar radiance is an accumulated output, time interval in the calculation needs to be determined. Therefore, solar radiation estimates with seven-day and one-day interval settings, as well as one-hour and half-hour settings were compared for sensitivity analysis. The test results did not show apparent differences. In this case, by maintaining a reasonable processing time, time interval for the monthly irradiance was set hourly per week. The yearly calculation was set with time interval of hourly per month. The year setting for time configuration in this model is used to determine the leap year. It does not have any other influence on the solar radiation estimation (ESRI, 2011). In this study, 2011 was set as the input year, and the yearly accumulated solar radiation maps were generated for 365 days.

Furthermore, sunlight has high transmissivity through the atmosphere and only a small proportion is diffused in clear-sky conditions. According to Fu and Rich (2000), the transmissivity parameter has an inverse relationship with the diffuse proportion. Before defining the values of these two parameters, an experiment using EV buildings as an example to test the impact of these two parameters on the output radiation was conducted. According to the calculated one-year solar radiation by different combinations of these two parameters (in Appendix B), the maximum and minimum radiation shows a significant pattern. For example, when the diffuse proportion stays the same but the transmissivity value increases, the estimated radiation increases, and vice versa. These combinations reflect radiation changes under different weather conditions. According to ESRI (2011), typical observed values of diffuse proportion and transmissivity for a clear sky are 0.3 and 0.5, respectively. For very clear sky conditions, the diffuse proportion is 0.2 and transmissivity is 0.6 or 0.7 (ESRI, 2011). The present study used a transmissivity of 0.7 and diffused proportion of 0.3 in the calculation for clear sky conditions. In contrast, overcast conditions have low transmissivity and high diffused rates. A transmissivity of 0.3 and diffused proportion of 0.7 were adopted for overcast conditions. Since solar radiation varies under different types of weather conditions, the clear-sky radiation was then compared with the radiation output under overcast conditions.

4.1.2. Other Datasets

In addition to the solar radiation maps, other datasets were clipped to either the UW campus or the City of Waterloo boundaries, and re-projected to a Universal Transverse Mercator (UTM) coordinate system. Since in the macro-scale analysis, information about land use accessibility could not be obtained directly, land accessibility was based on the Waterloo zoning by-law data from the City of Waterloo Municipal Data was conducted. The Waterloo zoning by-law data contains information about potential/current land use types for each predefined zone. It also shows usage regulations and restrictions. Zones unrestricted by buildings were selected as potentially accessible lands, including green zones and agricultural lands. Suburban areas were also considered to be accessible. Furthermore, slope and aspect information used in the present study was obtained based on a DEM processed using ArcGIS software. All the criteria layers used in the macro-scale analysis were generated with a 10-m spatial resolution.

4.2. Micro-scale Analysis

In the present study, micro-scale installation refers to solar panel placement on building rooftops. Essentially, factors taken into account should ensure efficacy of energy generation with a long-term viability. First, shadow effects caused by surrounding trees and objects on the rooftop have a direct impact on the output of solar panel. Second, orientation and tilt of solar panels in different seasons and at various time periods within a day can also influence solar power generation. This section focuses on how the micro-scale site selection was carried out, while considering ambient environment shadow effects.

As mentioned in Section 4.1.1, the solar radiation model involves considering of shading effects caused by buildings, slope, and other surface objects. According to the monthly- and yearly-accumulated solar radiation maps, areas impacted by shadow show significantly different incoming radiation levels compared to those fully exposed to sunlight. Therefore, histograms of solar radiation values of each building of interest were used to differentiate and categorize the shaded and unshaded areas. According to an example of histogram of a rooftop solar radiation map shown in Figure 4.4, pixels

aggregated on the right side of the solar radiation value axis are identified as unshaded areas, whereas pixels with small solar radiation values shown on the left side of the radiation axis are completely shaded areas. Since areas obscured by shadows are time specific, their accumulated solar radiation amounts are various, which leads to a valley as shown in Figure 4.4. In this study, a low valley closed to the peak of shaded pixels was used as a threshold (T) for separating the shaded and unshaded areas.

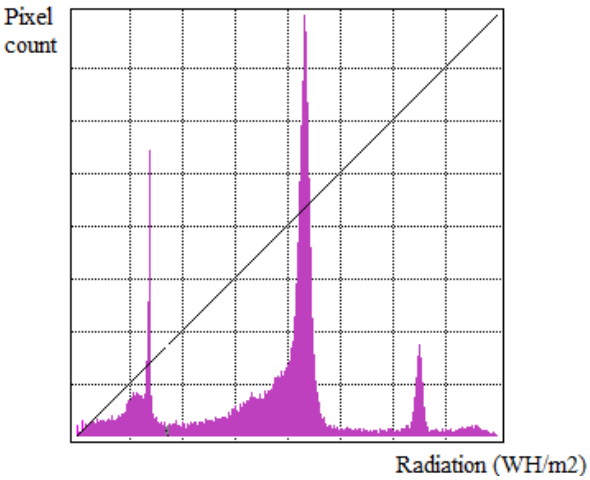

Figure 4.4 - An example of a histogram of a roof solar radiation map

After obtaining the monthly shaded/unshaded maps, a shadow mask based on the probability of shadow present over a year was then created. The probability of shadow presenting (P) throughout one year was calculated as follows:

$$P = (T_1 + T_2 + \ldots + T_{12}) / 12 \times 100\% \quad (8)$$

where T_i is the radiation threshold for each month indicating shadow presence and absence. This results in a total of 12 output (i.e., $\frac{1}{12}, \frac{2}{12}, \ldots, \frac{12}{12}$), which is difficult to consider in decision-making for site selection. Therefore, the shadow presenting probabilities were divided into four classes. Areas with 0% to 25% probabilities were considered as non-shaded areas, 25% to 50% were seldom shaded areas, 50% to 75% were almost shaded areas, and 75% to 100% were completely shaded areas. According to the shadow mask and the radiation maps, small discrete areas were excluded, whereas areas with large or sufficient space for solar panel placement were highlighted and

considered as potential sites. Areas that fit one industry-standard c-Si PV module[1] were considered to have sufficient space available for installing solar panels. It was then possible to calculate the total electricity output, if the electricity conversion factor was known.

4.3. Macro-scale Analysis

Apart from rooftop installations, solar panels can also be mounted on the ground for commercial, residential, or industrial applications. For the proposed ground-mounted panel installations in this thesis (i.e., macro-scale level analysis), a range of criteria related to study area characteristics were considered. An MCA approach was adopted due to the numerous criteria involved in the decision-making process. As shown in Figure 4.5, the first step of the analysis was to determine which factors should be included. Considering that each factor has different levels of importance or degrees of impact on the site selection process, each factor was given different weights based on its importance to the study area. The Analytical Hierarchy Process (AHP) was employed for assigning weights due to the numerous factors involved. The close adjacency of both sites to residential areas may raise several concerns. For example, the aesthetics and reflectivity of sunlight from the PV farms could be problematic to the surrounding residential community. For PV farms, positioning near high population density areas may incur vandalism. Therefore, after the MCA, a buffering procedure of residential areas was implemented to exclude immediate boundary areas. Areas were then ranked by their scores, ranging from 0 to around 0.8. The higher score the more suitable. This study considered areas with scores of greater than 0.6 as priority sites for solar panel installation, since most criteria were considered by those areas. In order to select optimal sites for large-scale solar PV installation, small sized selected sites with less than 1 acre[2] were filtered out. Finally, on-site inspection or ground truth data collection were performed to evaluate the final site selection and to view conditions on the ground.

[1] According to IRENA (2012), c-Si module size ranges from 1.4 m^2 to 2.5 m^2. This study used the minimum size 1.4 m^2 as a minimum area that is required for solar panel installation.
[2] 1 acre was adopted as the smallest dimension of a PV power station in this study.

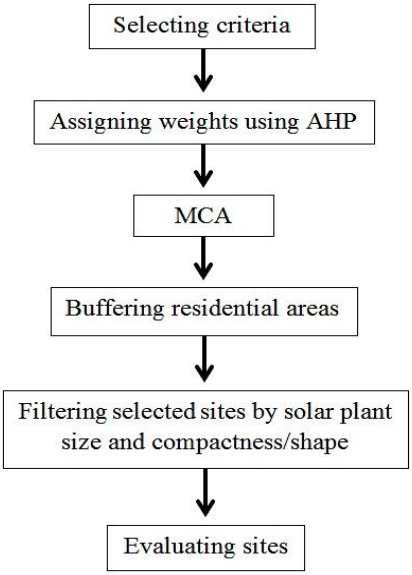

Figure 4.5 - Analytical procedure of the macro-scale analysis

4.3.1. Multicriteria Analysis

Although residential areas have mostly concentrated on rooftop solar panel installations, due to the increasing demands for renewable energy, ground-mounted solar panels on nearby vacant lands have become an additional source of capturing solar energy. Many regions have begun to implement so-called PV solar farms or solar power plants in their regions based on their potential for high energy capacity and returns. In comparison to micro-scale roof installations, the macro-scale ground mounting installation requires consideration of more factors in the site selection process, including environmental impacts and protection regulations. In this study, the main objective of the macro-scale site selection is to apply MCA to determine potential sites of solar installation within the City of Waterloo.

The analytical hierarchy process (AHP) method was adopted as a multicriteria decision-making tool in this study. The AHP is a robust structured approach dealing with complex decisions (Gastli and Charabi, 2010b), with ability to mix qualitative and quantitative criteria in the same decision framework (Pohekar and Ramachandran, 2004). The AHP method builds on a pair-wise comparison model for determining the weight of each criterion (Wang et al., 2009). It was proposed primarily by Saaty (Saaty, 1980). As

shown in Figure 4.6, the nature of the process is the decomposition of a complex problem into a hierarchy with the goal at the top of the hierarchy. Criteria and sub-criteria are at levels and sub-levels of the hierarchy. Criteria considered in the present study were grouped into three categories: (a) generation efficiency, (b) economic, and (c) environmental factors (Figure 4.7), which sometimes interact with each other. Among the criteria, only generation efficiency and economic factors were compared and analyzed in the AHP.

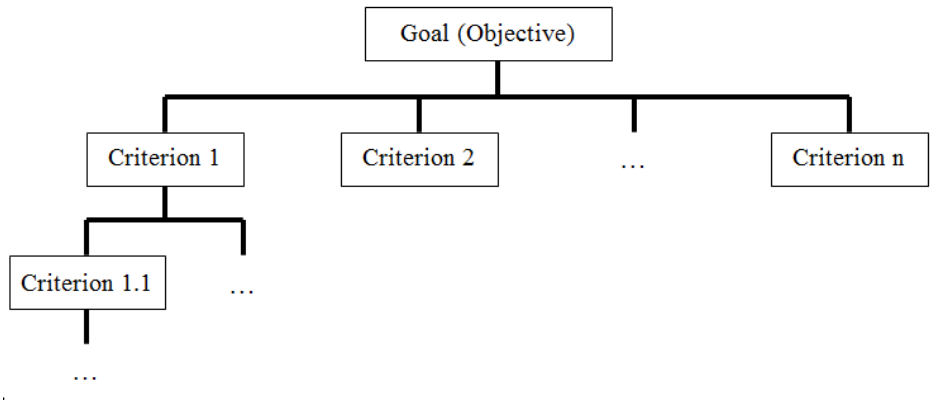

Figure 4.6 - Schematic diagram of analytical hierarchy process (AHP)

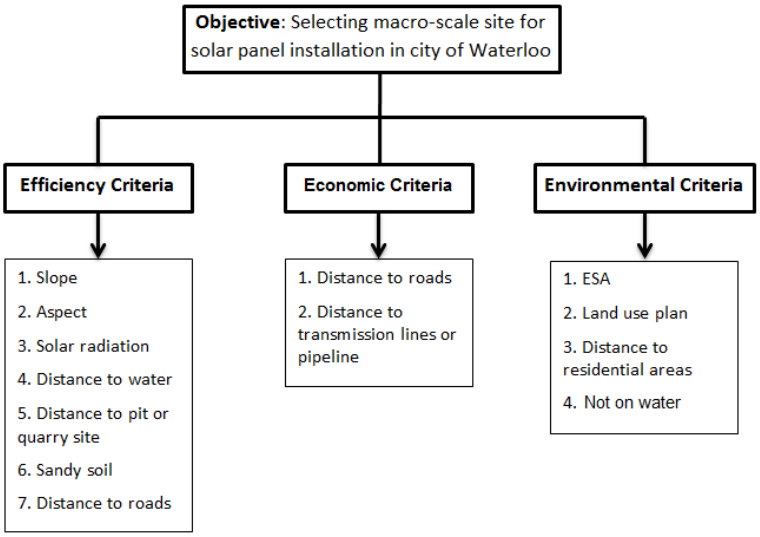

Figure 4.7 - Hierarchy structure of multiple criteria used in the multicriteria analysis

For energy generation efficiency, incoming solar radiation is the most important consideration. Shadow effects due to aspect and slope were also taken into account. Since

PV performance can be affected by the increasing temperature of PV cells and dust cover, accessibility to water resources for cooling and cleaning was considered but with less relative importance. In addition, PV panel performance can be influenced by dust risk from adjacent pit/quarry sites or roads. Distance to road network was determined by considering the road density of the city. Areas covered by sandy soil were avoided in the site selection process for reducing dust risk.

Economic factors were considered in the site selection process. For example, areas should be accessible to roads for the ease of construction. In addition, PV farm should be constructed close to electricity transmission lines to reduce energy loss and transmission costs. In this study, proximity to transmission lines was deemed to be more important than distance to road networks.

From an environmental perspective, solar panels should avoid environmentally sensitive areas (ESA) and water bodies. Solar panels should also be installed in locations that are difficult to be accessed by residents or passersby to decrease the probability of vandalism or deliberate damage. Overall, eleven evaluation criteria were incorporated in the site selection process, which collectively addressed energy, economic, ecological, and land use concerns. Each criterion is described in Table 4.1.

Table 4.1- Criteria used in the MCA with corresponding standards/restrictions

ID	Criterion	Standards and restrictions
C1	Slope	Slope < some slope limit (< 4%)
C2	Aspect	Southeast to southwest facing orientation only
C3	Solar radiation	The higher incoming solar radiation the better (>= 1.15 $MWh/m^2/yr$)
C4	Water source	Not too far to water sources (=< 200 m) but not water bodies
C5	Road networks	Farther away from certain distance of major roads (>= 10 m)
C6	Transmission lines	Within certain distance of transmission lines (=< 1 km)
C7	ESA	Not on ESA
C8	Pit & quarry site	Within certain distance of pit and quarry site (>= 50 m)
C9	Sand content	No more than 50% content
C10	Land suitability	Not on reserved or in-use areas
C11	Residential area	Not adjacent to residential areas (>= 100 m)

To meet the criteria shown in Table 4.1 above, Boolean and fuzzy set membership functions were applied. Boolean function reclassifies input data into 0 or 1 with Boolean logic (False or True). Fuzzy membership functions transform input data to a 0 to 1 scale based on the possibility of being a member of a specified set (ESRI, 2012c). More specifically, input values that are definitely a member of the specified set are assigned with 1, while values that are definitely not a member of the specified set are assigned with 0 (ESRI, 2012c). The entire range of possibilities between 0 and 1 are assigned to some level of possible membership - the larger the number, the greater the possibility (ESRI, 2012c). For example, it was desirable for a solar panel installation site to be located in close proximity to water source yet not located directly on top of water. In other words, distance to water source should be less than a minimum set distance, while distances greater than a minimum set distance are completely unsuitable. Since a potential site should not be located directly on a water body, a distance equal to 0 is considered to be unsuitable. The schematic diagram of this type of fuzzy linear membership function is shown in Figure 4.8. Models of all criteria built and implemented in ArcGIS Model Builder are shown in Appendix C.

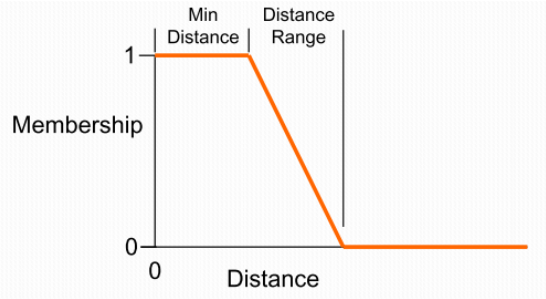

Figure 4.8 - An example of fuzzy membership function – a negative slope linear transformation

After determining the criteria, elements at a given level are compared in pairs to assess their relative importance to each other (Aragonés-Beltrán, 2010; Saaty, 1980; Kahraman and Kaya, 2010). The relative importance can be scaled as seen in Figure 4.9. Weights that emphasize the relative importance of one criterion to another are often determined by stakeholders, research specialists, managers, or interest groups to improve the decision-making process (Janke, 2010). This study determined the weights based on previous studies and fact of the study area. To elicit pair-wise comparisons performed at

a given level, a reciprocal matrix A (where the number of rows and columns is defined by the number of criteria), is created by putting the result of the pair-wise comparison of element i with element j into the position α_{ji} as shown below:

$$A = \begin{bmatrix} a_{11} & a_{12} & \dots & a_{1i} \\ a_{21} & a_{22} & \dots & a_{2i} \\ \vdots & \vdots & \ddots & \vdots \\ \alpha_{j1} & a_{j2} & \dots & a_{ji} \end{bmatrix} \quad (9)$$

Subsequently, a priority vector (also eigenvector) was computed to establish weights (w_j), (i.e., the normalized principal priorities). The procedure consists of two steps: (1) to raise the matrix to a power; and (2) to sum and normalize the row. This process must be iterated until the eigenvector solution does not change from the previous iteration. These weights are a quantitative measure of the consistency of the value judgments between pairs of factors (Carrion et al., 2007; Saaty, 2003).

1/9	1/7	1/5	1/3	1	3	5	7	9
Extremely	Very	Strongly	Moderately	Equal	Moderately	Strongly	Very	Extremely

Less Important ⟶ More Important

Figure 4.9 - Relative importance of one criterion over another in criteria pairwise comparison

After obtaining the eigenvector, it is multiplied with the weight coefficient of the element at a higher level (that was used as a criterion for pair wise comparisons). The procedure is repeated upward for each level, until the top of the hierarchy is reached. The overall weight coefficient, with respect to the goal for each decision alternative is then obtained. The alternative with the highest weight coefficient value should be taken as the best alternative (Pohekar and Ramachandran, 2004).

In this study, as shown in Figure 4.7, three types of factors were taken into account. Since the environmental criteria were factors that must be considered due to environmental regulations, they were excluded in the criteria comparison. In other words, ESA and water bodies were strictly avoided. In addition, land use was considered in that potential sites were not to be situated directly next to residential housing. Therefore, only criteria of efficiency and economy were compared and assigned weights. In the present study, efficiency is considered to be moderately more important than economy (e.g.,

Aragonés-Beltrán, 2010; Chen et al., 2010). Among the efficiency and economic factors, solar radiation availability, transmission lines proximity, and shadow effect reduction are considered to be the most important. By altering the values of factor weights but retaining their relative importance, the sensitivity of the alternatives' ranking with respect to changes in efficiency and economic variables was evaluated. In particular, a criterion in the reciprocal matrix was selected as the candidate to be examined, and then assigned a scale of weights showing different levels of importance. This study selected major criteria into the sensitivity analysis. Slope was compared to aspect or solar radiation potential[1] with a weight ranging from 1/6 to 1/2, and distance to transmission lines was compared to distance to roads from 2 to 6. For the higher level, efficiency was compared to economic criteria by assigning weights from 2 to 4. The resultant maps were then analyzed based on locations and sizes of the highly ranked sites.

Since solar availability directly determines energy generation potential, and aspect determines the amount of irradiance received by a solar panel surface. Therefore, in this study, amount of irradiance received and aspect were considered to be the most important criteria with equal weights. Flat topography is considered to be less important, since the receiving solar radiation flux is mainly affected by solar panel tilt. Dust risk was considered as a minor factor affecting PV system performance, since dust on solar panels can be washed off by rainfall. Therefore, dust risk factors (i.e., distance to quarry site and not on sandy soil) were weighted equally but less than slope, aspect, and solar radiation. Proximity to water sources for panel cleaning was considered to be the least important factor impacting efficiency. From an economic perspective, proximity to the existing grid was deemed to be more important than proximity to the road networks (Charabi and Gastli, 2011). The matrices and calculated weights are shown from Table 4.2 to Table 4.4.

[1] In this study, topographic aspect and solar radiation potential were treated equally.

Table 4.2 – High level criteria ranking

Higher level	Efficiency	Economic	**Weight (Eigenvector)**
Efficiency	1	3	75%
Economic		1	25%

Table 4.3 - First level criteria ranking (economic constraints)

Economic	Distance to Roads	Distance to transmission lines	**Weight (Eigenvector)**	**Final weight**
Distance to Roads	1	1/6	14.29%	3.6%
Distance to transmission lines		1	85.71%	21.4%

Table 4.4 - First level criteria ranking (factors of efficiency)

Efficiency	Slope	Aspect	Solar radiation	Distance to water	Distance to quarry site	Sandy soil	**Weight (Eigen-vector)**	**Final weight**
Slope	1	1/2	1/2	5	3	3	18.46%	13.8%
Aspect		1	1	6	4	4	29.76%	22.3%
Solar radiation			1	9	5	5	33.99%	25.5%
Distance to water				1	1/2	1/2	3.85%	2.9%
Distance to quarry site					1	1	6.97%	5.2%
Sandy soil						1	6.97%	5.2%

4.3.2. On-site Feasibility Assessment

Since the datasets employed in this study may be over-generalized or not be up to date, it was necessary to perform an on-site assessment or verification of identified sites from the MCA analysis. Consequently, selected potential sites were evaluated by site visit to collect ground truth observations, including land use changes and topography. For example, residential areas may have expanded rapidly in recent years and encroached on selected sites. The location of transmission lines and roads were also verified during the on-site assessment.

4.4. Survey

For the purpose of investigating how these companies determined an optimal site for solar panel installation, as well as gauging maintenance practices after installation, a survey was designed with a focus on both ground-mounted and roof-mounted solar panel installation site selection. Participants in the survey could be technicians or employers with knowledge of solar panel installation site selection. These companies were considered to be qualified by providing solar panel installation to their customer, or else having specialists with installation knowledge. Twenty Ontario solar companies were selected and invited to participate in the survey. Company selection was not restricted by company size, and companies included both panel manufacturers and installers.

The survey was implemented in the form of a questionnaire, and included 7 open questions, which are shown in Appendix D. At the beginning of the questionnaire, participants were asked to provide background information about their company. The following sections asked respondents questions regarding factors and data considered by the company when assessing potential sites for solar panel installation. Participants were asked to rank a list of factors based on their relative importance to the site selection process. The factors provided were efficiency of energy generation, economical/budget considerations, and environmental considerations. In addition, companies were asked about the challenges often encountered during the solar panel installation process. The surveyed companies were also asked to provide information about maintenance services provided after installation. Last, a question related to different factors considered in a grid-connected solar system and a stand-alone system was included at the end of the questionnaire.

During the survey implementation, invitations were first sent to twenty solar companies in Ontario via email. A reminder e-mail was distributed one week after the invitation. In the end, three companies responded to the survey by answering most of the questions (15% response rate). Analysis of survey responses included comparing types of customers that companies worked with, considerations and concerns involved in the installation site selection process, and the importance of such factors in project

implementation. In addition, challenges that the companies encountered when installing solar panels correctly were discussed. After obtaining findings from comparison of solar companies, factors considered or excluded in solar panel installation site selection by solar companies compared to this study were identified and discussed. When possible, survey results were used to better inform the thesis research and to tweak weighting criteria to further improve site selection results.

Chapter 5. Results and Analysis

5.1. Micro-scale Analysis

As mentioned in sections 3.2 and 4.2, five buildings on the UW campus were selected for the micro-scale level of analysis. First, monthly- and yearly-accumulated solar radiation maps of the building rooftops were generated to obtain spatial information about solar radiation availability. Second, standard deviation maps of solar radiation were calculated to show the temporal variation of solar radiation across a year. Last, shadow maps were produced from solar radiation maps to identify areas potentially affected by shadows from surrounding structures or obstructions.

Before the site suitability analysis was conducted, solar radiation estimates under clear-sky and overcast conditions were compared. Figure 5.1 shows an example of one-year accumulated solar radiation maps of EV buildings under two types of sky conditions with standardized and uniform legends. Areas exposed to the sun receive greater amounts of incoming solar radiation under clear-sky conditions than under the overcast scenario. Therefore, the maximum solar radiation of clear-sky conditions (about 1,300 KWh/m^2) is much greater over a year than under overcast conditions (about 1100 KWh/m^2). Since similar spatial patterns under both conditions were observed as shown in the two maps in Figure 5.1, this study used incoming solar radiation under clear-sky conditions for solar radiation spatial pattern analysis.

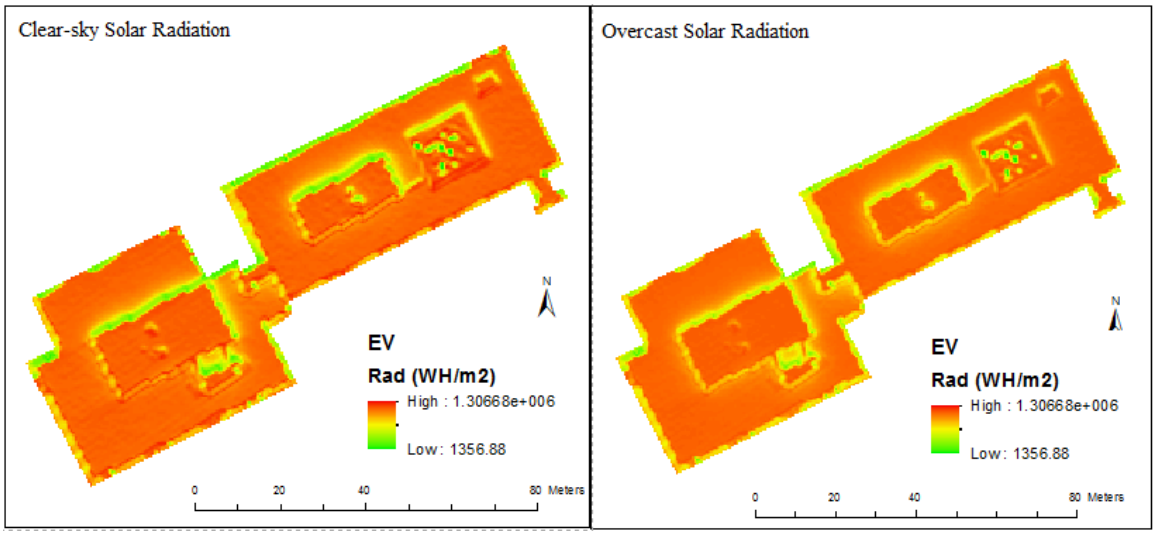

Figure 5.1 - Solar radiation map under clear-sky and overcast conditions

5.1.1. Physical Activities Complex

In Figure 5.2, monthly-accumulated solar radiation distribution maps of the PAC building rooftop throughout the year are shown with standardized and uniform legends. According to the maps, the seasonal variation of radiation values can be observed. January and December show the least amount of solar radiation received, while June and July received the greatest levels of solar radiation. Roof corners and edges that are completely shaded throughout the year were evident. In each monthly map, the southern, northern, eastern and main rooftops (labeled in Figure 5.6) receive more solar radiation than other rooftops. In order to explore the detailed spatial variation of solar radiation for each month, different legend ranges were adopted with red areas indicating the greatest amounts of solar radiation received, while green areas represent shadow areas with the least incoming solar radiation. Figure 5.3 shows the monthly maps with map legends displaying different ranges of radiation values. Maximum radiation values in each month show that the radiation values in October, November, December, January, February, and March are much lower than during the rest of the year.

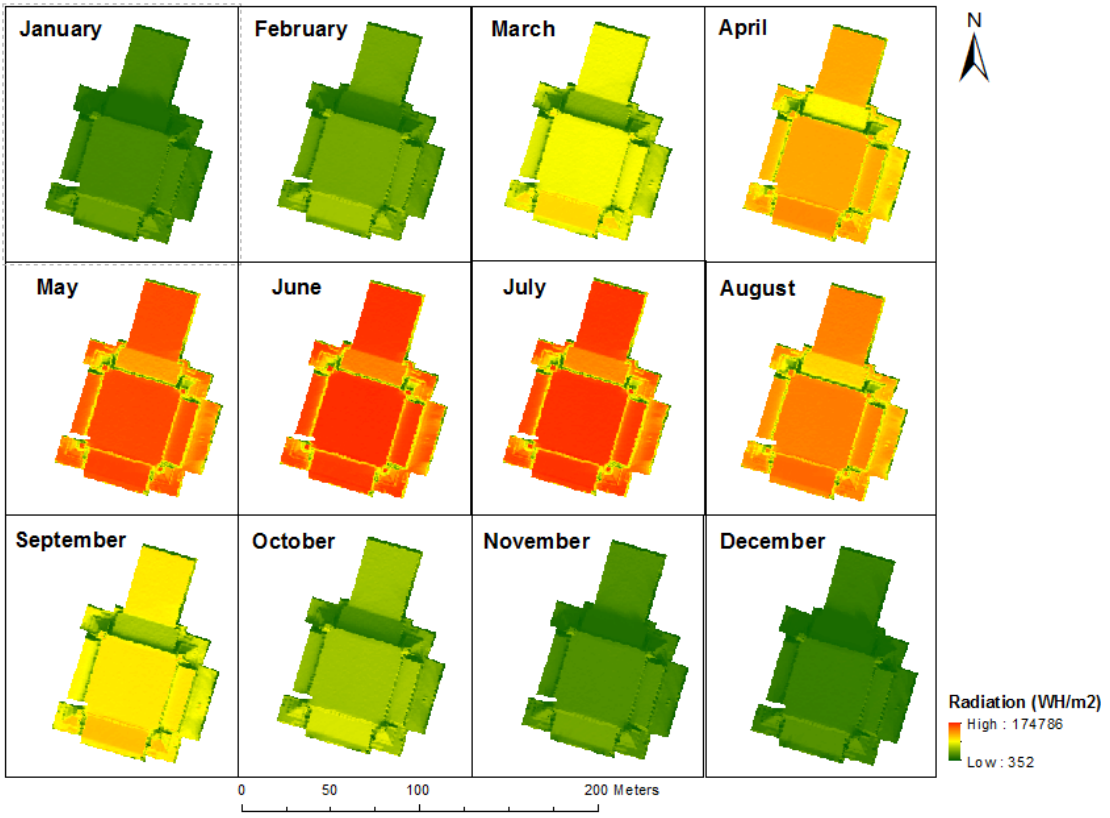

Figure 5.2 - Monthly solar radiation maps of the Physical Activities Complex (PAC) Building with standardized legends

In Figure 5.3, it is apparent that edges and corners of the rooftops receive less insolation than the roof center areas throughout the year. Comparing the lower eastern and western rooftops (labeled in Figure 5.6), it was noticeable that the eastern rooftop receives more solar radiation than the western, especially during the winter months. The PAC rooftops with higher elevation show greater insolation received than rooftops with lower elevation, since the taller roof shadows surrounding nearby areas, especially when the angle of incidence decreases. This pattern can be easily noticed from the northern lower rooftop, which is constantly shaded by the main rooftop. However, there is an exception for the lower rooftop of the southern side of the building (namely the southern rooftop), which has an approximately 10 ° slope with a south orientation. Due to the building's latitude, this rooftop is not blocked by the taller roof on the northern side (namely the main rooftop) and hence, not obscured by shadow effects. During summer months, the sun's rays reach the ground at a more perpendicular angle in the northern

hemisphere than in other seasons, and the insolation amount is higher overall. The main rooftop receives the greatest amount of insolation in June and July, while the southern rooftop tends to receive the greatest insolation, except in June and July due to the increased solar incidence angle in summer.

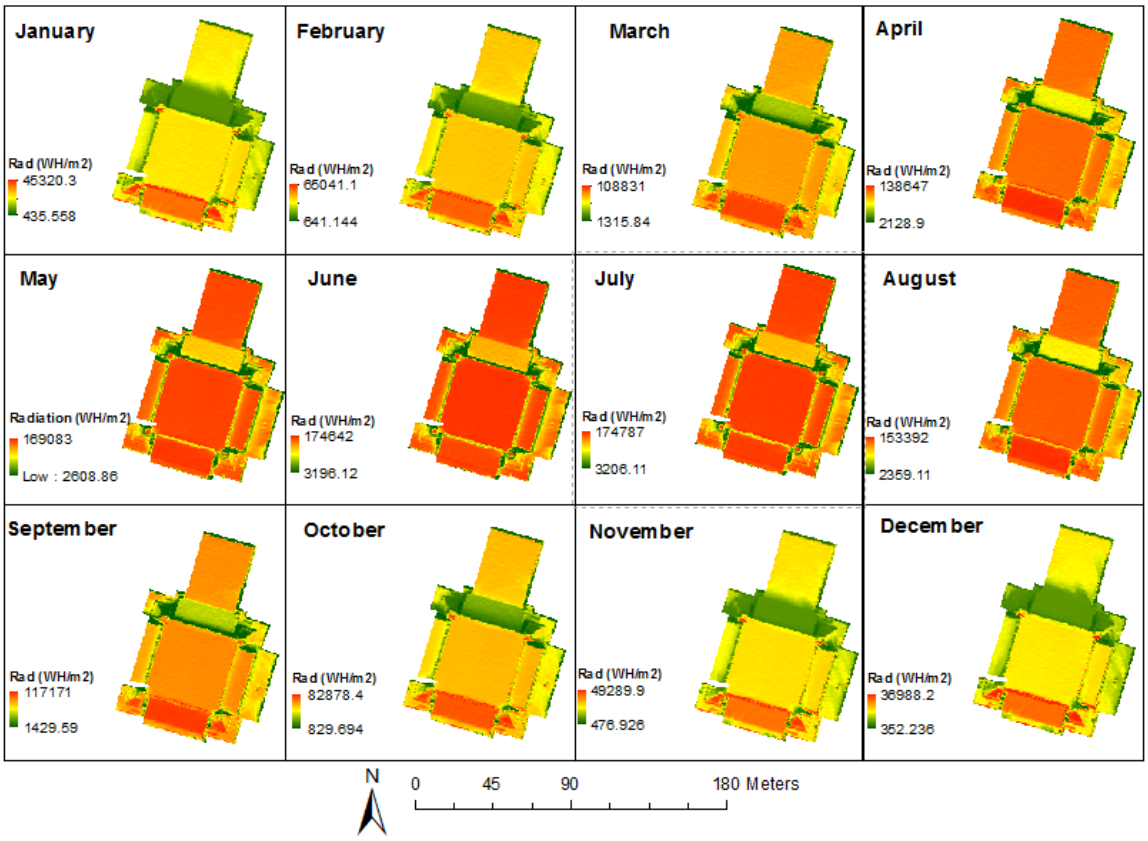

Figure 5.3 - Monthly solar radiation maps of the Physical Activities Complex (PAC) Building with different individual legends

Figure 5.4 (A) shows a one-year accumulated solar radiation map of the PAC building under clear-sky conditions. In order to better interpret the one-year accumulated solar radiation map, as well as the monthly-accumulated maps, a standard deviation map providing information about how much variation exists in average incoming solar radiation is shown in Figure 5.4 (B). Overall, the standard deviation values are high, since solar radiation varies widely seasonally.

In Figure 5.4 (A), areas with the highest accumulated insolation amount through the entire year are displayed in red, while the lowest are in green. Specifically, the southern

rooftop receives the most accumulated solar radiation (around 1300 kWh/m^2/yr). As mentioned above, the southern rooftop consistently receives the highest amount of incoming solar radiation; therefore, it shows a very low standard deviation. The standard deviation of the southern rooftop compared to its yearly average radiation is approximately 51,175 WH/m^2 to 52,924 WH/m^2. Area receiving the second highest amount of insolation over a year is the main rooftop. However, according to the monthly maps and the standard deviation map, the amount of solar radiation that strikes the main rooftop varies greatly within one year. Due to the higher height of the main rooftop, a significant shading effect is caused along the northern lower rooftop and northern rooftop below. The northern rooftop obtains less accumulated insolation compared to rooftops located in the south. The south-most part of the northern rooftop, displayed in red in Figure 5.4 (B), shows the highest variation in one year because shadows caused by taller buildings vary according to seasonal changes in solar angle. The deviation of this part is about 58,171 WH/m^2 to 64,557 WH/m^2. Areas consistently shaded throughout the year, such as roof corners and roof edges, show the lowest standard deviation.

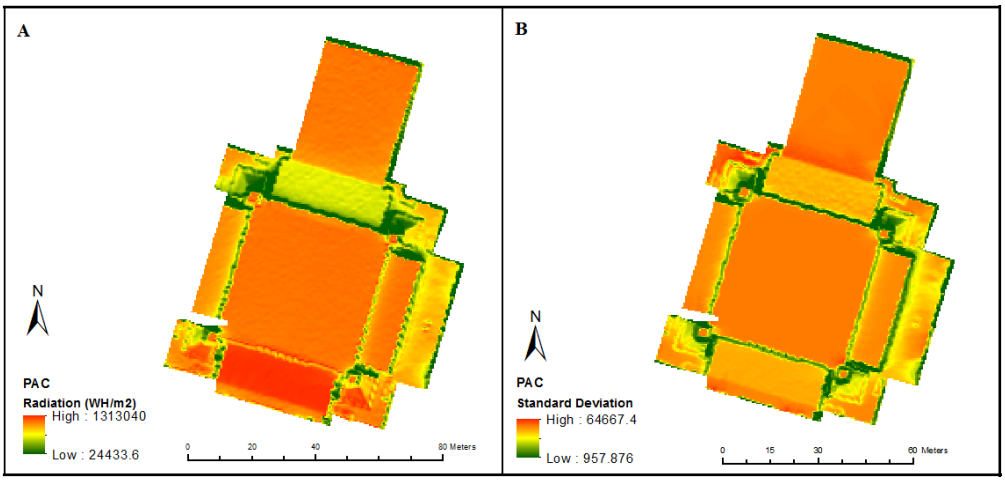

Figure 5.4 - A: One year accumulated solar radiation map of the PAC building; **B:** Standard deviation of solar radiation of the PAC building.

A shadow mask map of the PAC building was produced and shown in Figure 5.5 (A), which shows areas covered by shadow versus areas exposed to the sun. According to the shadow map, there are about 4000 m^2 of the rooftop areas that are free of shadow effects throughout the year, while the overall rooftop area is almost 7000 m^2. Pixels in light grey

on the northern rooftop have an 8.3% probability of being shaded, indicating a one-month probability. It appears that potential shadow effects are caused by trees close to the PAC building in December. 4.4% of the PAC rooftop area has shadow probabilities of 16.7% and 25%, and these areas are almost located at the roof edges. Probabilities greater than 25% indicate that areas have more than one season of probability to be blocked from the sun.

In the classified map (Figure 5.5 (B)), areas shown in white are the non-shaded areas. In contrast, areas in black mean that the probability of shadow covering those areas is greater than 75%, indicating that throughout the year over nine months those areas are influenced by shadow effects. Such areas are considered to be completely shaded, and should be avoided for solar panel installation. Areas having 50% to 75% of shadow risks are almost shaded areas, indicating that the areas are shaded more than half of a year. By comparing the shadow mask of the PAC building to its yearly-accumulated solar radiation map, it was verified that areas with high shadow risks do indeed receive much less solar radiation than other areas. Areas classified as unshaded areas are considered as optimal installation places in the present study.

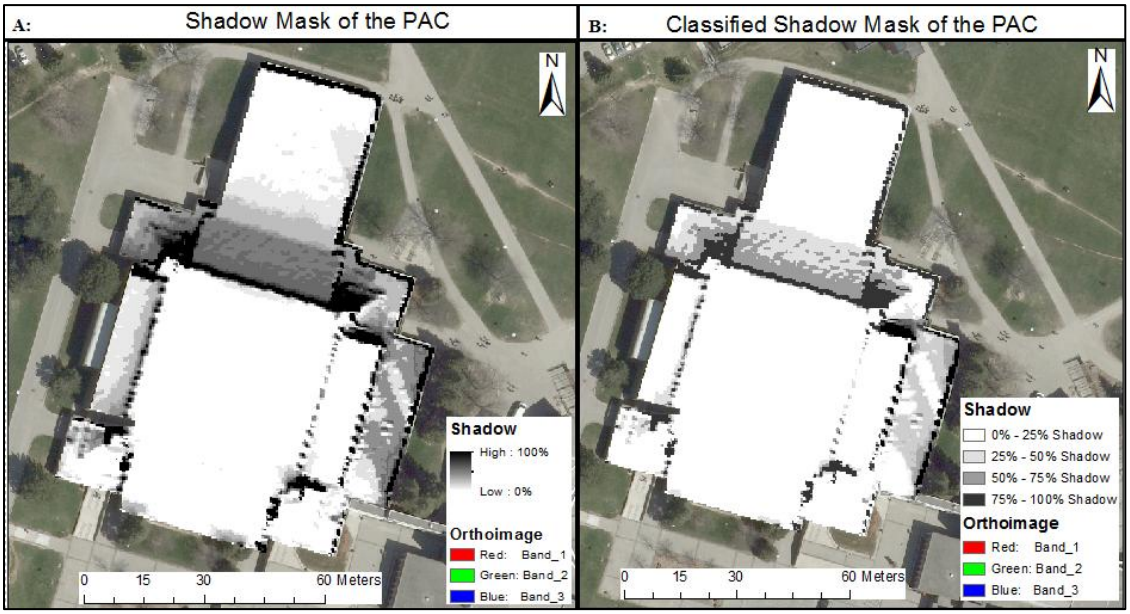

Figure 5.5 - Shadow masks of the PAC building. **A:** Unclassified shadow mask; **B:** Classified shadow mask.

Since dimension and shape of the site should be taken into account when considering suitable installation sites, a minimum area of 1.4 m^2 were used to screen appropriate areas for solar panel installation. As a result, roof corners and small discrete shapes may be excluded. In Figure 5.6, areas with less than 25% probability of shading effects are highlighted. The overall dimension of these areas is about 3,705 m^2. Associated with the annual solar radiation map, the yearly average radiation output is about 1,162.9 kWh/m^2, while the minimum yearly output is 1,023 kWh/m^2. If the future installed panels have a conversion efficiency of 15%, which is an average efficiency for typical solar panels (e.g., Bielinskas, 2012), the average annual electricity output would be 174.4 kWh/m^2.

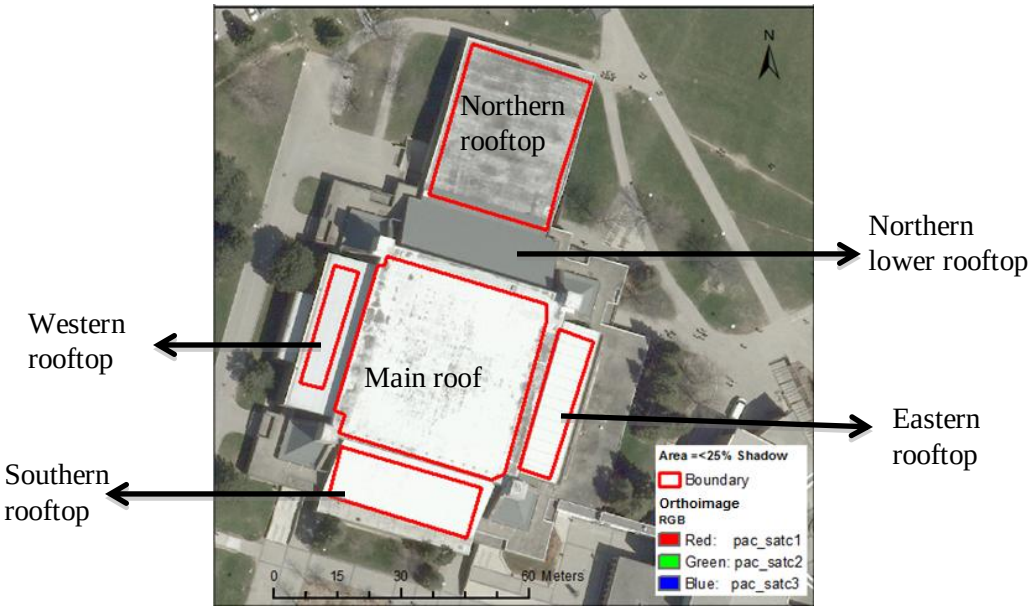

Figure 5.6 - Areas on the PAC building rooftop with less than 25% of shadow risks overlaid on an orthoimage

5.1.2. Environment Buildings

The second case study includes two adjacent buildings of the Faculty of Environment Building. From the monthly average solar radiation maps with standardized legends in Figure 5.7, seasonal variation of solar radiation is shown. Figure 5.8 shows the monthly maps with different individual legend, indicating detailed spatial variation of solar radiation within each month. According to both Figure 5.7 and Figure 5.8, shadow effects from stacks and roof constructions to the lower roof edges and corners are evident.

Unlike the PAC, the EV buildings have a more complex roof structure. Objects on the rooftop cause shadow effects on surrounding areas. Rooftop stacks and other obstructions on the EV buildings cause larger shadows to obscure rooftop areas in January, February, March, April, September, October, November, and December compared to other months, since the incidence angle of the sun is smaller during spring, fall, and winter. The southern sides of both EV buildings are less susceptible to shadow effects and receive greater insolation than the northern side from September to March. In addition, planes at higher altitudes tend to obtain more insolation than lower or shorter planes.

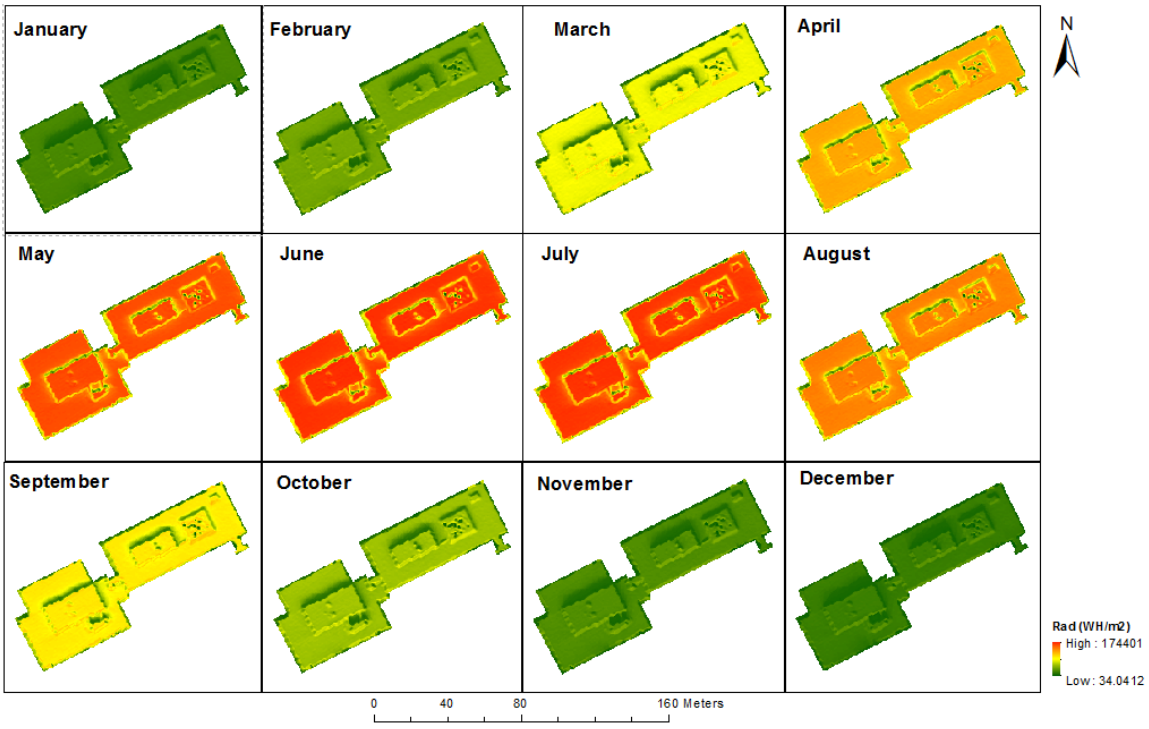

Figure 5.7- Monthly solar radiation maps of Environment buildings with standardized legends

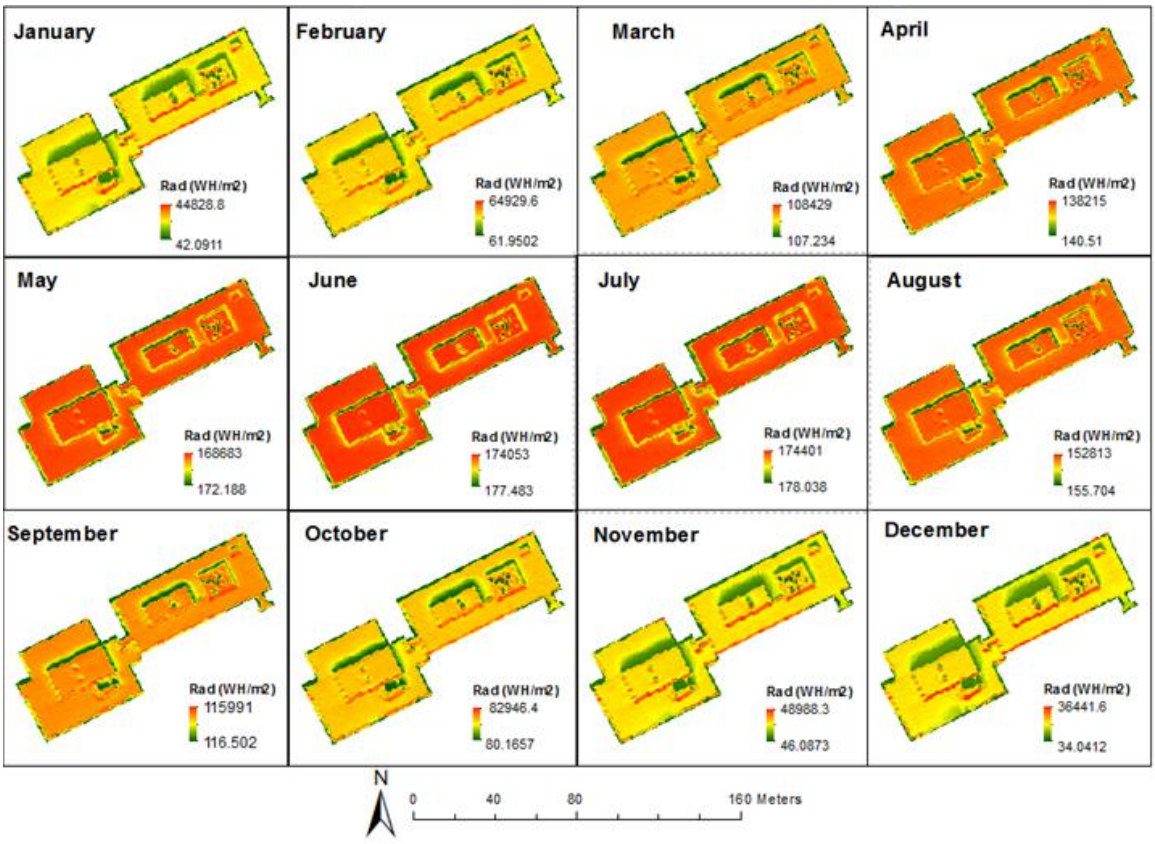

Figure 5.8 - Monthly solar radiation maps of Environment buildings with individual legends

To better interpret the solar radiation variation of complex EV building rooftop structures, a 10-cm spatial resolution orthoimage was obtained to enable more detailed analysis of roof physical shapes and structure, as shown in Figure 5.9. In the orthoimage, the first circled area on the EV1 rooftop was identified to be a stack, which creates shadows around the surrounding rooftop areas, as shown in the radiation maps. The second circled area on the EV1 rooftop was identified to be a pyramidal skylight. Since laser pulses from LiDAR sensors can pass through the glass material of skylights and be reflected from the underlying ground surface from inside the room, it was determined that the collected laser elevation data was indeed not the actual rooftop altitude, but indicative of floor height of the room directly below the skylight. These observations help to explain why this specific area of the rooftop appears irregular or uneven in Figure 5.7 and Figure 5.8. The third highlighted area on the EV1 roof is a rooftop construction, as shown in Figure 3.3, which can cause shadows to fall on surrounding areas. Areas highlighted on the EV2 rooftop contain several devices or stacks. Solar panel installation site selection

should avoid such devices or stacks, while favoring open and flat rooftop areas.

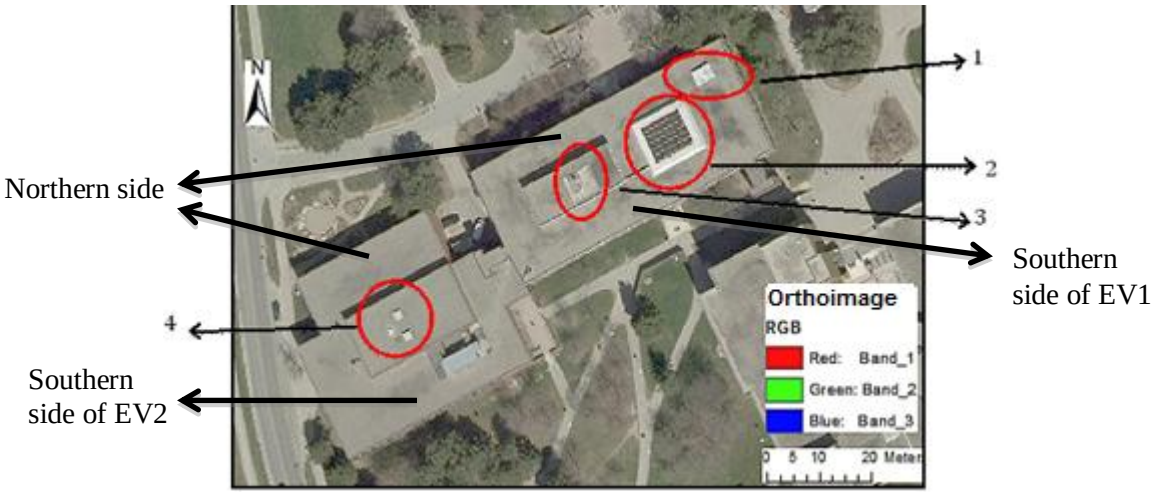

Figure 5.9 - 10-cm spatial resolution orthoimage showing roof structure of Environment (EV) buildings

As shown in Figure 5.10 (A), for a flat rooftop structure, edges and corners appear to be more susceptible to shadow effects; hence it is preferable to install solar panels in central or interior areas of building rooftops rather than at the edges or boundaries. Moreover, northern side of EV2 rooftop receives slightly more solar radiation during a year than the other sides. However, shadow caused by the rooftop constructions to parts of the northern sides is also significant. According to the standard deviation solar radiation map shown in Figure 5.10 (B), the rooftops towards the north receive a wide variation of solar radiation within a year due to seasonal changes in the solar incidence angle. Specifically, the northern areas are shaded when the incidence angle was low, while they are exposed to the sun when the angle increased during the year. Also, as the sun angle increases, incoming solar radiation also tends to increase. Remaining shadowed areas show less variation throughout the year, as they remained more or less constantly in the shade, as shown in Figure 5.10 (B) in green.

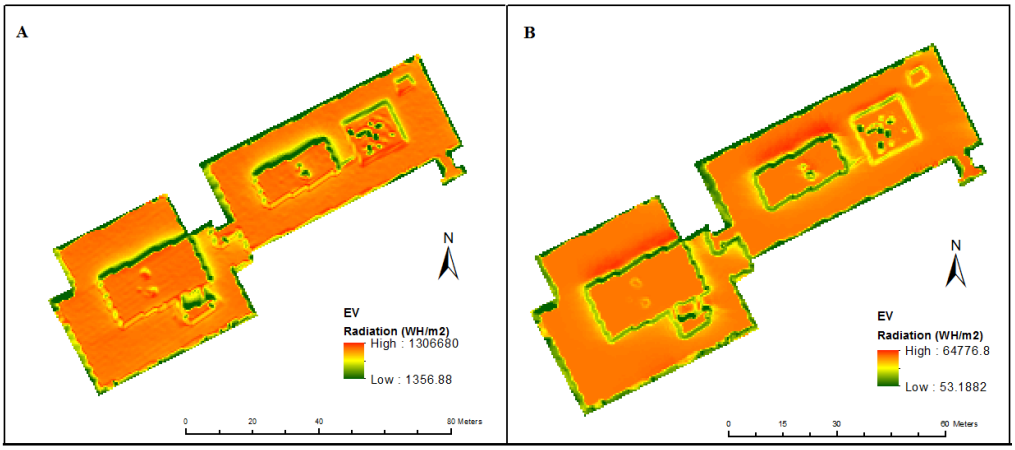

Figure 5.10 - A: One-year accumulated solar radiation of Environment (EV) buildings; **B:** Standard deviation of solar radiation of EV buildings.

Figure 5.11 (A) shows an unclassified shadow mask of the EV buildings. Pixels in light grey on the northern EV1 and EV2 rooftops have shadow probability of 8.3% or 16.7%, indicating that one- or two-month probability of being shaded throughout the year. By analyzing the rooftop structure, the potential shadow is due to the rooftops' obstructions (i.e., pyramid skylight rooftop and facility rooms) in January and December. The eastern side of the EV1 building has an 8.3% of shadow cast probability due to the adjacent building (J.G. Hagey Hall of the Humanities building). This shadow effect only occurs in December. The southern edge of the EV2 building is affected by shadow with a probability of 8.3% or 16.7% due to nearby trees in January and December. The southern edge of EV 2 is more or less affected by shadow cast throughout the year with significant effects during the winter months (November, December, and January). Similar to the previous analysis of the PAC building, shadow probabilities of less than 25% were considered to be non-shaded or exposed. In the classified map (Figure 5.11 (B)), areas in black represent completely shaded areas that have a greater than 75% probability of having shadows present, while the white areas are exposed to the sun with less than 25% of shadow risk. Excluding the skylight rooftop and areas with stacks or devices, lower rooftops particularly on the south and southeast sides were determined to be more suitable for solar panel installation. For higher rooftops of the rooftop constructions, flat regions are preferred for panel placement, while the strength and stability of the rooftop for supporting the weight of solar panels in the first place should be considered.

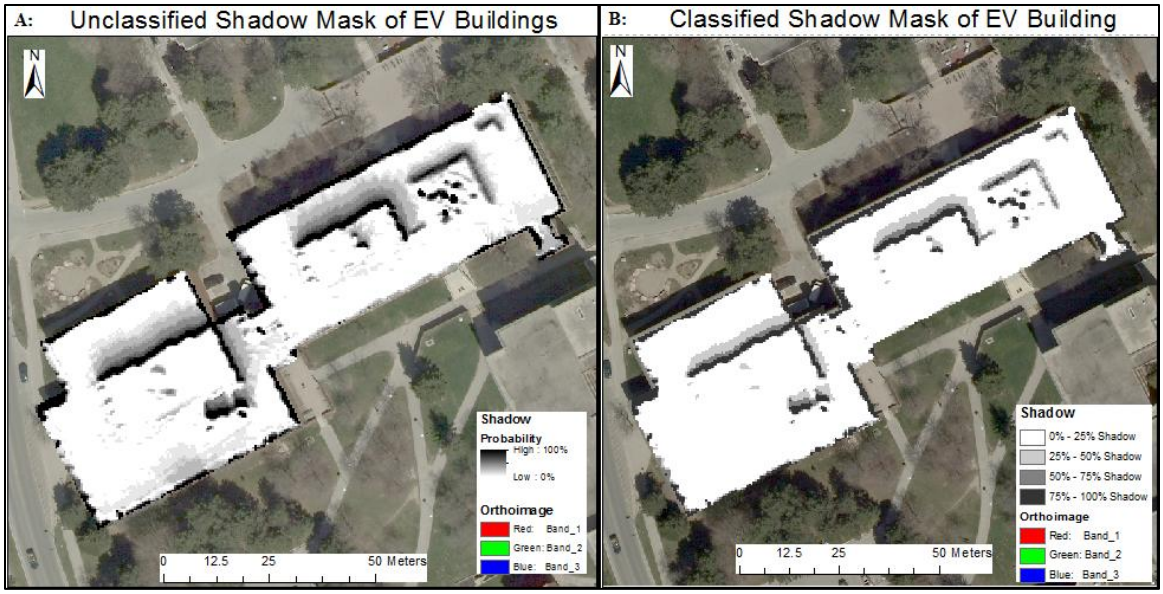

Figure 5.11 - Shadow masks of EV buildings. **A:** Unclassified shadow mask; **B:** Classified shadow mask.

According to the classified shadow mask, as well as the rooftop structure and stability, appropriate roof areas with less than 25% of shadow risks are highlighted in Figure 5.12. These potential areas have an overall dimension of about 1,704.2 m^2. The average annual incoming solar radiation is approximately 1,140 kWh/m^2 and the minimum radiation output is about 1,000.9 kWh/m^2. If solar panels have a conversion efficiency of 15%, the average annual electricity output is about 171 kWh/m^2. According to the selected areas highlighted in red in Figure 5.12, the northern side of EV1 has a 2.8 m by 58.3 m area. If a 1-m setback from the rooftop edge for occupation safety is required, the width of the northern side of EV1 will shrink to 1.8 m, which is sufficient for a 1.4 m^2 solar panel to be installed. If areas with shadow risks from 25% to 50% are included as potential installation areas shown in Figure 5.12 in blue, the available area of the northern side of EV1 for solar panel installation will increase to 5.2 m × 58.3 m. If a minimum 1-m setback is required, the available area would decrease to 4.2 m × 57.3 m. In addition, the suitable area of the northern side of EV2 for solar panel placement will increase with this new criterion. The final area of this new selected site would result in about 1,845.2 m^2, and the increased area would be 141 m^2. Since this new site also includes areas with less than 25% of shadow, the final average incoming solar radiation

only decreases slightly to 1,138 KWH/m^2. The minimum radiation output of the newly selected area changes to 860.9 KWH/m^2.

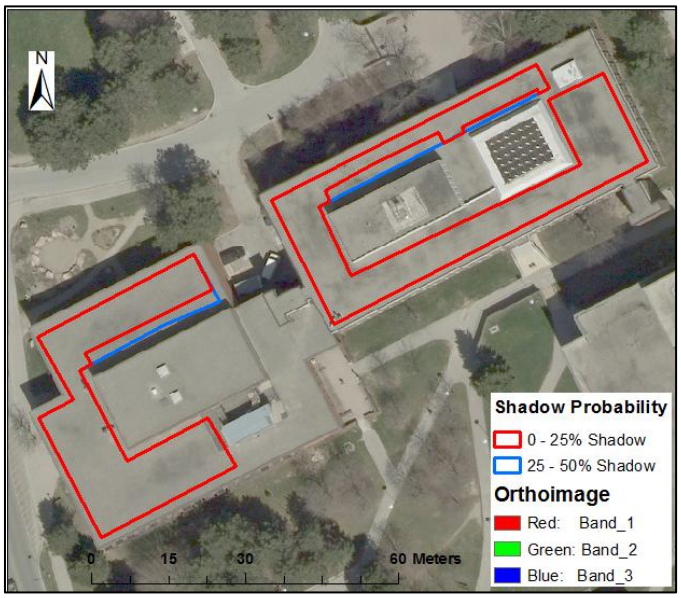

Figure 5.12 - Areas on Environment (EV) rooftops with less than 25% and 50% of shadow risks overlaid on an orthoimage

5.1.3. Dana Porter Library

From monthly solar radiation maps of the DP Library with standardized legends shown in Figure 5.13, it is observable that December and January received the lowest solar radiation throughout the year. In Figure 5.14, spatial variation of solar radiation of one month is shown based on the original legend scale. It is also evident that edges of the library building rooftop receive much less insolation than inner rooftop areas due to shadow effects. This was similar to previous buildings that were discussed. Constructions and obstructions on the building rooftop cause shadow effects to the surrounding areas, while the shadow caused by such constructions tends to vary depending on the time period in the year. The outer edges of the building were identified as the rooftop of the main floor (1st floor rooftop), which is labeled in Figure 5.17. Overall, the southeast side of the 1st floor rooftop receives more solar radiation than layers in the northeast and northwest. The lower south corner receives the highest solar radiation during the year. Southwest and southeast parts of the building rooftop show less obstruction from shadows than the northern and northwest rooftops, especially in the winter months.

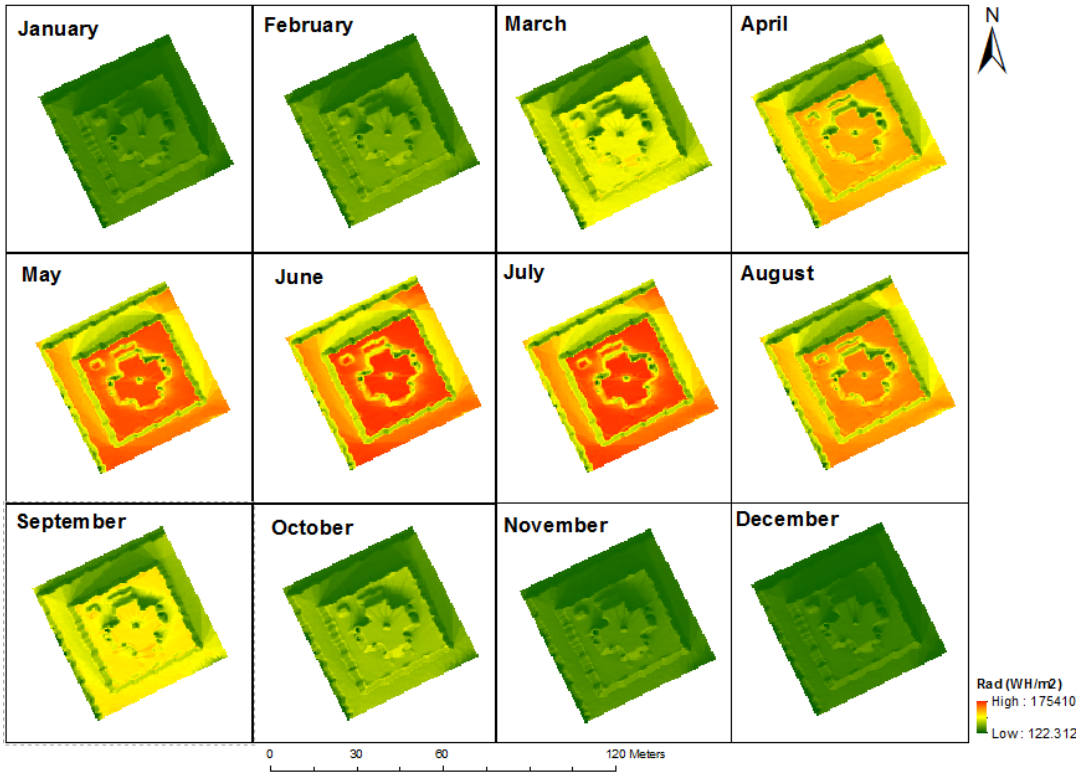

Figure 5.13- Monthly solar radiation maps of the Dana Porter (DP) Library with standardized legends

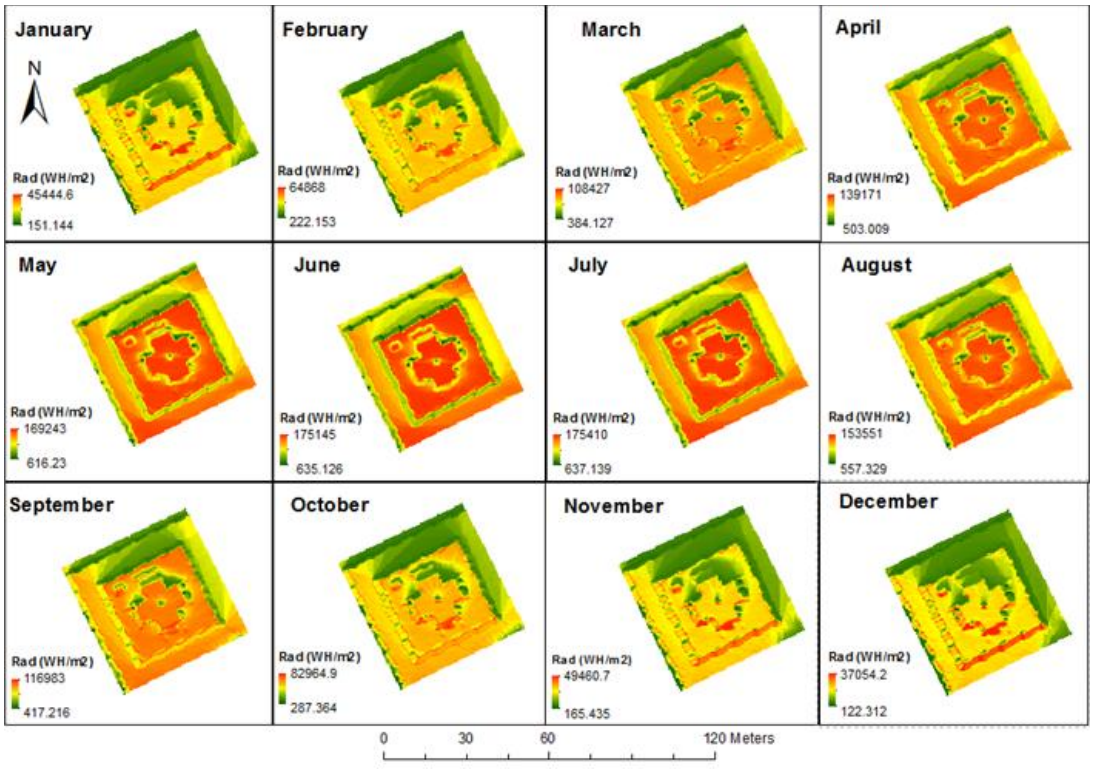

Figure 5.14 - Monthly solar radiation maps of the Dana Porter (DP) Library with individual legends

Figure 5.15 (A) shows a one-year accumulated solar radiation map of the DP Library. As illustrated in the map, the southern corner of the 1st floor rooftop receives the greatest insolation throughout the year. Although the building rooftop obtains a significant amount of radiation, since the roof structure is complicated with a crisscross construction above, shading effects on the northern side are significant. This construction does not make the area suitable for solar panel installation. Figure 5.15 (B) shows a standard deviation map of the Library. It is noticeable that monthly radiation of most of shadow areas compared to the yearly average radiation throughout the year has less variation than the radiation of fully exposed (non-shaded) areas. The southern side of the building rooftop shows relatively less variation than the northern side during the year.

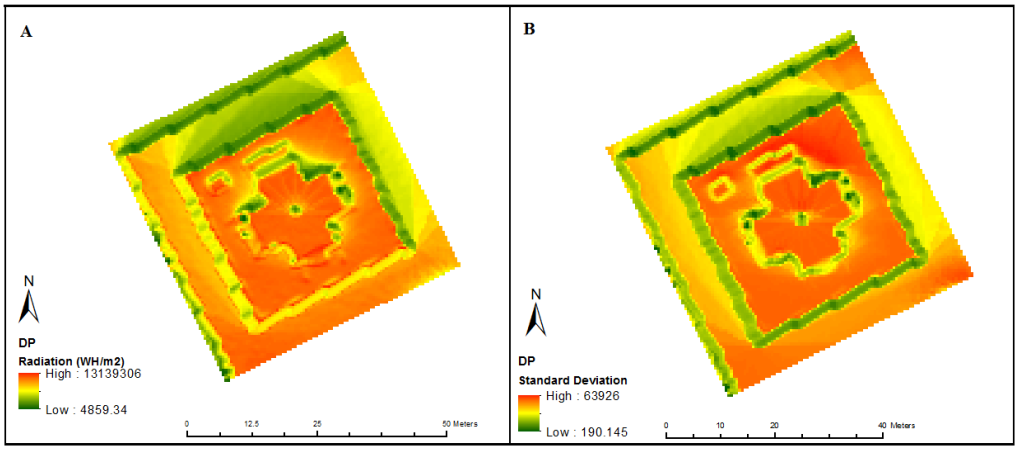

Figure 5.15 - A: One-year accumulated solar radiation map of the Dana Porter (DP) Library; **B:** Standard deviation of solar radiation of the DP Library.

Referring to the shadow mask of the DP Library shown in Figure 5.16 (A) and (B), combined with the results from the previous analysis, potential sites for solar panel installation can be readily identified. Figure 5.16 (A) shows the original calculated shadow risk map for the DP Library with an average shading probability of about 38.2%. Most of the building rooftop and 1st floor rooftop have no shadows cast throughout the year, although the northern side remains completely shaded. In the classified map (Figure 5.16 (B)), white areas indicate a shadow probability of 0% to 25%, which are classified as unshaded areas. Black areas indicate that the probability of shadows is greater than 75%, suggesting that these areas are overcast by shadows during most of the year. The southwest and southeast sides of the building rooftop can be identified as potentially

suitable installation sites. Due to the cross-shaped construction at the center of the DP rooftop, the outer perimeter of the rooftop may be more desirable for solar panel placement. The southwest and southern sides of the 1st floor rooftop are also considered as potential sites for solar panel installation.

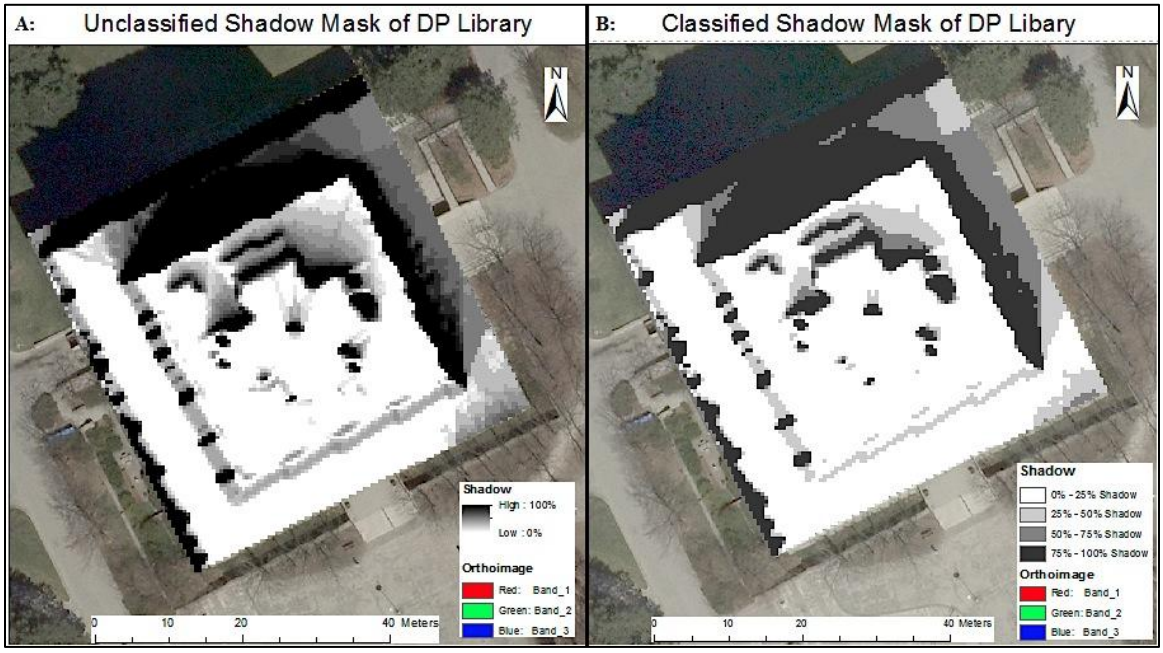

Figure 5.16 - Shadow masks of the Dana Porter (DP) Library. **A:** Unclassified shadow mask; **B:** Classified shadow mask.

According to the classified shadow mask, as well as the rooftop structure of the DP Library, appropriate roof areas with less than 25% of shadow risks are highlighted in Figure 5.17. These potential sites encompass an overall area of about 492.5 m^2. As shown in the 10 cm spatial resolution orthoimage in Figure 5.17, the library roof is distorted, since the airborne camera did not acquire the image vertical to the nadir or perfectly perpendicularly. As a result, the highlighted areas do not match exactly with the corresponding true color orthoimage. 3D ground control points must be acquired to rectify this distortion, which were not available for this study. However, referring to Figure 5.17, it is easy to visually identify that areas 1 and 2 (marked in red) correspond to the main rooftop structure, while areas 3 and 4 correspond to the first-floor roof eaves. The average annual incoming solar radiation of this area is approximately 1,079.4 kWh/m^2, while the minimum radiation is about 821 kWh/m^2. If solar panels have a

conversion efficiency of 15%, the average annual electricity output would be about 161.9 kWh/m^2. According to Figure 5.16, areas with shadow risks of 25% to 50% are mostly located along the northern side of the building rooftops. If a 1-m minimum setback is required for installation safety regulation, the available area would be of insufficient size to accommodate a 1.4 m^2 PV module.

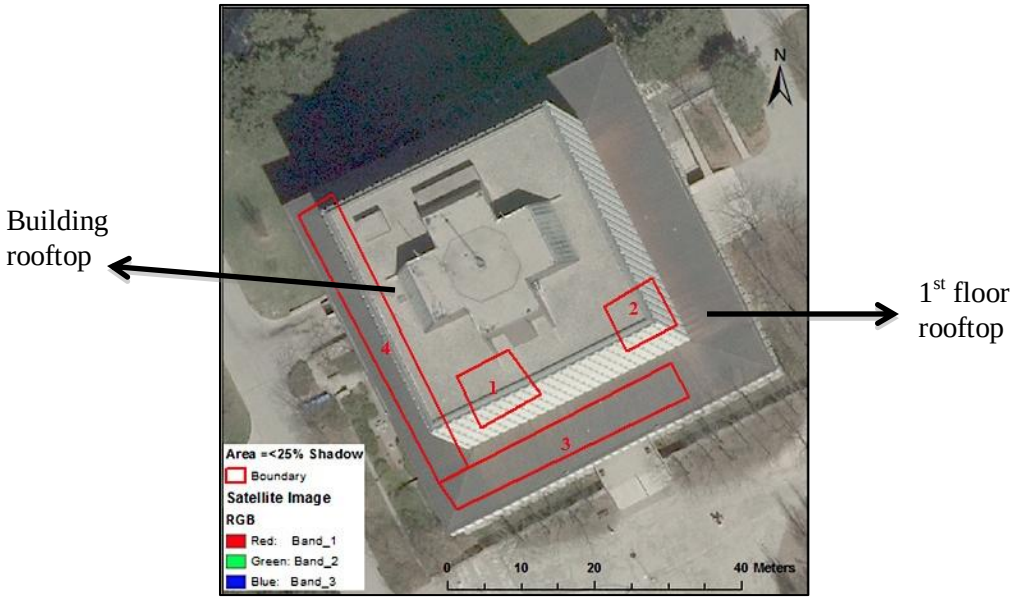

Figure 5.17 - the Dana Porter (DP) Library rooftop with less than 25% of shadow risk overlaid on an orthoimage

5.1.4. Federation Hall

Figure 5.18 shows a series of monthly-accumulated solar radiation maps of the FED Hall with standardized legends, while Figure 5.19 shows the monthly maps with original legend scales. In order to better identify and visualize roof structures, a 10 cm spatial resolution orthoimage displaying the FED Hall is shown in Figure 5.20, in which rooftops of the FED Hall are labeled. The previously installed solar array on the southeast side is clearly visible. From Figure 5.18, not only the seasonal pattern, but also shadow effects on the northern tilted rooftops and roof edges can be noticed. According to Figure 5.19, the flat plane of the FED Hall rooftop receives a maximum amount of solar radiation from April to August months, while from September to March the southwest tilted roof receives the most insolation compared to other rooftops. For the southeast tilted roof, since solar panels were installed prior to 2006, which is when the LiDAR

points were collected, the thickness of the PV panels may account for different height readings. Consequently, incoming radiation values in the region differ greatly due to the surface roughness and gap spacings between solar panels. As shown in Figure 5.18, the PV panels on the southeast tilted rooftop receives higher levels of radiation from October to February. The northern tilted roofs are influenced substantially by shadows from surrounding structures during most of the year. Moreover, the lower rooftop has a considerably large area susceptible to shadow effects, as shown in Figure 5.20. The main rooftop is unobstructed without any stacks blocking incoming solar radiation, while the lower roof has several objects in view.

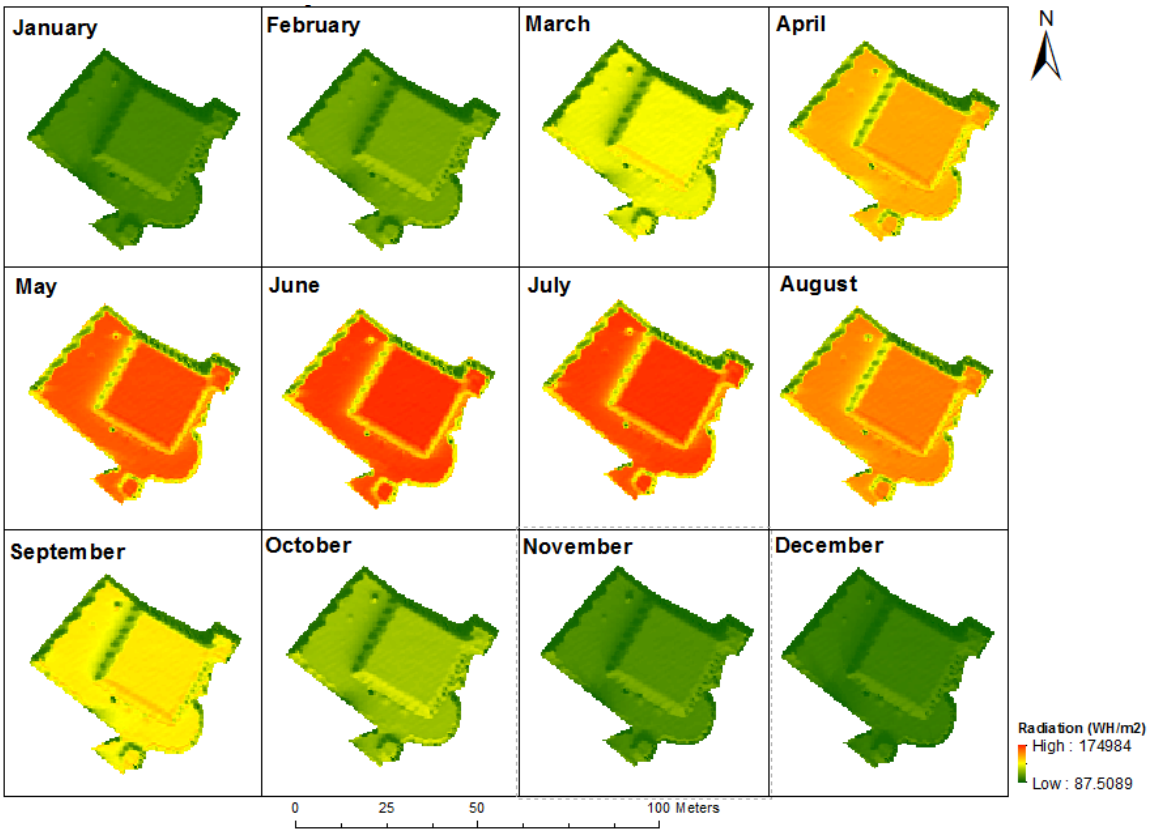

Figure 5.18 - Monthly solar radiation maps of the FED Hall with standardized legends

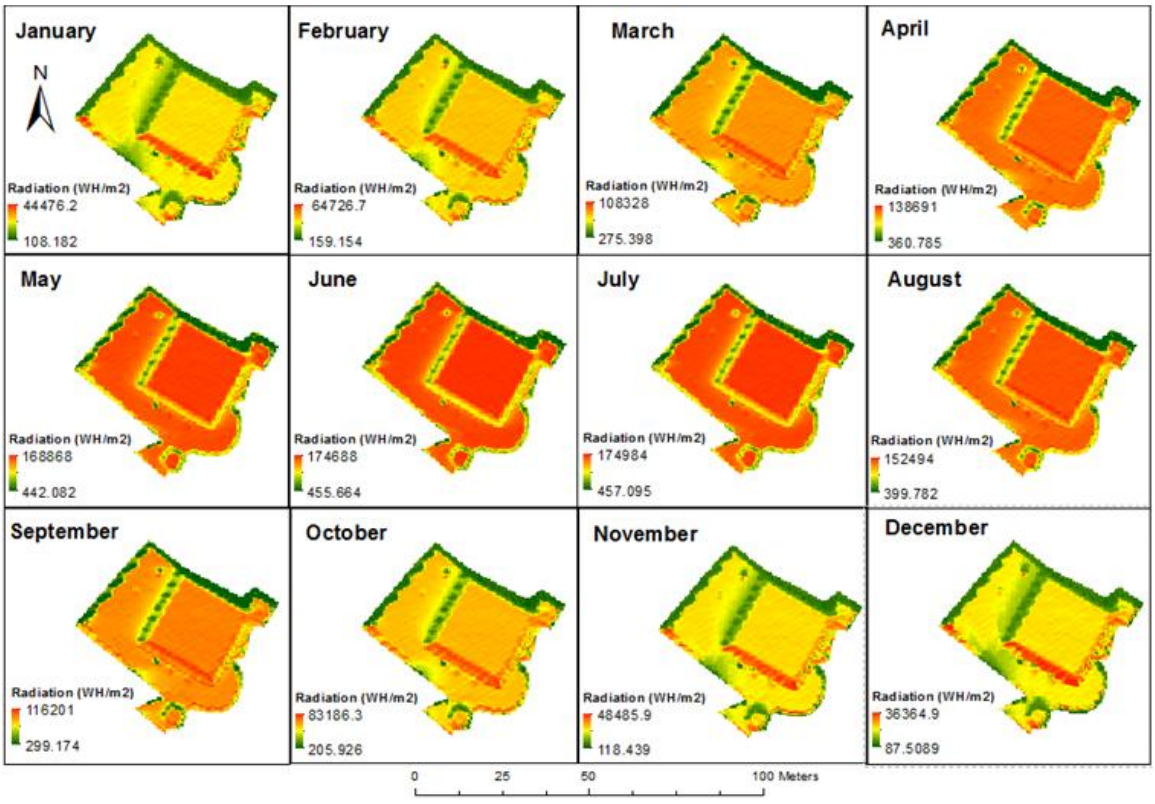

Figure 5.19 - Monthly solar radiation maps of the FED Hall with individual legends

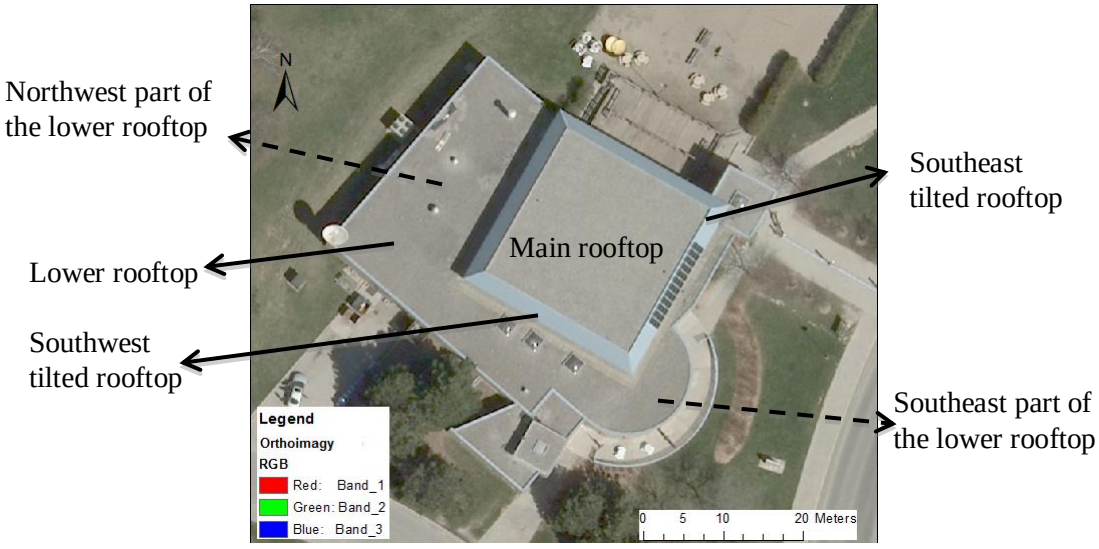

Figure 5.20 - 10 cm spatial resolution orthoimage of the FED Hall

Figure 5.21 (A) shows the one-year accumulated solar radiation map of the FED Hall. Overall, the flat rooftop receives the greatest amount of incoming radiation throughout the year, especially along its southwest edge. Referring to the standard deviation map

shown in Figure 5.21 (B), even though the flat roof has the greatest total incoming radiation, its deviation from the yearly average is high due to seasonal effect. In contrast, the two smaller southern-tilted rooftop structures receive a relatively constant amount of radiation throughout the year.

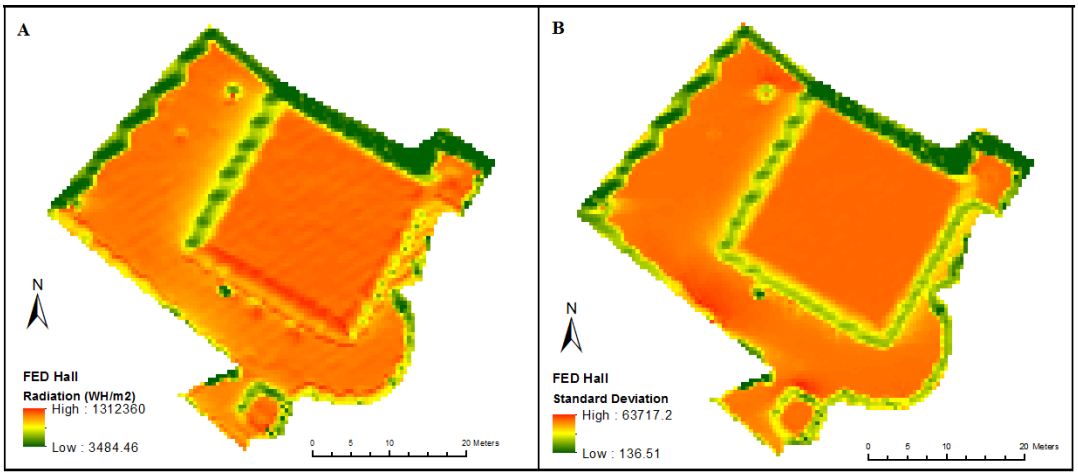

Figure 5.21 - A: One-year accumulated solar radiation map of the FED Hall; **B:** Standard deviation of solar radiation of the FED Hall.

Figure 5.22 (A) shows an unclassified shadow probability map of FED Hall. Some areas of the lower rooftop have a low shadow probability of 8.3% and 16.7%, which is likely due to the main rooftop structure in December and January. Some parts of the lower rooftop are shaded by nearby trees during winter months. The southern tilted rooftops and the main rooftop structure are shadow-free throughout the year, except for some edge effects. Figure 5.22 (B) shows a classified shadow risk map, which has the shadow probability range separated into quartiles. From this map, the northern tilted rooftops are shadowed constantly throughout the year. Both the southern tilted and flat rooftops were fully exposed to the sun and deemed suitable for solar panel placement.

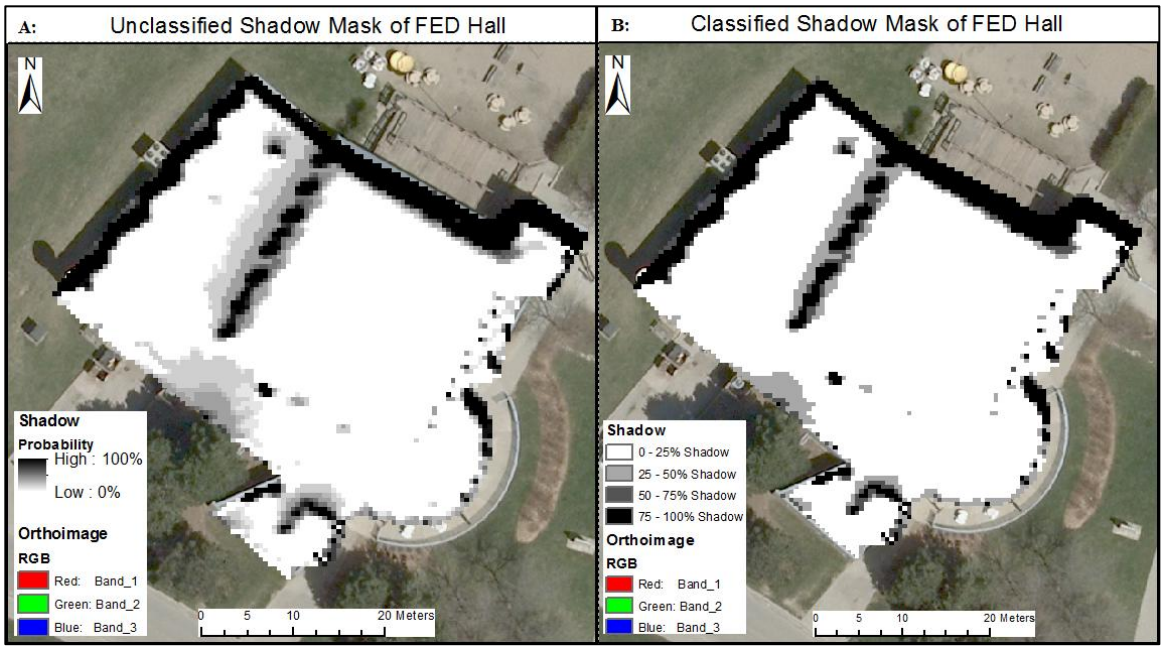

Figure 5.22 - Shadow masks of FED Hall. **A:** Unclassified shadow mask; **B:** Classified shadow mask

According to the classified shadow mask, as well as roof structure of the FED Hall, appropriate roof areas with less than 25% of shadow risks are digitized and highlighted in Figure 5.23. These potential sites encompass a total area of about 715.3 m^2. The average annual incoming solar radiation of these areas is approximately 1,167.6 kWh/m^2, while the minimum radiation output is about 835.7 kWh/m^2. If solar panels have a conversion efficiency of 15%, the average annual electricity output is about 175 kWh/m^2. If areas with shadow risks of 25% to 50% are included as potential sites for solar panel installation, the final site at the lower level of the roof will be slightly larger, as displayed in black in Figure 5.23. The final dimension increases to 297.2 m^2. The corresponding average annual radiation is 1,093.8 kWh/m^2, and the minimum radiation of these areas changes to 754.7 kWh/m^2.

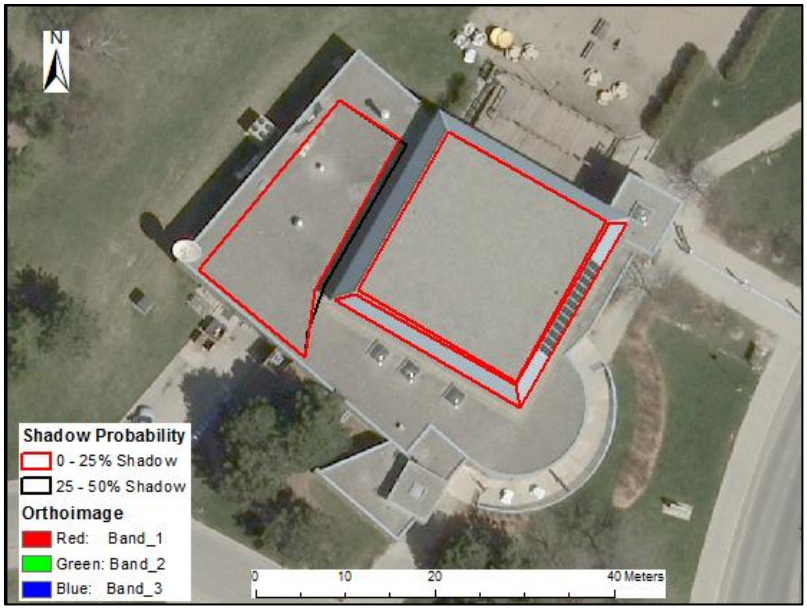

Figure 5.23 - Areas on FED Hall roofs with less than 25% and 50% of shadow risks overlaid on an orthoimage

5.1.5. Student Village 1

Student Village 1 (V1) is a dormitory located on the northwest side of the main UW campus. A 10 cm spatial resolution orthoimage of the V1 buildings is shown in Figure 5.24 (A). It has one main building and four groups of small buildings, some of which are interconnected. The groups of buildings have identical rooftop shapes and structures. The southwest (SW) cluster of buildings is highlighted in orange, the northwest (NW) cluster is highlighted blue, the eastern cluster is highlighted yellow, and the northern cluster is highlighted green. A zoomed image showing detailed roof structures of the NW buildings is provided in Figure 5.24 (B). There are few obstructions on these rooftops and structures are mostly simple and flat. The main building is shown in Figure 5.24 (C), which is a more complex structure with several obstructions, including air conditioning units and chimneys. Trees are also located throughout the V1 grounds, which can potentially contribute to shadows cast over edges of building rooftops.

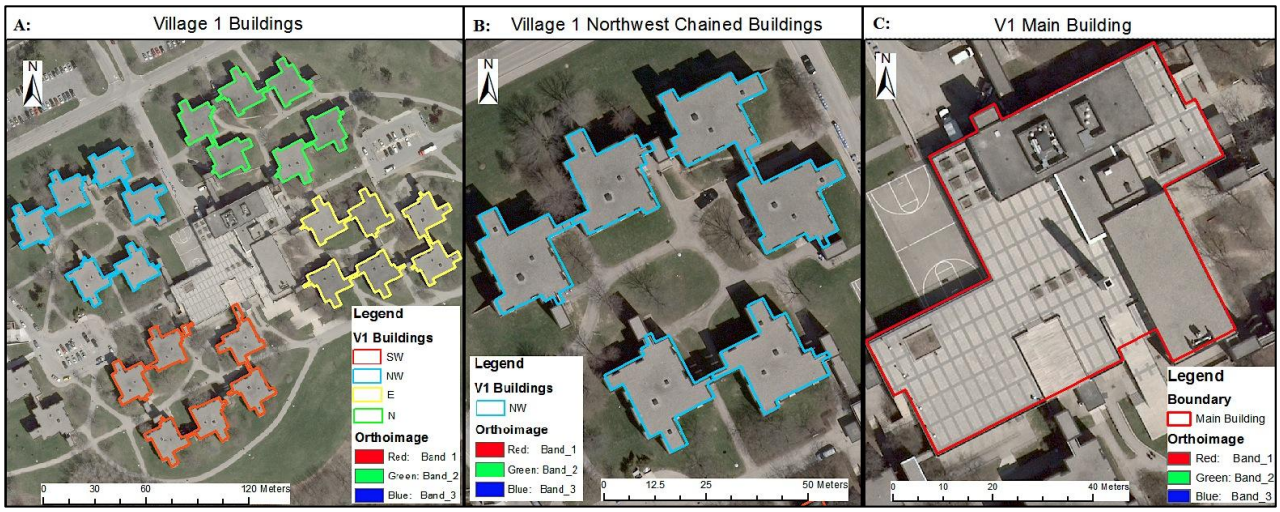

Figure 5.24 - A: 10-cm spatial resolution orthoimage of Village 1 (V1) buildings; **B:** Northwest buildings of V1; **C:** Main building of V1

According to the monthly-accumulated solar radiation maps with standardized legends in Figure 5.25, solar radiation flux reaches the highest level in June and July, and decreases dramatically in the winter months. Shadows caused by rooftop stacks and chimney can be identified from these maps. Figure 5.26 shows the monthly maps with individual legends, and from the maps, roofs in green are shaded surface areas. Since trees are in close proximity to some dormitory buildings, shadows are cast near the building edges. The northern and northeast parts of the main building rooftop have obstructions blocking incoming solar radiation, which significantly reduces the suitability of the rooftop for solar panel installation. The southern-most part of the main building rooftop receives greater solar insolation from April to October than other time periods.

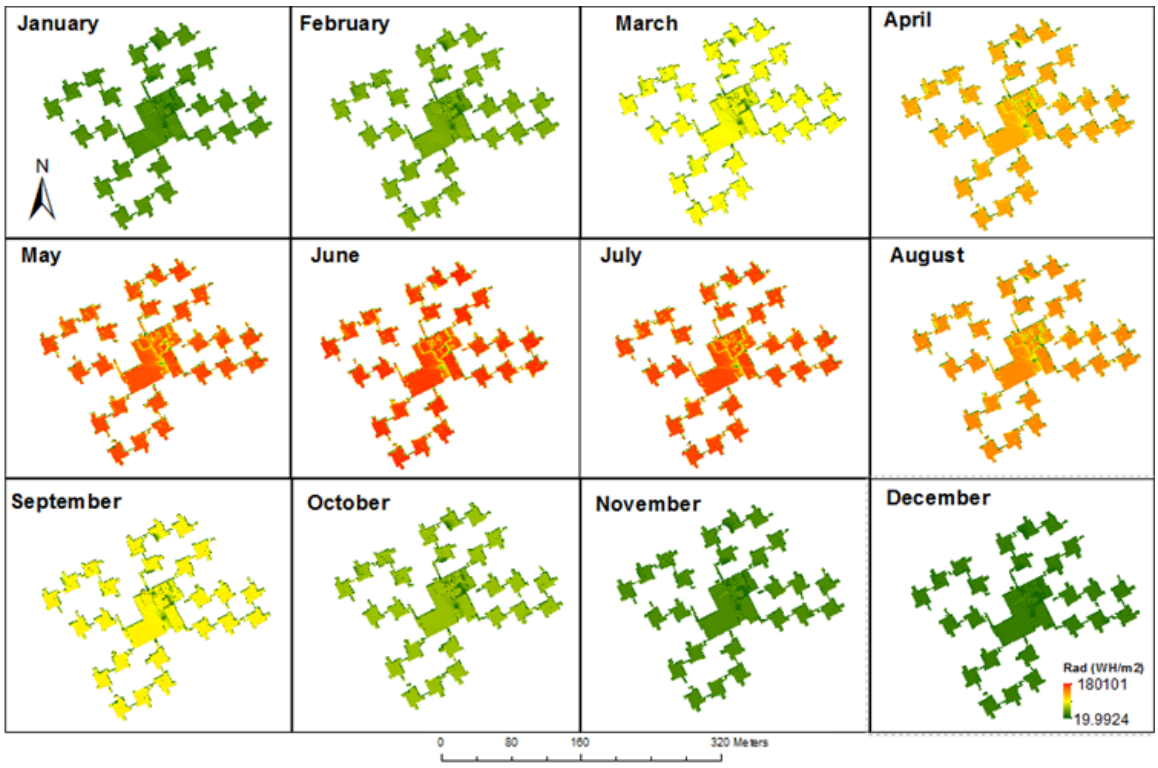

Figure 5.25 - Monthly solar radiation maps of the V1 buildings with standardized legends

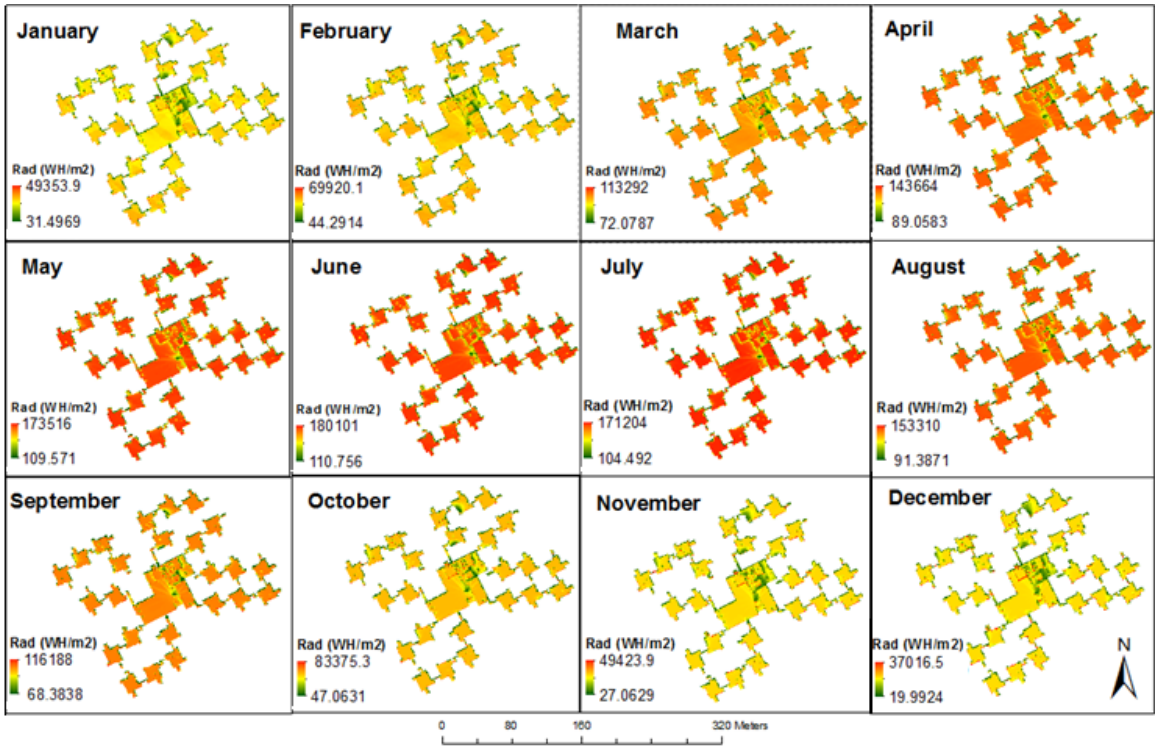

Figure 5.26 - Monthly solar radiation maps of the V1 buildings with individual legends

Figure 5.27 (A) shows the one-year accumulated solar radiation map of the V1 buildings. The solar radiation map displays a very similar spatial pattern to the monthly maps. The four groups of V1 buildings show that some of the rooftops receive greater incoming solar radiation within a year, while some are affected by shadows from surrounding vegetation and building obstructions, and such stacks will reduce the suitability of local areas on the rooftops. For the main V1 building, more complex rooftop structures including chimneys and stacks would complicate the installation process and also contribute to more shadow effects. The standard deviation map in Figure 5.27 (B) shows that shaded areas of the main/central building rooftop and other dormitory rooftops have less deviation than other roof surfaces. The northern building rooftops show the greatest variability throughout the year due to seasonal changes in the solar incidence angle and shadow effects.

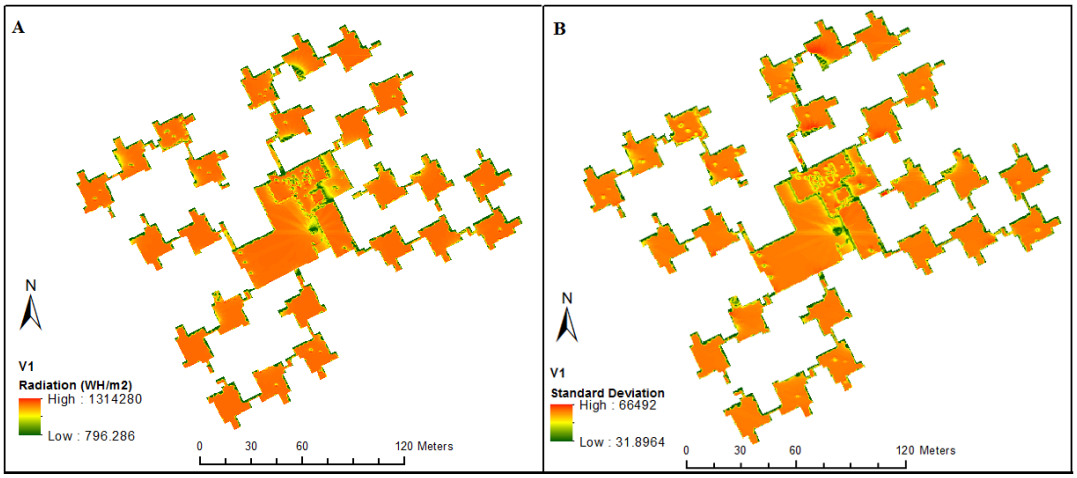

Figure 5.27 - A: One-year accumulated solar radiation map of the V1 buildings; **B:** Standard deviation of one-year solar radiation of the V1 buildings

Figure 5.28 (A) shows the unclassified shadow mask of the V1 buildings. The average shading probability of the building rooftops is approximately 22.4%. Pixels in light grey on the rooftops of grouped dormitory buildings have a probability value of 8.3%, indicating a very low probability of shade effects in these areas. The southern part of the main building rooftop (Figure 5.24 (C)) has an 8.3% of shadow risk due to the presence of a chimney. Figure 5.28 (B) shows the classified shadow risk map that divides shadow probability into quartiles. From this classification, areas with 8.3% and 16.7%

shading probabilities are classified as appropriate sites, resulting in a potential area of approximately 1,122 m^2. Overall, among the small groups of dormitory buildings, the southwest and eastern buildings are least affected by shadows, while the northern and northwest buildings are affected the most. The main building rooftop has more shadows along the northern side due to shadows caused by the complex roof structure.

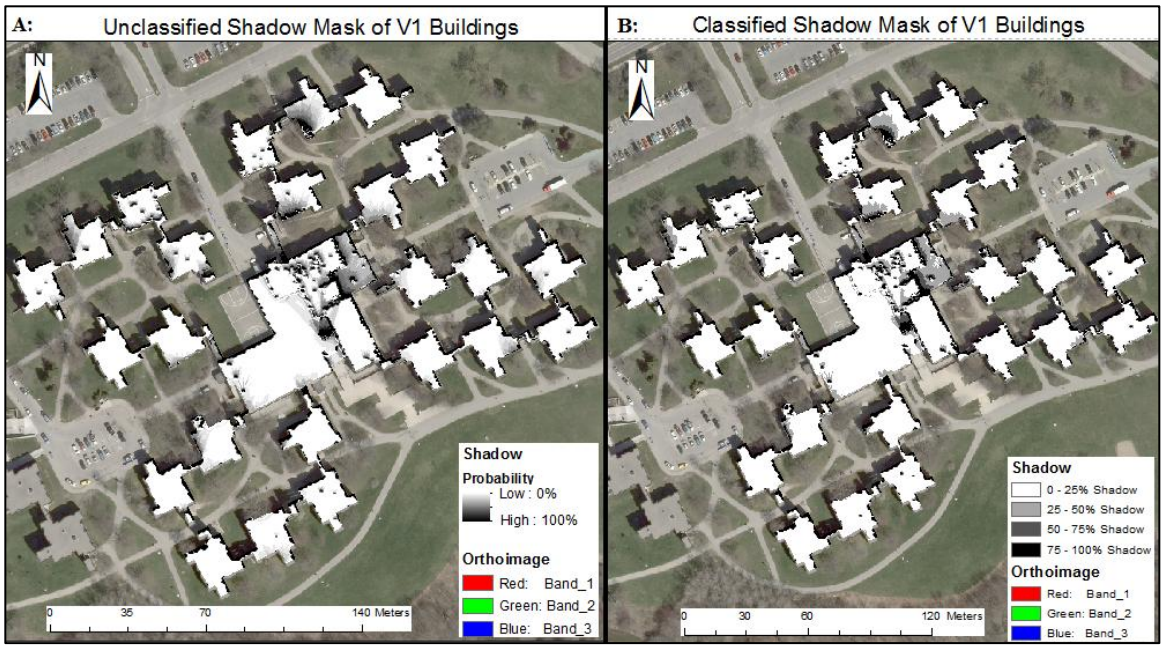

Figure 5.28 - Shadow masks of the V1 buildings. **A:** Unclassified shadow mask; **B:** Classified shadow mask.

According to the classified shadow mask, as well as observed roof structure of the FED Hall, appropriate roof areas with less than 25% of shadow probability are highlighted in Figure 5.29. These potential areas have an overall dimension of about 4,912.8 m^2. Each small building rooftop has an area of about 160 m^2. The average annual incoming solar radiation of these areas is approximately 1,153.7 kWh/m^2, while the minimum radiation output is about 885.5 kWh/m^2. If solar panels have a conversion efficiency of 15%, the average annual electricity output would be about 173 kWh/m^2. According to Figure 5.29, if areas with shadow probabilities of 25% to 50% are included, this would enlarge the final site dimensions, as highlighted in black in Figure 5.29 with a final area of 5,474.6 m^2. The corresponding average annual radiation would be 1,151.2

kWh/m^2, indicating that areas with shadow risks greater than 25% but less than 50% could be selected as potential sites for solar panel installation.

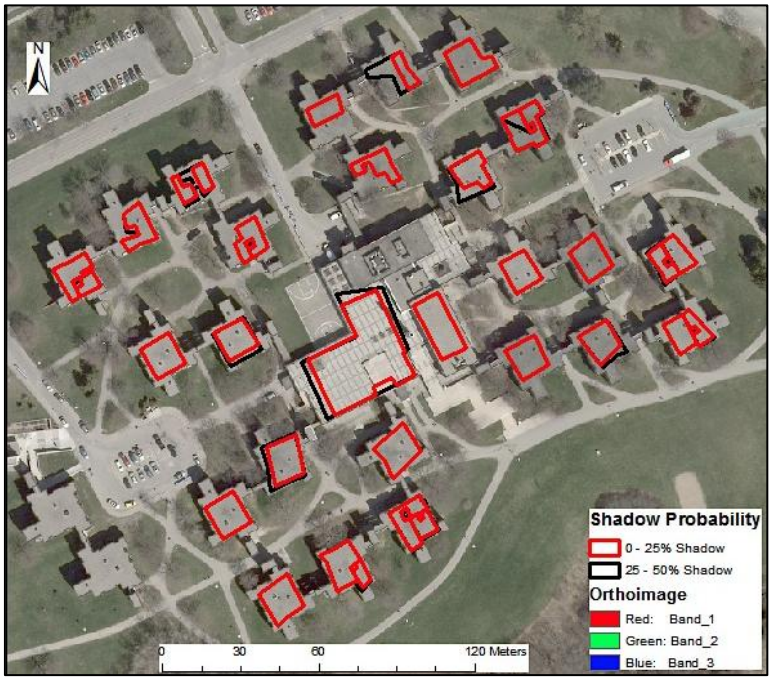

Figure 5.29 - Areas on Village 1 roofs with less than 25% and 50% of shadow risks

5.2. Macro-scale Analysis

In order to select potential optimal sites for solar panel farms in the City of Waterloo, a multicriteria analysis was applied. This section first provides results of the multiple criteria analysis and corresponding weights selected by AHP. The selected sites are then evaluated based on an on-site feasibility assessment and groundtruth observations.

5.2.1. Multicriteria Analysis

Criteria selected for the macro-scale analysis include slope, aspect, solar radiation, distance to water, distance to road networks, distance to transmission lines/pipelines, environmentally sensitive areas, distance to pit and quarry sites, sand content, land plan, and distance to residential areas. Yearly accumulated solar radiation map was generated with ArcGIS Solar Analyst and shown in Figure 5.30. As described in Section 4.1.1, the macro-scale calculations of solar radiation were similar to the micro-scale calculations, applying the same atmospheric and time interval settings. Solar radiation map used in the

macro-scale analysis also applied clear-sky conditions, since relative spatial variations of insolation were similar under both clear-sky and overcast scenarios (i.e., although absolute values differ, spatial patterns remain the same). According to Figure 5.30, red highlighted areas have high levels of incoming radiation, whereas green areas have low levels of radiation. The yearly-accumulated solar radiation map was reclassified to a raster layer ranging from 0 to 1 (i.e., unsuitable versus suitable) in the MCA.

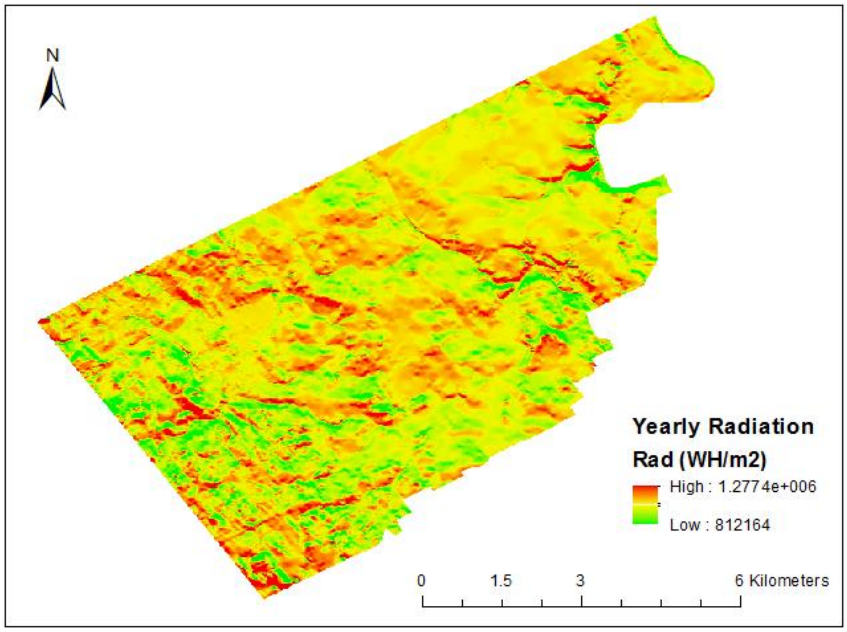

Figure 5.30 - One-year accumulated solar radiation map of the City of Waterloo

Results of the processed criteria are shown in Figure 5.31. Terrain slope was calculated from the DEM data and differences in land elevation. Almost 80% of the areas have a terrain surface less than or equal to 2% of gradient. In this study, the MCA model was tested with threshold gradient values of 3%, 4%, and 5% individually. Results from these three settings showed no significant difference; therefore, a final threshold setting of 4% was selected as a mid-range value. In other words, areas with a gradient greater than 4% were considered to be unsuitable for PV array installation. Since land surfaces facing towards the south have the most solar exposure in the northern hemisphere (e.g., Chaves and Bahill, 2010), areas facing the southwest to southeast were classified to 1 (suitable areas) and other orientations were classified to 0 (unsuitable areas).

Distance to road networks, water sources, transmission lines, and quarry/pit sites were calculated using the Euclidian tools and Fuzzy Membership. From a system performance perspective, road networks should not be directly adjacent to the potential site to avoid dust risk, while from an economic point of view, proximity to roads is desirable for ease of access, construction, and maintenance. Therefore, a maximum road distance threshold was set as 10 meters (Figure 5.31 (C5)). Since road density in the City of Waterloo is relatively high, distance to roads greater than 50 meters did not result in any potential sites identified in the MCA analysis. Maximum distance to water sources for solar panel cooling and cleaning purposes was set at 200 m (Figure 5.31 (C4_1)). Maximum distance thresholds were tested from 100 m to 300 m, but did not have significant impact on the MCA results. For distance to transmission lines, closer proximity was desirable and a 1-km maximum distance threshold was set in the MCA (Figure 5.31 (C6)). When considering dust risk, the farther away from industrial quarry sites the better. Hence, a minimum threshold distance of 50 m was set in the MCA (Figure 5.31 (C8)). To test the sensitivity of the selection result with various minimum distances to quarry sites, 30m to 40 m thresholds did not affect the MCA results.

Environmentally sensitive features such as ESA and water bodies were excluded from the solar panel site selection process. These were classified into a binary data format with suitable and non-suitable classifications (1 or 0, respectively) (Figure 5.31 (C4_2) and (C7)). Only sandy soil or topsoil with a sand content of greater than 50% was considered to pose as a significant source of dust risk to PV panels. Land use classification was a more complicated consideration compared to other criteria due to the number of available classes. This study considered agricultural land and open space uses as the most accessible or suitable land use for siting ground-mounted solar panels based on ease of accessibility and land vacancy (or lack of pre-existing land uses). Such areas were deemed to be the most easy to acquire with the best odds of being suitable for solar panel placement, which could be further evaluated with acquired groundtruth data. Last, based on the density of residential houses in the City of Waterloo, a 100-m buffer of residential areas was created to maintain a distance of accessibility to the potential solar panel sites and namely to exclude immediate boundary areas.

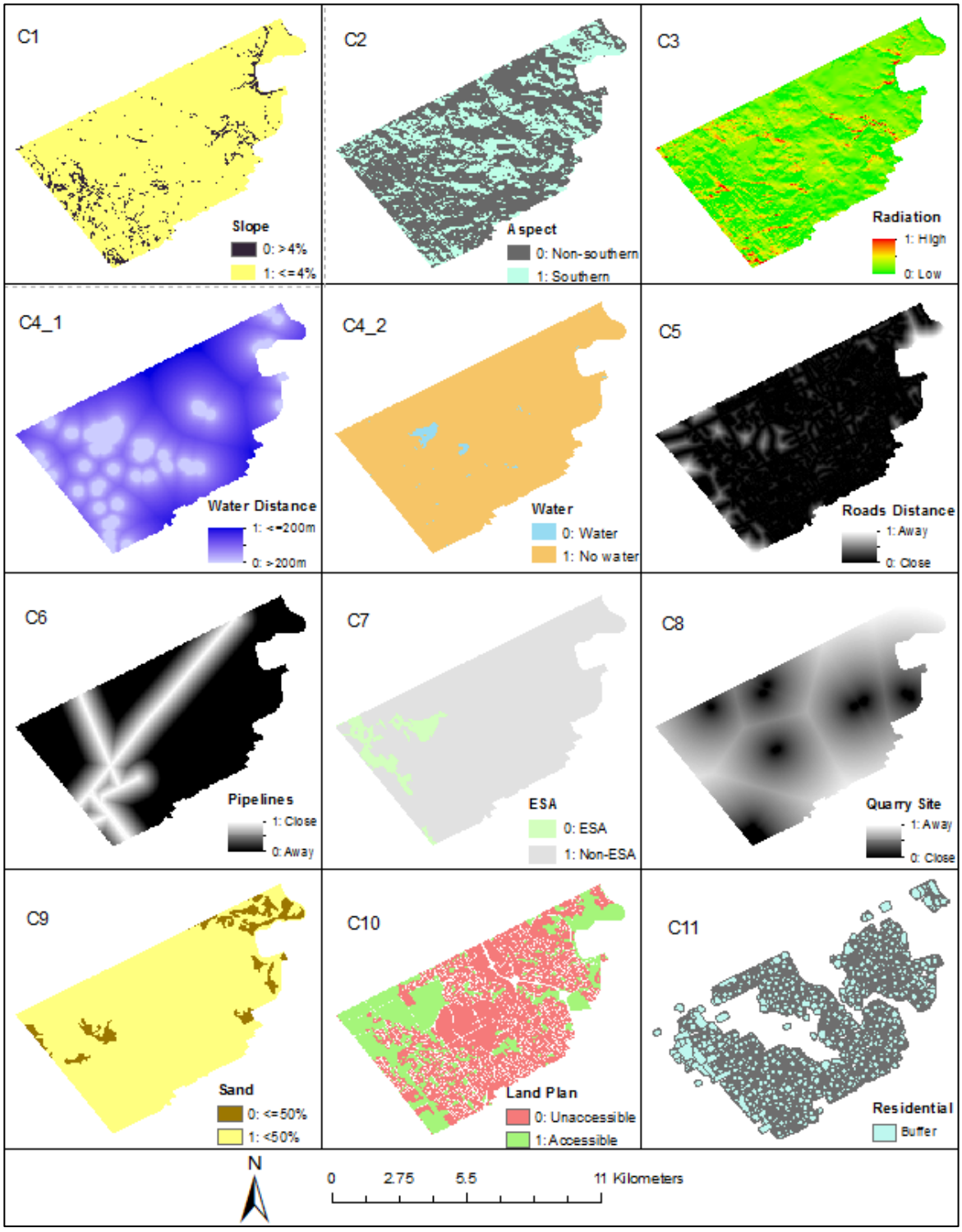

Figure 5.31 - Processed criteria layers used in MCA. **C1:** Classified slope layer; **C2:** Classified aspect layer; **C3**: Transformed solar radiation layer; **C4_1:** Transformed distance to water layer; **C4_2:** Binary water source layer; **C5:** Transformed distance to roads layer; **C6:** Transformed distance to pipelines layer; **C7:** Binary ESA layer; **C8:** Transformed distance to quarry sites layer; **C9:** Binary sandy layer; **C10:** Binary land accessibility layer; **C11:** Residential area buffer layer.

The ranking results of the present study are shown from Figure 4.2 to 4.4. In the last column, final weights for economical and efficiency criteria are listed. Based on this weight assignment, sensitivity analysis by changing weights of important criteria was conducted. The sensitivity analysis resultant maps under seven scenarios are shown in Figure E1 to Figure E3 in Appendix E. In particular, Scenario B is the base setting of this study. The MCA results were classified into four classes, highly suitable (i.e., areas with priorities), moderate suitable, marginal suitable, and unsuitable. This study considered highly suitable areas as potential installation sites. It is noticeable that locations of suitable sites are consistent, and the only alteration is sizes of the selected sites. In Scenarios A, B, and C, the upper level of criteria were added different weights. According to Figure E1 (Appendix E), as the weight of efficiency increases, scales of suitable sites are enlarged from 10.1% to 13.5%. Within Scenarios B, D and E, comparison between slope and aspect or solar radiation[1] was tested. In Figure E1 (B) and Figure E2, as the importance of solar potential increases, overall percentage area of potential sites shrinks from 11.4% to 8.7%. During Scenarios B, F, and G, as the importance of proximity to transmission lines compared to distance to road networks decreases from 6 to 2, the suitable sites shrink slightly with a decreasing rate of 1%.

After the MCA, four large potential sites with the highest scores were selected by filtering out small discrete areas, as shown in Figure 5.32 (A). The first and second sites are located in the northwest of the city with the final score of 0.6 and 0.62, respectively. The first site is at the edge of the city boundary occupying an area of 164,136.47 m^2 (Figure 5.32 (B)), and the second site is located close to the Columbia Lake, which is the largest area of about 393,520 m^2 (Figure 5.32 (C)). The third and fourth potential sites (shown in Figure 5.32 (D)) are located at the edge of the southwest city boundary, and these two sites are located in close proximity to each other. Their dimensions are 88,635.61 m^2 and 9,110.02 m^2, respectively. Site 3 has the highest score among these four sites, which is 0.69, while Site 4 has the second highest score of 0.65. In order to verify the feasibility of using these sites for solar panel placement, an on-site assessment was conducted to collect groundtruth data and observations.

[1] As mentioned in Section 4.3.1, topographic aspect and solar radiation potential were treated equally.

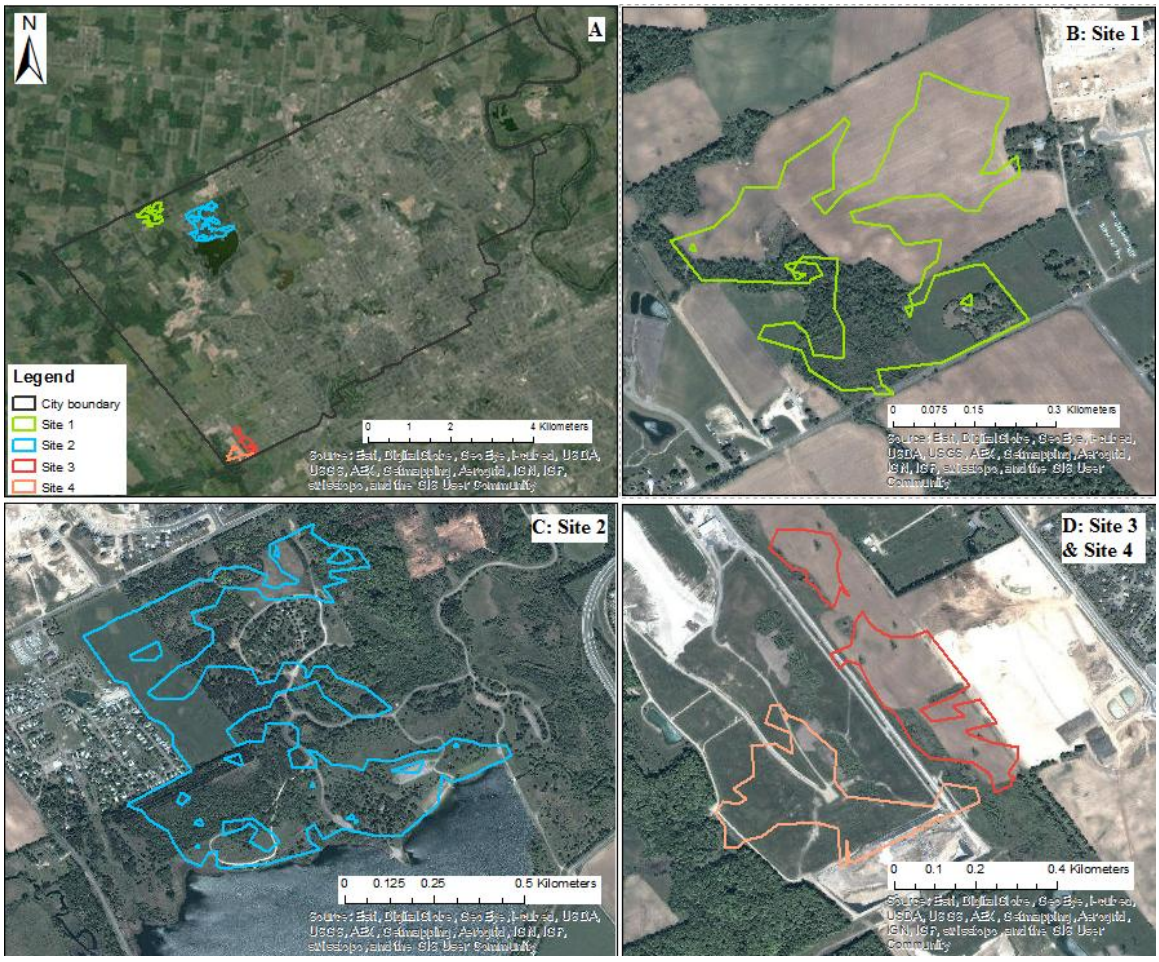

Figure 5.32 - Selected sites for solar panels installation in the City of Waterloo. **A.** Locations of four selected sites; **B.** Selected Site 1; **C.** Selected Site 2; **D.** Selected Site 3 and Site 4

5.2.2. On-site Feasibility Assessment

The feasibility assessment of the selected site was performed by collecting ground truth information. This information was obtained by visiting the sites in the Waterloo Region and recording observations with a camera. Figure 5.33 shows four maps. Map A of Figure 5.33 shows a satellite image of the first potential site (Site 1) with the boundary highlighted in green. The red arrow points in the direction of shooting the photo shown in Figure 5.33 (C), while the blue arrow points in the direction of taking the photo shown in Figure 5.33 (D). Figure 5.33 (B) shows a Google street view picture taken from direction 1 and a 2.5 m spatial resolution SPOT image of the corresponding street-view position. The Google street view image was captured in August 2011, which clearly verifies the agricultural land use of this site, as well as the relatively flat terrain. The eastern side of

the crop field is bordered by residential land use, as shown in Figure 5.33 (D). Both photographs were taken on March 17, 2013, with snow cover visible in both pictures. Another interesting observation is the proximity of an electricity line closely situated to the site, which would be advantageous for facilitating energy transmission for a new solar energy installation.

Figure 5.33 - On-site view from two directions for Site 1 validation. **A**. Selected Site 1 with two labeled observation directions 1 and 2; **B.** Google street view of Site 1 from direction 1, and satellite image with street-view position; **C.** Photo taken from direction 1; **D.** Photo taken from direction 2

The on-site feasibility assessment helped to identify advantages and disadvantages of the site for potential future solar plant development (summarized in Table 5.1). The primary advantage offered by the site is flat topography, which benefits solar panels by minimizing shadow effects by ambient objects. The second advantage of this site is its proximity to a transmission line that helps to reduce energy loss during transmission. Third, this site encompasses an area of approximately 0.16 km^2. A solar farm can range

from a few acres to hundreds of acres in size. For example, the SPV#1 Korat, a 6 MW solar farm in Don Chomphu, Thailand, was built on a 0.136 km^2 land. Another example is a 1,000 km^2 solar farm in Scotland with a capacity of 200,000 MWp (Megawatts peak). Therefore, Site 1 is large enough in size and dimensions to accommodate a substantial solar plant installation. The site's rectangular shape is also conducive and desirable for ease of installing and maintaining an array of solar panels. Last, this site is located at the edge of the City of Waterloo boundary; thus it is located away from the city center yet relatively close to residential areas where the energy can be used. Since the land use is predominantly agricultural cornfield, current private ownership and occupation of the land may also limit future prospects of developing a PV farm. Since residential houses and potential consumers of solar energy are located close to the site, visual aesthetics of a PV farm may be a concern to the local community. The close proximity of the site to local communities may also endanger the facility to vandalism or conflicting land use (e.g., recreation). Average annual solar radiation of Site 1 is about 1,184.5 kWh/m^2

Table 5.1 - Advantages and disadvantages of selecting Site 1 as a solar panel installation site

Pros	**Cons**
Flat land surface and topography	Corn field (agricultural land use)
Proximity to transmission lines	Proximity to residential houses
Relatively large area	
Ideal shape/ compactness	
Located far from city center	

For the second potential site (Site 2) considered in this study, corresponding groundtruth observations and maps are shown in Figure 5.34 with a Google street view shown in Figure 5.34 (B). The street view shows that several trees are located along the northern boundary of the site. Photographs taken from the on-site assessment show more information about the surrounding land use and local environment. The first site view picture is shown in Figure 5.34 (C), and the direction and position from which the picture was taken is highlighted in red in Figure 5.34 (A). Although the picture was taken on a winter day with heavy snow cover, the cropland and agricultural land use is still evident. A grove is also identified along the eastern side of the cropland area, while the western side of the cropland is occupied by residential land use, which was identified as open

space in the land use data. The direction and position from which the photo was taken are shown in blue in Figure 5.34 (A). Both groundtruth photographs verify that the potential site is flat in topography and the areal dimensions are also quite suitable for solar PV placement. The presence of a nearby transmission line was also verified during the on-site assessment.

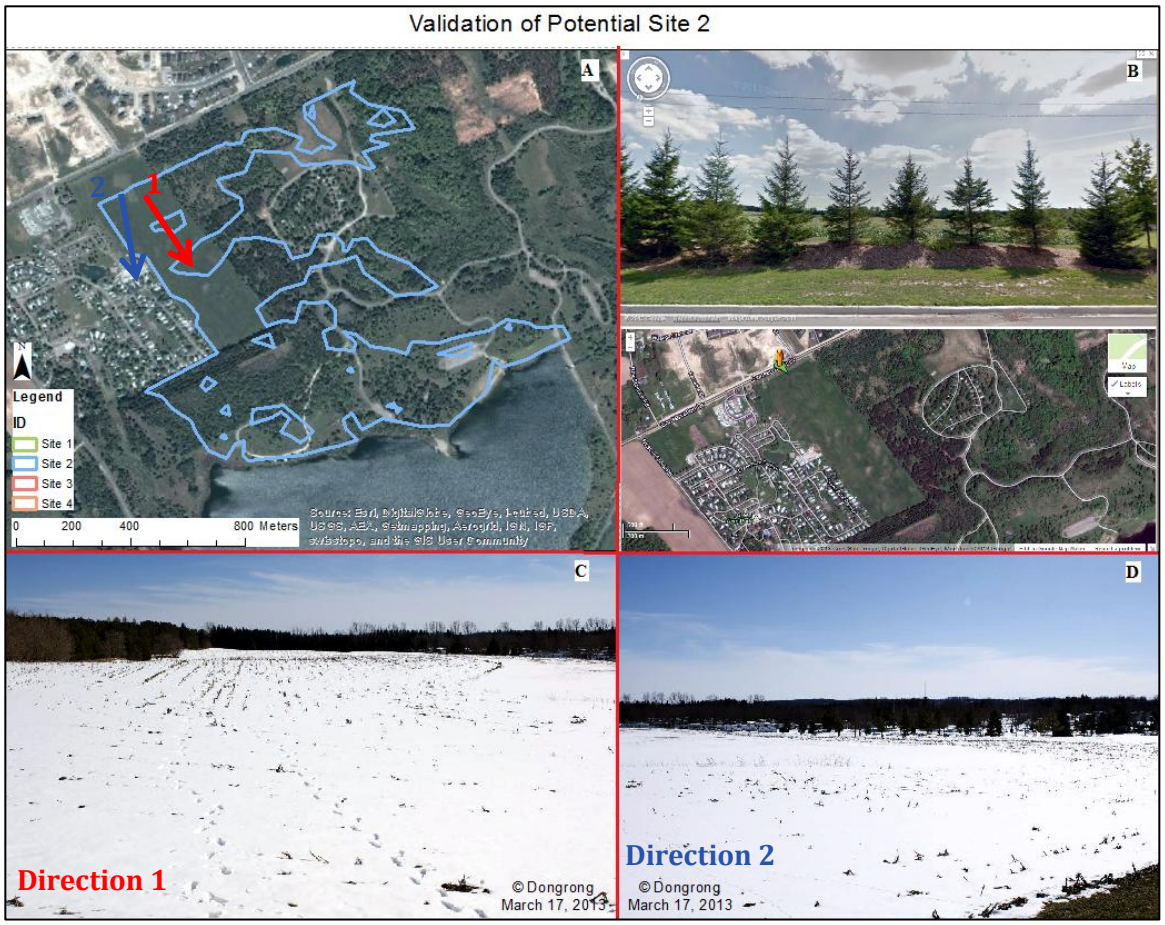

Figure 5.34 - On-site view from two directions for Site 2 validation. **A.** Selected Site 2 with two labeled observation directions 1 and 2; **B.** Google street view of Site 1 from direction 1, and satellite image with street-view position; **C.** Photo taken from direction 1; **D.** Photo taken from direction 2

Based on groundtruth observations, advantages of selecting this site for solar PV installation can be summarized as follows: 1) the flat topography reduces shadow effects; 2) close proximity of the site to transmission lines can avoid energy losses during transmission; 3) areal dimensions of the site is suitable for macro-scale ground-mounted PV panel installation; and 4) the compact dimensions of the site is conducive for PV array installation. However, ownership of the agricultural cornfield should be considered

for future decisions relating to land use planning. This selected site also occupies a large area of groves and trees at the northern Columbia Lake, which should be eliminated due to environmental concerns. Since the site is located in close proximity to residential land use and water bodies, the aesthetic and recreational value of the land may be important considerations when developing this site. Average annual solar radiation of this site is about 1,183.5 kWh/m^2. The advantages and disadvantages of the site for solar panel installation are summarized in Table 5.2.

Table 5.2 - Advantages and disadvantages of selecting Site 2 as a solar panel installation site

Pros	**Cons**
Flat land surface or topography	Agricultural corn field and groves
Proximity to transmission lines	Proximity to residential houses
Large land area/size	Proximity to ESA/water bodies
Ideal shape/ compactness	

Figure 5.35 shows on-site pictures taken for the third and fourth sites (Site 3 and 4) identified for solar panel installation. In Figure 5.35 (A), the third and fourth sites are highlighted in red and orange, respectively. Since no streets are located around these two sites, a Google street view picture was not available. Figure 5.35 (B) shows a photo taken at the northern Site 3 with the position and direction of taking this picture highlighted in Figure 5.35 (A). Since the picture was taken on April 9th, 2013, snow cover was melting with more bare ground visible. Several transmission lines located within the selected site were readily observable. Pictures shown in Figure 5.35 (C) and (D) were taken within the Site 3, as shown in Figure 5.35 (A) marked in blue and green, respectively. Site 4 can also be seen in pictures shown in Figure 5.35 (C) and (D). Site 3 was identified as cropland land use, while Site 4 was identified to be an active landfill site. Unlike Sites 1 and 2, both Sites 3 and 4 have more variable topography and the area is not flat, while Site 3 has a more level land surface than Site 4. Referring to the slope map shown in Figure 5.31 (C1), the gradient of Site 3 is less than 4%, whereas Site 4 has a steeper surface due to the landfill structure. Even though the slope in this area is relatively steep, the land surface is more or less south facing. Based on ground truth observations, it was observed that a newly developed commercial area is currently being constructed along the eastern side of the sites.

In order to verify the suitability of the landfill site for solar energy development, more information about the Waterloo landfill was acquired from its municipal website. The official map available for the landfill is shown in Figure 5.36. The Waterloo Landfill with an area of approximately 1.26 km^2 includes the original landfill area and the north and south expansion areas. From Figure 5.35 (A) and Figure 5.36, it was determined that the northern Site 4 is the original landfill site, whereas a small part of the area towards the south is the newly expanded landfill site being developed to receive municipal waste.

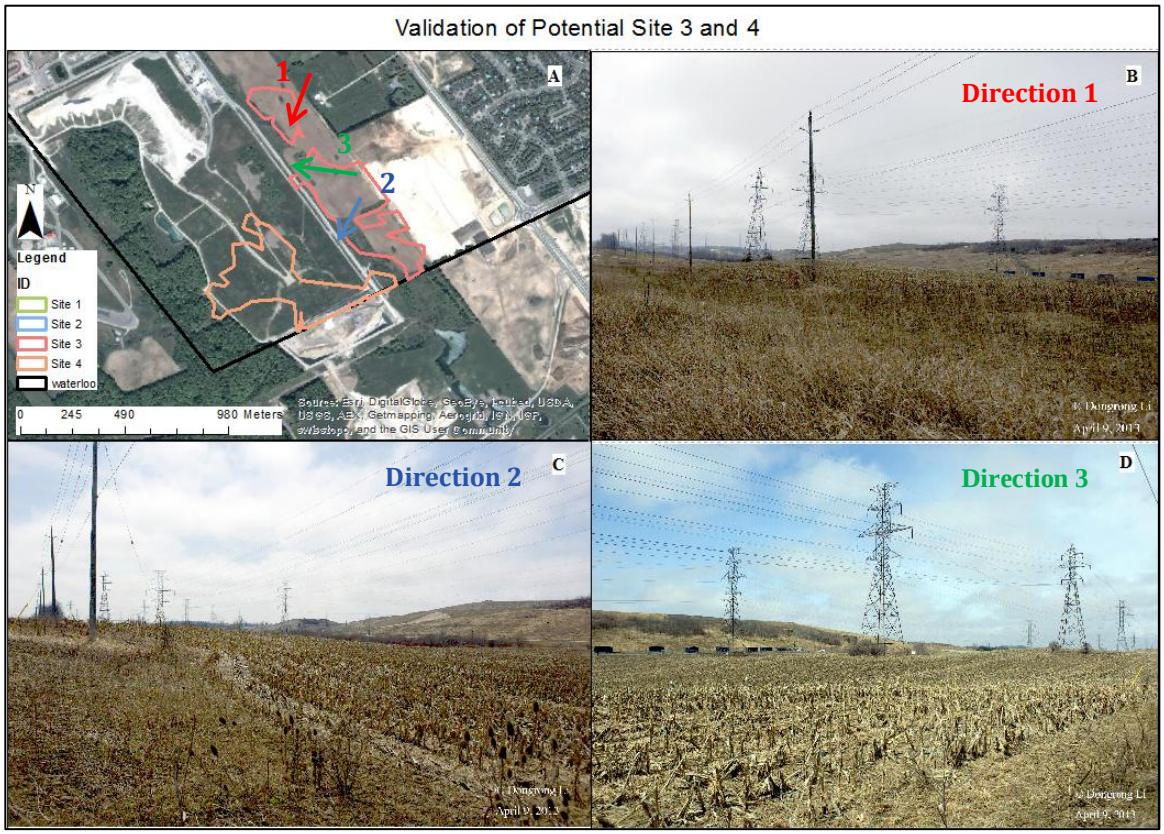

Figure 5.35 - On-site view from three directions for Site 3 and Site 4 validation. **A.** Selected Site 3 with three labeled observation directions 1, 2, and 3; **B.** Photo taken from direction 1; **C.** Photo taken from direction 2; **D.** Photo taken from direction 3

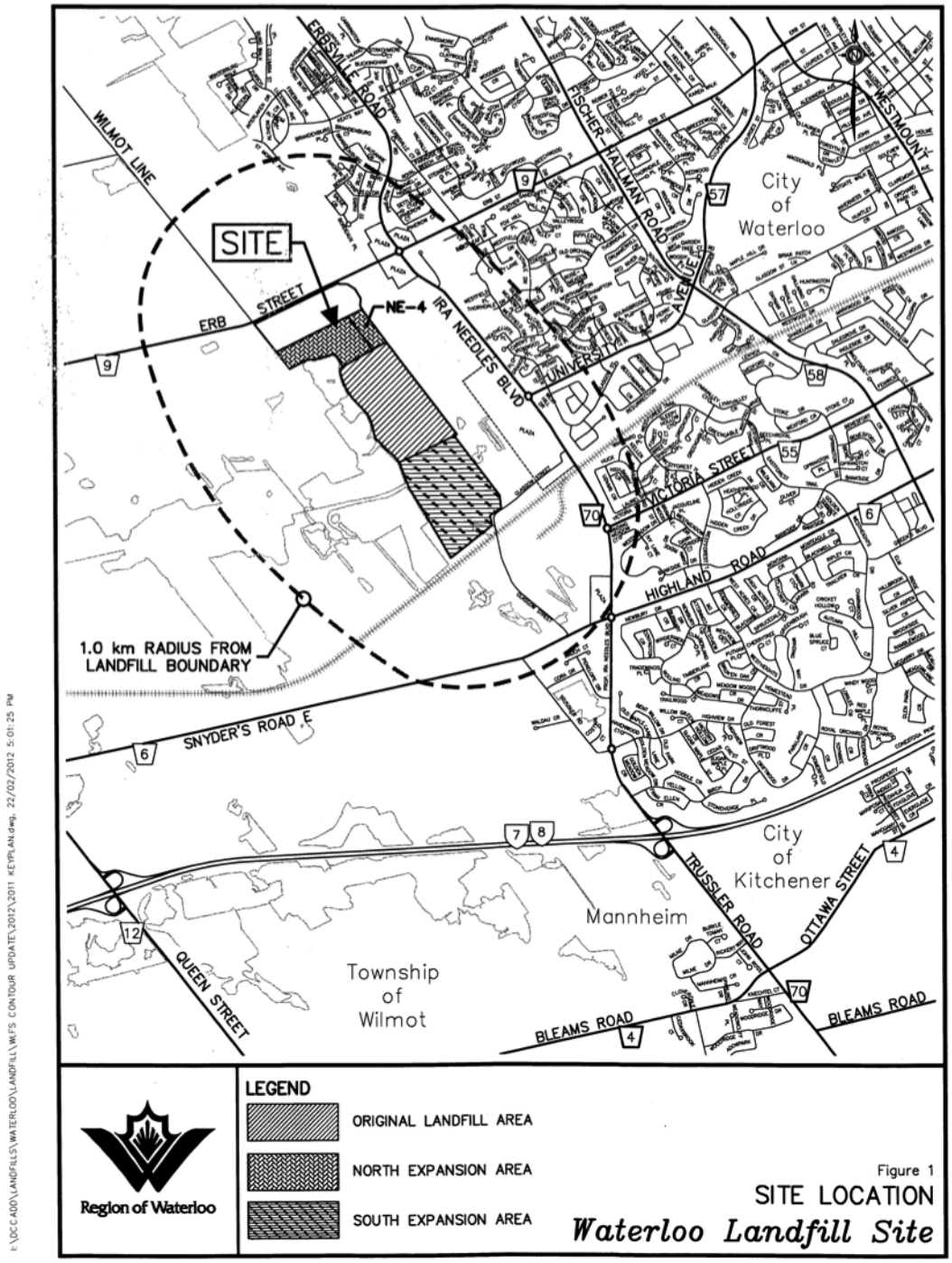

Figure 5.36 - Map of the Waterloo Landfills (Region of Waterloo, 2012)

The advantages and disadvantages of Site 3 for being developed into a potential PV site are summarized in Table 5.3. Benefits include a flat land surface providing ideal topographic conditions for PV panel installation. The location far away from residential

land use also reduces concerns related to aesthetics and/or recreation. However, since the site is located close to commercial land use, it may be more susceptible to vandalism from passersby. The neighboring landfill site may also contribute more dust pollution, which may reduce PV panel efficiency. Three transmission lines are located inside the chosen site, which may benefit energy transmission and reduce losses. However, with the presence of lattice towers, solar panel installation should avoid such structures. Average annual solar radiation of Site 3 is about 1,184.8 kWh/m^2.

Table 5.3 - Advantages and disadvantages of selecting Site 3 as a solar panel installation site

Pros	**Cons**
Flat land surface or topography	Proximity to commercial land use
Located away from residential houses	Dust risk from landfill
Proximity to transmission lines	Lattice towers on the site

Table 5.4 summarizes the advantages and disadvantages of Site 4. As previously discussed, the slope of this site is almost southern oriented and thus ideal for maximizing solar exposure. Similar to Site 3, Site 4 is located in very close proximity to transmission lines, which is vital for saving energy transmission costs from a future solar power installation. Also, this site is located far away from residential houses. Although this area is currently an active landfill site, once the landfill life cycle is completed, the former dump may be an ideal site for conversion into a site for a PV farm operation. Examples of where former landfills have been successfully converted into solar projects include the Forbes Street Landfill project in Rhode Island and the Hickory Ridge Landfill project in Conley, Georgia. The Forbes Street Landfill project has approximately 13,000 solar panels installed over 0.12 km^2 of the 0.89 km^2 site (Rupp, 2013). For the Hickory Ridge project, within over 0.19 km^2 of the total area, an integrated 1 MWp PV array is located on the southwest and southeast slopes of the landfill in an area approximately 0.04 km^2 (HDR, Inc., 2013). If successfully implemented, Site 4 has potential to be developed into a PV farm that could cover about 0.09 km^2 of area. Average annual solar radiation of Site 4 is about 1,216 kWh/m^2, which is much greater than other sites.

Table 5.4 - Advantages and disadvantages of selecting Site 4 as a solar panel installation site

Pros	Cons
Southern facing slope and topography	Developed landfill area
Former landfill solar project potential	
Proximity to transmission lines	
Located far away from residential houses	

5.3. Survey

The questionnaire survey was designed to acquire information about how solar companies in Ontario select potential sites for solar PV installation. Factors and adopted data in solar panel site selection by the participated companies and the present study are compared. During the survey, three responses were received from Company A, B, and C, and the response rate is 15%. Two of the companies service residential customers for the roof-mounted installations. Grid-connected solar systems were identified as more popular with customers, since no batteries are required and less maintenance costs are entailed. One of the companies surveyed is a solar panel manufacturer, and their customer types include the installer, developer, farmer, and small and large contractors.

Table 5.5 summarizes the data used, factors considered, and challenges faced during solar panel installation projects cited by the three companies. The three companies are arbitrarily referred to as Companies A, B, and C to protect their identify for confidentiality reasons. All three companies regularly referred to Google maps and Google street view for preliminary site assessment. However, Company A also referred to building survey plans in diverse forms, such as CAD drawing maps. Building survey plans include information such as interior/exterior buildings/rooms/yards dimensions.

The main client type of Company B is residential. In addition to using Google maps and Google street view for preliminary site assessment work, they also employed satellite and aerial photo images for initial screening of sites and to conduct site measurements for more detailed assessment. Company C indicated usage of Google maps and GIS datasets online or from municipalities for acquiring initial site observations. Detailed on-site measurements were then conducted or else building survey plans were consulted for more detailed analysis.

Table 5.5 - Survey results of data used, factors considered, and challenges faced during solar panel installation projects by three Ontario solar energy companies

	Company A	**Company B**	**Company C**
Data	Google maps/street view	Google maps/street view	Google maps/street view
	Building survey plans	Satellite & photo imagery	GIS datasets
		Site measurements	Site measurements
			Building survey plans
General Factors	Building dimensions	Available surface area	Building dimensions
	Shadow effect	Tree & building shadows	Shadow effect
	Snow impact	Roof surface orientation	Obstructions (e.g., chimneys, vents, etc.)
	Height of the array (Flat roof)	Minor factor: building height	
	Tilt angle		
	Pitch		
	Loads		
	Operating temperature (e.g., air gap)		
Challenges	Good building survey	Good building survey	Extra weight of panels to roof
	Accurate structural analysis	Accurate structural analysis	Proper mounting to avoid leaks
	Efficient array design and setup	Considerate planning	
		Skillful execution of installation work	

In terms of factors taken into account for solar panel site assessment, the companies surveyed in this study all mentioned availability of surface area/dimensions and shadow effects as primary considerations. Company A also considered the impact of snow cover on system performance during wintertime. In order to avoid obstructions caused by solar arrays, the height of PV arrays on a flat roof and tilt angle of the arrays were considered in the primary assessment. Company A also considered roof pitch of the flat building roof, as well as roof load or mass. For panel performance, the increasing operating temperature caused by air gaps or deflector impacts was another concern expressed by Company A. Other than the dimension and shadow effects, Company B considered roof surface orientation for the optimal site selection in order to maximize solar exposure. Building height was cited to be a minor factor. For Company C, considerations included structures or obstructions such as chimneys, vents, skylights, etc. on the rooftop.

In order to install PV panels correctly, both Companies A and B found that lack of good building survey plans and accurate site data adversely affects the accuracy of the site structural analysis of potential sites. In addition, building and design code compliant arrays are considerably challenging to install, since an efficient PV array system could cost more than a less efficient system. For Company B, primary challenges were identified as planning of array installation location and support locations, as well as skillful execution of installation work. However, according to Company C, since the building structure is not designed for supporting the extra weight of solar panels, roof upgrades were considered to be much more important than the installation itself. Therefore, appropriate evaluation of roof support and extra prohibitive costs of significant roof reinforcement can be challenging and deter potential clients from proceeding with a solar project. Another challenge cited by Company C was the avoidance of leaks with properly mounted solar panels or damage to rooftop structure during the installation process. Usually solutions are to use new technology that does not penetrate the roof or use highly trained installers and have someone double-check every penetration. After the installation, two inspections during the first 4-year of service was provided by one of the companies, while another installer had data monitoring on their systems, performing maintenance as required by automatic email reports.

Even though the surveyed companies mostly serviced residential customers, all of the companies provided their perspective on considerations for ground-mounted PV panel placement. In particular, from an environmental perspective, Company A speculated that ground-mounted solar panels may lead to potential soil loss. It was suggested that an appropriate landscape orientation should be determined. In addition, an ideal landscape orientation can help to reduce snow cover and reduce shadow effects. Company B suggested proper zoning for subsidy programs and proximity to grid infrastructure as essential factors for site selection of a ground-mounted PV array. Company C indicated that ground-mounted systems are limited to building on certain types of land (i.e., non-productive land) and proximity to electrical transmission infrastructure as primary considerations.

5.4. Chapter Summary

This chapter introduced potential solar panel installation site selection results at the micro and macro scales and presented responses from a questionnaire survey of three Ontario solar companies. For the micro-scale analysis, solar radiation availability was considered as the main criteria for selecting optimal sites for rooftop-mounted solar installations, while the macro-scale analysis considered additional factors, such as environmental criteria in its site assessment.

For the micro-scale study, monthly and yearly solar radiation maps of selected buildings on the University of Waterloo campus were adopted for spatial solar radiation variation analysis and standard deviation maps were generated for temporal solar variation analysis. In order to easily identify shadows on building rooftops, a shadow mask for each building was generated. According to the solar radiation maps and corresponding shadow masks of five campus buildings, it was observed that building roof edges and lower elevation rooftops tend to receive less incoming solar radiation compared to other parts of the rooftop. In addition, roof obstructions cause significant shadows to be cast over surrounding areas and disrupt incoming solar radiation from being received. Furthermore, southern parts of the rooftops receive a greater amount of solar radiation throughout the year due to the solar incidence angle. Similarly, for tilted rooftops, the south-oriented roofs receive more radiation than other parts of the building roof structure. Therefore, roofs with a southern exposure without obstructions were considered as sites with the highest potential for rooftop solar installations.

For the macro-scale site selection study, apart from incoming solar radiation, other factors such as environmental, economic and efficiency factors were taken into account when considering ground-mounted solar installations. After ranking these factors using AHP and integrating them in an MCA, four potential sites located at the periphery of the city were identified. All of the sites were large enough in terms of area and dimensions to be suitable for siting centralized ground-mounted PV plants or so-called solar farms. The MCA was supplemented with groundtruth observations to better inform the site selection process. An on-site feasibility assessment involved obtaining observations and verifying

land use type, transmission lines, slope and aspect, as well as inspecting the surrounding environment. Sites 1, 2 and 3 were identified as cropland, whereas Site 4 was located on a landfill site. Sites 1 and 2 were both located on relatively flat land, while Sites 3 and 4 were situated on a relatively rugged terrain. Since Site 3 and 4 are south-oriented, sunlight can still strike the land surface. From a land use change perspective, converting completed landfill sites to solar farms provides long-term environmental benefits in comparison to converting cropland or agricultural fields. Therefore, among the four selected sites, Site 4 is the most ideal site for ground-mounted solar panel installations.

A questionnaire survey was distributed to 20 Ontario solar companies to consider current business practices in the thesis project. Three companies responded to the survey, indicating Google maps/Google street view as commonly used references for preliminary site analysis. They also used different data sources for analyzing rooftop structures, such as building survey plans and GIS datasets. Even though factors taken into account during the site selection process varied, the primary factors considered by all solar companies were site dimensions and shadow effects which was consistent with the criteria used in this study. Accurate roof structural analysis and appropriate solar panel installation practices were commonly cited as primary challenges for any solar energy project.

Chapter 6. Discussion and Conclusions

The first section of this chapter discusses limitations regarding the data used in the micro-scale analysis, and compares it with data considered by solar companies surveyed in this study. Differences in the solar panel site selection process between surveyed solar companies and considerations from this GIS study were also compared. This section concludes with discussing the findings from the site selection analysis of UW campus buildings. In the second section of this chapter, limitations and summary findings of the macro-scale level study are discussed. Finally, the third section discusses limitations of this research and future work that could be carried out for improving the solar panel installation process.

6.1. Micro-scale Analysis

6.1.1. Data

Availability of incoming solar radiation and shadow effects were the primary considerations when assessing potential solar panel installation sites on building rooftops. The solar radiation calculation was implemented by the area solar radiation tool in ArcGIS associated with elevation data as the primary input. The elevation raster was derived from LiDAR point cloud data collected in 2006. Since the data were collected six years ago and several new buildings on the UW campus have since been constructed, including Environment 3 (EV3), it was not possible to model shadow impacts of these new buildings and to factor them into the analysis. A source of error in this study is dated DEM data and the lack of accurate and up-to-date building plans that include the new EV3 building. Moreover, obstructions on or around rooftops may change as time progresses, including surrounding vegetation and tree growth, which will also change shadow effects on rooftops.

The accuracy and quality of collected LiDAR data were not investigated in this study. The data have known geometric errors due to systematic and random errors from the instrument during the collection phase by Optech. Geometric calibration could not be performed without available ground control points (GCPs) for reference. Consequently,

the elevation and georeferencing of buildings may not be very accurate, which may result in errors in the solar radiation estimations. Fortunately, information about rooftop structures could still be achieved from recorded elevation information, which allows for reliable assessment of spatial patterns of incoming solar radiation. In other words, although the absolute heights of buildings were not recorded correctly during the LiDAR data collection phase, the relative comparisons of the buildings' roofs were correct. Based on these heights, roof structures can be easily recognized and analyzed. All of the analyses at the micro-scale level were based on solar radiation maps deduced from LiDAR data.

In the survey of Ontario solar companies conducted for this study, it was found that it was commonplace for companies to refer to Google maps/street view for preliminary observations of potential sites. However, on-site measurements provide the most accurate information about rooftop structures, allowing for more detailed assessment of potential sites for solar panel installation. Building survey plans are also commonly used for detailed assessment of roof structures. However, these can be difficult to obtain. If on-site measurements cannot be performed, or accurate building survey plans are unavailable, this study has shown that using LiDAR data can provide another means of assessing roof structures.

To better assess the application of GIS techniques and remote sensing for solar panel site selection, advantages and disadvantages of Google maps compared to LiDAR data are summarized in Table 6.1. Google maps provide the easiest way for people to view the building roof without any costs, whereas LiDAR data are expensive to acquire. Applying Google maps is much faster and accessible than LiDAR data for the preliminary assessment, since LiDAR point clouds require calibration and processing before being used for analysis. In addition, the Google street view provides a direct view of houses, especially those with pitched roofs, which enables more information in the preliminary analysis. Nevertheless, trees and other structures can obscure the view of houses and pitched rooftops. Moreover, Google street view is only available for areas were roads/streets are accessible and may not be regularly updated.

Table 6.1 - Advantages and disadvantages of using Google map/Google earth and LiDAR data for solar panel site selection

Google map/Google street view	**LiDAR data**
Pro	**Pro**
Easy access and zero cost	Available elevation & geographic position raw data
Much faster access for preliminary assessment	Able to build 3D model for visualization
Direct and high-resolution view of houses by Google street view	High spatial resolution dataset
3D view by Google earth	No cloud cover
Con	**Con**
Limited display of Google street view	High cost for data acquisition
Availability of data based on road accessibility	Expertise required
No elevation or raw data available	Software for processing
Inconsistency of data at various spatial scales	
Outdated data issues	
Cloud cover	
Google maps unavailability of some regions	

Furthermore, LiDAR data do not show visual images of the area of interest, but only its elevation and geographic location information that can be used to build a 3D model. Although Google Earth enables users to have a 3D view, similar to LiDAR data, the basic free version of Google Earth does not provide access to the raw elevation information. Since Google maps apply a pyramid structure to display different satellite images for the same site based on the required spatial resolution at a particular scale, satellite images with different resolutions may show different levels of detail for the same location due to different dates of acquisition. For example, images for a specific region could be taken in August 2011, but a larger-scale image could be taken in October 2011. Changes during this time period would be missing or inconsistent between scale levels, such as a newly constructed facility. Spectral differences in images may also affect data compatibility, such as an image captured on a sunny versus cloudy day. Information shown in the maps will be inherently different. Since LiDAR measures distances by illuminating a surface with an optical laser beam, cloud cover is generally not a concern.

6.1.2. Factors

As previously described, solar radiation availability and shading effects are two main factors for determining optimal sites in the micro-scale building site assessment, while shading effects were taken into account during the solar radiation calculation. However, incoming radiation estimates may not be accurate, since the estimates are highly dependent on weather conditions, while in this study, only clear sky conditions were considered. As a result, potential energy production was estimated based on an ideal circumstance, and actually results would be less than the estimates.

The solar radiation model in ArcGIS requires several parameter settings, which can impact output radiation estimates. In particular, the day interval setting of the monthly-accumulated solar radiation calculation was set as seven days, and hour interval was set as one hour. The smaller the interval is, the more accurate the solar radiation is estimated. For example, a seven-day interval calculation applies one-day solar radiation results to represent results of the other six days within a seven-day period, and ignores variations existing in the seven days. However, the processing time will increase dramatically due to the required iterations, especially when the spatial resolution of the input elevation data is high. The time interval was tested with a variety of settings, including daily interval settings, as well as half-hour and one-hour settings. The test results did not show apparent differences, suggesting that the default seven-day and one-hour settings would be sufficient and help to achieve a balance between accuracy and processing time. The sky size parameter specifies the resolution of the viewshed, sky map, and sun map rasters that are used in the radiation calculations. Since sufficient resolution is required to adequately represent all sky directions and sun positions, the larger the sky size is, the more accurate calculation is achieved; however, calculation time increases considerably. A resolution of 1,400 cells per side was adopted in this study, which was set high enough for sun tracks to be achieved with a 7-day interval (ESRI, 2011).

The remaining two parameters in this model that will lead to a significant difference in radiation estimation calculations are the diffuse proportion and transmissivity parameter settings. As mentioned in Section 4.1.1, different combinations of the two parameters will lead to different solar radiation values estimated. However, comparing

the solar radiation maps under overcast and clear-sky conditions shown earlier in Figure 5.1 as an example, spatial patterns of solar radiation of the area of interest were almost the same. That is, roof surface areas receiving high solar radiation or affected by shadows are consistent between overcast and clear-sky conditions. The only differences of different conditions were the ranges of solar radiation values (Appendix B). Therefore, the two parameter settings do not appear to have a significant impact on the site selection findings.

According to Table 5.5, the solar companies surveyed in this study consider a range of factors in the site selection process. Most of the criteria relate to solar radiation availability and shadow effects, which are consistent with the adopted methodology of this study. However, some factors considered by the solar companies, including the solar array height and space between arrays were not incorporated into the GIS analysis based on a number of constraints. For some buildings, array height is usually limited with a specific value for ventilation. The total amount of solar radiation received at the Earth's surface varies seasonally. Solar radiation flux reaches its maximum during the summer months, which in turn, will have a higher impact on the yearly optimum tilt angle. It is also important to consider that a minimum structural setback from roof edges should be applied for safety. This factor was discussed in this study but was also not considered by the companies included in the survey.

Roof load and penetration were not considered in this study due to a lack of detailed roof information. According to Finamore et al. (2002), the flat rooftop of FED Hall cannot support PV panels if snow or rain covers are not removed. For roofs that can only support thin and lightweight PV panels, roof penetration may be required during the installation process for improved stabilization. However, penetration can also increase the probability of roof leakage. Apart from using this approach to stabilize the panels, mounting with concrete or steel bases that use weight to secure the panel system in position is also a commonly adopted approach. Given that the optimal site for receiving solar radiation is chosen, the next stage should entail an evaluation of roof structural capacity. A full building assessment should consider the necessity of additional roof reinforcement before making recommendations for solar panel installation.

Finally, a remaining factor that was not considered in this study was snow cover. In the wintertime, snow cover on solar panels is a concern for areas usually affected by heavy snowfall and may significantly reduce electricity output. Flat rooftops are usually more affected than pitched roofs. Heavy snow cover leads to extra weight to the building roof and snow cover also prevents solar panels from receiving sunlight. Snow removal maintenance is seldom provided during the wintertime, thus roof load capacity should be considered prior to solar panel installation. Snow cover was not considered in this study, since it was difficult to model and to mask out covered regions of rooftops accurately during wintertime conditions, and also the accumulated snow on solar panels varies when solar panel tilt changes.

6.1.3. Micro-scale Selection

In this study, areas consistently receiving large amounts of radiation throughout the year were selected as optimal sites for solar panel installation. Patterns of building electricity demand and usage should be considered in the assessment. For example, the PAC main rooftop receives the highest monthly radiation of approximately 174 kWh/m^2 in summer, especially in June and July, whereas it receives little radiation in the winter. If the PAC consumes more energy for heating in the wintertime but less power during the summer, solar panel installation on the main rooftop may not meet seasonal energy demands. However, the generated solar energy during summer may assist with powering air conditioning units for cooling. Heavy snowfall during wintertime may also cause snow cover on solar panels and reduce solar exposure. Similarly, the FED Hall main rooftop receives the highest amount of solar radiation during the summertime but relatively less radiation during winter. Therefore, if more electricity is required for powering air-conditioners during summer months, rooftop mounted solar panels may be quite useful for assisting to meet seasonal energy demands.

Shadow masks were created for each building to distinguish shadow-cast regions of building rooftops from exposed areas. The shadow mask shows the probability of shadows being present or absent on average throughout a year. For each month, a threshold for distinguishing shaded and unshaded areas was selected based on differences

in solar radiation intensity, which was analyzed using the solar radiation histogram and corresponding solar radiation map and aerial imagery for spatial interpretation and analysis. The selected thresholds for separating shaded/unshaded areas are subjective due to the fuzziness between shaded and unshaded areas. A threshold with small solar radiation values considers more areas as suitable sites than a threshold set with a large solar radiation. Solar radiation values greater than the defined threshold were categorized as unshaded, whereas values less than the threshold represented a shaded scenario. After determining a threshold for each month, a shadow mask was then generated. Since areas with a shadow probability of less than 25% have less than three-month shadow risks, and these low shadow probabilities only occur in the winter months, when solar radiation intensity is the weakest, classifying these areas as unshaded is reasonable. As the shadow probability increases, solar radiation receiving amount reduces dramatically.

With the monthly- and yearly-accumulated solar radiation maps and classified shadow mask, suitable sites on each building rooftop were easily identified. According to the radiation maps and shadow mask of the PAC building, it was determined that the main, eastern, and southern rooftops were the most suitable site for mounting solar panels. If energy demand is higher in the summer, the northern and western rooftops (labeled in Figure 5.6) are additional sites that could be considered for PV array installation.

The two EV buildings have a more complicated roof structure than the PAC rooftops due to the presence of structural obstructions, such as stacks. Since the EV rooftop has a pyramidal glass roof (i.e., skylight), as well as stacks and two roof constructions, available space for solar panel installation is limited compared to the PAC. According to the shadow mask of the EV buildings (Figure 5.11), among areas available for panel installation, most of the northern side of the EV buildings is susceptible to overcast shadows over the year, while the southern sides were considered to be suitable for solar panel installation.

The DP Library rooftop has the most complex structure and the most limited space for PV panels among the five buildings examined in this study. Due to the greatest building height across the campus, its rooftop shows the maximum solar radiation

receiving amount in July compared to other studied buildings. Results from this study suggested placing solar panels along the southern side of the roof, although the physical dimension or available area may be a limitation. The final selected site of the library rooftop has an area dimension of 118 m^2. If a 1-meter setback is required, the final dimension would be reduced to about 90m^2. The 1st floor rooftop of the library is another option available for solar panel installation. Comparing the southeastern and southwestern sides of the 1st floor rooftop, this study found that the southeast rooftop received a greater amount of solar radiation, although less physical space was available.

For FED Hall, the southwest slanted roof received consistent incoming radiation throughout the year and was determined to be a suitable location for PV installation. The main/central rooftop can also be considered for solar panel installation, since a high level of radiation is received during summer months. From the shadow mask results, areas with a shadow risk less than 25% include the main roof, southeast and southwest tilted roofs, and northwest lower rooftop. When the constraints are weakened to 25% to 50% shadow risk, selected sites on the northwest lower roof are included, increasing by 31 m^2. However, the average annual solar radiation reduces as the constraints are weakened.

The V1 student dormitory was the final case study at the micro-scale level of analysis. From the results presented in Section 5.1.5, a group of rooftops on the south of the site consistently received high incoming solar radiation throughout the year, demonstrating good potential for solar panel installation. As previously mentioned, new vegetation or tree growth will change shadow effects, especially along building perimeters or rooftop edges. Therefore, rooftops shaded by trees may vary from season to season. As shown in the radiation maps, these roofs have small stacks, which cause shadows. If the height of solar panel installations is set high enough, it may be possible to avoid shadow effects. For the center main rooftop, although its large areal dimension is suitable for panel installation, the complex roof structure and obstructions would likely cause significant shadow effects. According to Figure 5.28 (B) and 5.29, areas that are temporarily affected by shadows from a chimney on the southern main rooftop are considered as suitable site due to a loose shadow threshold selection. If shadow

thresholds are set rigorously with high solar radiation values, most southern areas of the main rooftop will be eliminated.

6.2. Macro-scale Analysis

6.2.1. Data and Factors

This study applied MCA to select suitable sites for solar panel installation in the City of Waterloo. Similar to solar radiation estimation for the micro-scale building level, estimation for the macro-scale area was also obtained using digital elevation information and the ArcGIS radiation tool. The elevation data of the City of Waterloo was a 10 m spatial resolution DEM (Appendix A). Compared to the LiDAR data used in the micro-scale analysis, the DEM data have a relatively coarse spatial resolution. In addition, the DEM data only contain elevation information of the bare earth. Therefore, land surface features were not considered in the solar radiation, slope and aspect calculations. However, since only open space and agricultural land uses were considered as accessible lands for solar panel placement, building height information was not critical to this study. As a result, trees may be selected as ideal installation sites, which should be filtered out by subsequent analysis with land use data or aerial imagery. In light of the significant processing time required for solar radiation calculations, higher spatial resolution datasets may not have been desirable or beneficial to this study.

Compared to criteria used in the previous micro-scale study, this analysis only included important criteria when considering the study area location. As previously mentioned, the solar radiation calculation tool in ArcGIS already accounts for atmospheric effects, site latitude and elevation, land surface steepness and compass direction, daily and seasonal shifts of the sun angle, and effect of shadows cast by surrounding topography. Therefore, topography, including slope and aspect, may not have been critical to consider in the MCA. However, considering the importance of topography on solar radiation spatial variability, slope and aspect were still nevertheless included, although perhaps redundant. As regards to their relative importance, since amount of solar radiation received is dependent on solar panel tilt rather than topographic

slope after installation, assigning less weight to topographic slope compared to solar potential and topographic aspect was reasonable.

Weather conditions were not considered due to their instability and unpredictability and the difficulty with modeling cloud patterns. In reality, atmospheric conditions could range from overcast sky, clear sky, partly cloudy sky, direct sunlight, to uniform sky. As mentioned in previous sections, even though radiation values vary depending on the sky conditions, relative spatial variation or pattern of radiation was deemed to be more essential to the site selection process than obtaining accurate absolute radiation values. Therefore, the solar radiation of the study area was calculated under clear-sky conditions.

Since radiation values were not used for estimating total energy supply from potential sites, an energy demand-supply balance calculation was not included in the final site analysis. Population density for energy demand estimation was not included, since the study was not an economic assessment of potential sites, but focused primarily on physical, environmental, and land use criteria for site selection. Since the goal of this study is to determine optimal sites within the city, configuration of final solar panel installations was treated as a subsequent consideration. The detailed visual impact to surrounding residential communities was also not considered to be an important criterion, although this could be studied separately as a viewshed analysis. Further development of the site for solar energy generation would also require consultation with neighbors, as well as additional urban planning and land zoning details. It is important to note that factors such as flood pathways, dams, and cultural heritage sites were not included in the analysis, since land cover and land use were more critical in the site assessment.

For dust risk assessment in the MCA, the sand content in soil, proximity to pit and quarry sites, and distance to roads were considered. Locations with pit and quarry land uses within the study area were excluded. Since adjacent roads can increase dust pollution in the air, potential solar installation sites should maintain a certain distance from road networks. Since the road density in the City of Waterloo is relatively high, a buffer of more than 50 m would exclude most parts of the city. Roads located far away from the site would be costly to construct. Given such considerations, a buffer radius of

10 m around major roads was adopted in this study. Wind speed was also considered to be an important factor contributing to dust. However, due to unavailability of detailed wind speed data, this criterion was not considered in the final analysis.

6.2.2. Macro-scale Selection

MCA is an approach used to assist decision makers to choose between alternative choices according to criteria, some of which may be conflicting or controversial. This context often leads to an absence of an absolute optimal or perfect solution. Theoretically, this method formulates recommendations, while decision makers maintain their freedom to make choices. In the sensitivity analysis of weight assignments, the geography of areas with the highest scores remains the same. Only the area size changes during the analysis, while the location of selected sites is relatively consistent, since the relative importance between or among criteria were retained during the test. For example, for the higher level criteria, since efficiency is the basis of economic benefits of a PV project, efficiency was considered to be more important than economic, and relative weight of efficiency was tested ranging from 2 to 4. If more various levels of relative importance, such as 1/4 to 4 between economic criteria and efficiency, were added to the sensitivity analysis, locations of selected sites may be changed. However, importance of criteria was set based on solar panel site selection requirements according to previous research studies and answers from the surveyed companies, and thus, the tested value ranges in this study were reasonable.

After the site selection process in this study, the assessment considered ground truth information and observations. The ground truth data provided information about the current land use type, surrounding environment, and verification of certain criteria. Since secondary data about a potential site could be out of date, on-site inspection is necessary to acquire current status information. For example, current information about transmission lines, new road construction, and new residential houses and commercial buildings proved to be useful to the site selection process.

Potential sites for ground-mounted solar installations were selected close to the periphery of the city. Four of the sites considered in this study had potential for

centralized PV power plants to be installed. For the first two selected Sites 1 and 2, their locations were close to transmission lines and located away from the city center. The terrain is flat, although private land ownership issues may be challenging to install ground-mounted solar arrays. During the site evaluation, new residential houses next to Site 1 were identified. Houses on the western side of Site 2 were also observed, which were originally indicated to be open space on the land use map. As a result, the selected sites could be more exposed, which could potentially lead to vandalism and concerns about aesthetics. Although Site 2 has the largest areal dimensions, the southern section consists of natural green open space and is also bordered by Columbia Lake, which is a conservation area. Consequently, the boundary of Site 2 should be further adjusted.

Sites 3 and 4 differ significantly from Sites 1 and 2 in terms of land use. In particular, Site 4 is not a quarry/pit site but an active landfill site, while Site 3 is within 1-kilometer radius of the landfills (Figure 5.36). Due to current landfill practices, these two sites cannot be used for solar panel placement at present. However, after the landfill life cycle is completed, the land could be reclaimed and re-developed as potential sites for clean energy technologies, such as solar power. Many examples of using landfills or brownfields as PV farms exist around the world today. For example, Hickory Ridge Landfill was once a mountain of trash sitting idle on the outskirts of Atlanta, Georgia (Snedden, 2011). Now it has been developed with plastic solar panels as shown in Figure 6.1. A similar solar landfill project is underway in Madison County, New York, where the energy generated from eight acres of panels is being used to run the recycling center next door (Snedden, 2011). Similarly, industrial contaminated lands or brownfields can be used to develop PV farms. For example, the U.S. Department of Energy is currently taking bids in Colorado to build a PV farm on a 42-acre former uranium mine site (Barber, 2012).

Figure 6.1 - A landfill site on the outskirts of Atlanta, Georgia covered 10 acres of land with plastic solar panels (Snedden, 2011)

Landfills have many advantages as potential sites for PV farm projects. In particular, the tall structure of landfills enables the area to be unobstructed by shadows and often at elevations higher than average tree height (Snedden, 2011). In addition, landfill sites provide the advantage of being located near urban areas without sacrificing valuable green space that contributes to the overall "quality of life" (Barber, 2012). The stable surface of landfills makes it suitable for mounting thin and flexible solar panels (Roberts, 2010). Furthermore, criteria for a landfill site to accommodate current solar technologies, include the site being fairly level with little vegetation cover, being located away from ESA, and being adjacent to the local utility power line grid (Barber, 2012).

Mounting solar panels on landfills has a variety of benefits. First, even though it may cost more to develop a PV farm than to clean up the landfill site and to establish a new business, solar arrays pay off with low maintenance costs and avoid landfill post-closure care costs (Roberts, 2010; Snedden, 2011). The usage of renewable solar energy also benefits carbon cap and trade credits (Roberts, 2010). The commercial value of a PV farm also has long-term benefits. Overall, the design of the solar array cover provides an easily maintained, durable, and stable surface that benefits landfill sites by providing long-term reliability from energy generation and environmental protection. A solar energy cover also helps "communities to pave the road to energy independence with creative land re-use and potential for widespread application on many other types of brownfields" (Roberts, 2010, par. 15). Overall, compared to Sites 1 and 2, Sites 3 and 4 may be superior choices for ground-mounted solar panel installation.

6.3. Future Work

According to the limitations discussed in Sections 6.1 and 6.2, improved data sources and incorporating more criteria could improve the solar panel mounting site selection process. For example, more accurate and calibrated LiDAR point cloud would enable more reliable incoming solar radiation amounts to be estimated for each building. Since the DEM derived from LiDAR point cloud was interpolated with 0.5 m spatial resolution, a better resolution (i.e., 0.2 m) could offer more structural details to be discerned. Although the point cloud density of this LiDAR dataset is considerably high, a denser point cloud may further improve roof structure analysis and provide more detail about the physical form and structure. Although high spatial resolution datasets would require more time to process, the accuracy of insolation estimates of the study area could be further improved.

Availability of other datasets as additional criteria could further improve site selection results. For example, in the micro-scale site assessment, building roof load or strength of the roof structure could improve the analysis, providing information indicative of the ability of the building to support the extra weight of PV panels. Moreover, rooftop texture and materials could be assessed. For example, the PAC has significant damages to the roof making it unsuitable for solar panel placement (Finamore et al., 2002). In such cases, appropriate roof refitting may be required. Before mounting PV arrays on a rooftop, solar panels height, tilt and distance between arrays are required to accurately calculate solar radiation, so as to avoid shading effects from other panels. When determining the shadow threshold for shading probability calculation, a fuzzy logic may be adopted for a more accurate representation.

In the macro-scale site selection, as discussed in Section 6.2.1, some criteria applied by previous research studies are not applicable to the City of Waterloo. Nevertheless, factors such as land ownership are necessary in the site selection process. As suggested by the surveyed companies, land cover and land use majorly limit the site selection; therefore, detailed land use plan and land information from the municipal government should be obtained. To address the aesthetics of a newly developed PV farm, producing a viewshed layer based on the residential houses present could help to address such

concerns. For the macro-scale on-site feasibility assessment, a more reliable assessment could entail consulting neighbors and conducting a household survey.

For both micro and macro scales, electricity demand and supply of the building or area(s) of interest should be assessed. In order to implement an economic demand and supply analysis, assumptions, such as daily or seasonal power usage for lighting, heating, etc., are necessary. The specific type of solar panel should then be determined according to budget availability and energy output expectations. Sky-condition indicators (i.e., transmissivity and diffuse proportion) in the solar radiation calculation can be adjusted using monitoring data from local weather stations for accurate solar potential estimation. However, a full energy supply-and-demand economical analysis was outside the scope of this study.

6.4. Conclusion

The rapid growth in the level of greenhouse gas emissions, the increasing amount of energy demand, and the increase in fuel prices are the main driving forces for turning to renewable sources of energy. Solar energy has few adverse environmental effects compared to conventional fossil fuels, such as greenhouse gas emissions or smog-causing pollutants, has become a preferred source of energy. The goal of this study was to select potential sites for mounting solar panels on both micro- and macro-scales of analysis. In order to find out how solar panel site selection is conducted in current business practices, a questionnaire survey was conducted involving select solar companies from Southern Ontario. This study demonstrated the use of spatial analysis and GIS techniques for identifying potential solar panel installation sites at micro- and macro-scales.

The micro-scale analysis was for roof-mounted solar panel installations. Five buildings on the UW campus were selected as case studies. Optimal locations on rooftops were determined based on the generated monthly- and yearly-accumulated solar radiation maps and shadow masks. In order to generate the solar radiation maps, this study applied the ArcGIS area solar radiation analyst associated with elevation data inputs. This model accounted for atmospheric effects, orientation, daily and seasonal shifts of the sun angle, and shading effect caused by surrounding topography. Ultimately, solar radiation maps

provide spatial distribution information of insolation amounts. Shadow masks derived from monthly solar radiation maps allow quantitative analysis of shadow effects during the year. According to the surveyed solar companies, since a lack of accurate detailed building plan and roof structure analysis data were a challenge during the site evaluation, spatial analytical method of this study shows another feasible approach for rooftop site evaluation.

The macro-scale ground-mounted solar panel installation site selection was conducted by considering a range of criteria. By adopting an MCA approach, environmental, economic, and potential generation factors were assessed. After selecting the potential solar installation sites for the area of interest, an on-site feasibility assessment involving collecting groundtruth data was conducted. In the City of Waterloo, four sites were identified as potential sites for ground-mounted solar farm installations. The most suitable site was identified as an active landfill, which may be suitable for future development into a PV farm project.

This study faced a number of data limitations that if addressed, could potentially improve site selection results. For example, a lack of roof strength data was a significant limitation to the micro-scale analysis. Access to a detailed municipal land use plan and potential energy supply and demand information could potentially improve the macro-scale analysis. Nevertheless, this study demonstrated a spatial analysis approach that integrated remote sensing data and GIS techniques for determining potential sites for solar power production. Site selection results proved to be realistic and were verified with groundtruth observations. This study demonstrates a proof of concept and workflow that can be effectively applied for solar panel site selection at both micro- and macro-scales of analysis

References

Aragonés-Beltrán, P., Chaparro-González, F., Pastor-Ferrando, J.P. and Rodríguez-Pozo, F. (2010). An ANP-based approach for the selection of photovoltaic solar power plant investment projects. *Renewable and Sustainable Energy Reviews*, 14, 249-264.

Armstrong, A.S. (2009). Sustainable energy management for a small rural subdivision in New Zealand: a thesis presented in fulfilment of the requirements for the degree of Master of Technology in Energy Management, Massey University, Palmerston North, New Zealand. Retrieved from http://mro.massey.ac.nz/handle/10179/1659

Aydin, N. Y. (2009). GIS-based site selection approach for wind and solar energy systems: A case study from western: a thesis presented in fufilment of the requirements for the degree of Master of Science in Geodetic and Geographic Information Technologies, Middle East Technical University. Retrieved from http://etd.lib.metu.edu.tr/upload/12610774/index.pdf

Bakirci, K. (2012). General models for optimum tilt angles of solar panels: Turkey case study. *Renewable and Sustainable Energy Reviews*, 16, 6149-6159.

Balenzategui, J. and Chenlo, F. (2005). Measurement and analysis of angular response of bare and encapsulated silicon solar cells. *Solar Energy Materials and Solar Cells*, 86, 53-83.

Barber, D.A. (2012). Using landfills for solar farms. Retrieved from http://pv.energytrend.com/knowledge/knowledge_solar_20120730_2.html

Ben Salah, C., Chaabene, M. and Ben Ammar, M. (2008). Multi-criteria fuzzy algorithm for energy management of a domestic photovoltaic panel. *Renewable Energy*, 33(5), 993-1001.

Beringer, S., Schilke, H., Lohse, I. and Seckmeyer, G. (2011). Case study showing that the tilt angle of photovoltaic plants is nearly irrelevant. *Solar Energy*, 85, 470-476.

Bielinskas, V. (2012). Efficiency of solar energy harvesting. Retrieved from http://www.mesg.nl/wiki/images/f/fd/Paper_VGTU_03.pdf

Bravo, J.D., Casals, X.G. and Pascua, I.P. (2007). GIS approach to the definition of capacity and generation ceilings of renewable energy technologies. *Energy Policy*, 35, 4879-4892.

Broesamle, H., Mannstein, H., Schillings, C. and Trieb, F. (2001). Assessment of solar electricity potentials in North Africa based on satellite data and a Geographic Information System. *Solar Energy*, 70(1), 1-12.

Buttery, P., DeAngelis, S., Carwardine, W., Sheridan, S. and Siren, K. (2004). The feasibility of implementing a solar energy system on environmental studies two. Retrieved from http://environment.uwaterloo.ca/research/watgreen/projects/library/f04solarones2.pdf

Calabro, E. (2009). Determining optimum tilt angles of photovoltaic panels at typical north-tropical latitudes. *Journal of Renewable Sustainable Energy*, 1.

Carrion, J.A., Estrella, A.C., Dols, F.A., Toro, M.Z., Rodriguez, M. and Ridao, A.R. (2007). Environmental decision-support systems for evaluating the carrying

capacity of land areas: Optimal site selection for grid-connected photovoltaic power plants. *Renewable and Sustainable Energy Review*, 12, 2358-2380.
Charabi, Y. and Gastli, A. (2011). PV site suitability in Oman analysis using GIS-based spatial fuzzy multi-criteria evaluation. *Renewable Energy*, 36(9), 2554-2561.
Chaves, A. and Bahill, A.T. (2010). Locating Sites for Photovoltaic Solar. *ArcUser*, 24-27. Retrieved from http://www.esri.com/news/arcuser/1010/files/solarsiting.pdf
Chen, Y., Lee, C. and Wu, H. (2005). Calculation of the optimum installation angle for fixed solar-cell panels based on the genetic algorithm and the simulated-annealing method. *IEEE Transactions on Energy Conversion*, 20, 467-473.
Chen, H.H., Kang, H. and Lee, A.H.I. (2010). Strategic selection of suitable projects for hybrid solar-wind power generation systems. *Renewable and Sustainable Energy Reviews*, 14, 413-421.
Cheng, C.L/. Jimenez, C.S.S., Lee, M.-C. (2009). Research of BIPV optimal tilted angle, use of latitude concept for south orientated plans. *Renewable Energy*, 34, 1644-1650.
Clifton, J. and Boruff, B.J. (2010). Assessing the potential for concentrated solar power development in rural Australia. *Energy Policy*, 38, 5272-5280.
Dawson, L. and Schlyter, P. (2012). Less is more: Strategic scale site suitability for concentrated solar thermal power in Western Australia. *Energy Policy*, 47, 91-101.
Dornan, M. (2011). Solar-based rural electrification policy design: The Renewable Energy Service Company (RESCO) model in Fiji. *Renewable Energy*, 36, 797-803.
Dorvlo, A.S.S., Jervase, J.A. and Al-Lawati, A. (2002). Solar radiation estimation using artificial neural networks. *Applied Energy*, 71, 307-391.
Elizondo, D., Hoogenboom, G. and McClendon, R. (1994). Development of a neural network to predict daily solar radiation. *Agricultural Forest Meteorology*, 71, 115-132.
ESRI. (2011). Area Solar Radiation (Spatial Analyst). Retrieved from http://help.arcgis.com/en/arcgisdesktop/10.0/help/index.html#//009z000000t5000000.htm
ESRI. (2012a). Calculating solar radiation. Retrieved from http://webhelp.esri.com/arcgisdesktop/9.3/index.cfm?TopicName=Calculating%20solar%20radiation
ESRI. (2012b). How solar radiation is calculated. Retrieved from http://resources.arcgis.com/en/help/main/10.1/index.html#//009z000000tm000000
ESRI. (2012c). How Fuzzy Membership works. Retrieved from http://resources.arcgis.com/en/help/main/10.1/index.html#//009z000000rz000000
Ethiopian Rural Energy Development and Promotion Center. (2007). Solar and wind energy utilization and project development scenarios. Retrieved from http://swera.unep.net/typo3conf/ext/metadata_tool/archive/download/EthiopiaSWERAre port_258.pdf
Fluri, T.P. (2009). The Potential of Concentrating Solar Power in South Africa. *Energy Policy*, 37, 5075-5080.
Figuiera, J., Mousseau, V., Roy, B. (2005). ELECTRE methods. In: Figueira, J., Greco, S., Ehrgott, M. (Eds). Multiple Criteria Decision Analysis: State of the Art Surveys. 133-162.

Finamore, C., Phelan, S., Rudzki, R. and Sturk, C. (2002). The feasibility of implementing solar panels on Federation Hall: Shedding light on the situation. Retrieved from http://environment.uwaterloo.ca/research/watgreen/projects/library/f02solaronfedhall.pdf

Foster, R., Ghassemi, M. and Cota, A. (2010). *Solar energy – Renewable energy and the environment*. London : Taylor and Francis Group.

Fu, P. and Rich, P.M. (2000). The Solar Analyst user manual. Helios Environmental Modeling Institute, USA. Retrieved from http://www.precisionviticulture.com/files/fu_rich_2000_solaranalyst.pdf

Fu, P. and Rich, P. M. (2002). A geometric solar radiation model with applications in agriculture and forestry. *Computers and Electronics in Agriculture*, 37, 25-35.

Garg, H.P. and Gupta, G.L. (1978). Flat plate collectors-Experimental studies and design data for India. Proceedings of the International Solar Energy Society Congress, New Delhi, India, 2, 1134-1146.

Gastli, A., Charabi, Y. and Zekri, S. (2010). GIS-based assessment of combined CSP electric power and seawater desalination plant for Duqum, Oman. *Renewable and Sustainable Energy Reviews*, 14, 821-827.

Gastli, A. and Charabi, Y. (2010a). Solar electricity prospects in Oman using GIS-based solar radiation maps. *Renewable and Sustainable Energy Reviews*, 14, 790 - 797.

Gastli, A. and Charabi, Y. (2010b). Siting of large PV farms in Al-Batinah region of Oman. *IEEE*, 548-552.

Gray, A. (2012). Self-cleaning hydrophobic nano coating for solar panel glass generating great results for nanoShell. Retrieved from http://www.pv-magazine.com/services/press-releases/details/beitrag/self-cleaning-hydrophobic-nano-coating-for-solar-panel-glass-generating-great-results-for-nanoshell_100005577/#axzz2d6jF7EHg

Gunerhan, H. and Hepbasli, A. (2007). Determination of the optimum tilt angle of solar collectors for building applications. *Building and Environment*, 42, 779-783.

Haurant, P., Oberti, P. and Muselli, M. (2011). Multicriteria selection aiding related to photovoltaic plants on farming fields on Corsica island: A real case study using the ELECTRE outranking framework. *Energy Policy*, 39, 676-688.

HDR, Inc. (2013). Hickory Ridge Landfill Solar Energy Cover. Retrieved from http://www.hdrinc.com/portfolio/hickory-ridge-landfill-solar-energy-cover

Hofierka, L. and Suri, M. (2002). The solar radiation model for open source GIS: Implementation and applications. Manuscript submitted to the International GRASS user conference in Trento, Italy. Retrieved from http://skagit.meas.ncsu.edu/~jaroslav/trento/Hofierka_Jaroslav.pdf

Hoyer, C., Schillings, C., Heinemann, D., Mannstein, H. and Trieb, F. (2002). Solar Resource Assessment and Site Evaluation Using Remote Sensing Methods. World Renewable Energy Congress VII, Cologne, Germany.

Hussein, H.M.S, Ahmad, G.E., and El-Ghetany, H.H. (2004). Performance evaluation of photovoltaic modules at different tilt angles and orientations. *Energy Conversation and Management*, 45, 2441-2452.

Independent Electricity System Operator (IESO). (2012a). Supply overview. Retrieved from http://www.ieso.ca/imoweb/media/md_supply.asp

Independent Electricity System Operator (IESO). (2012b). 18-Month outlook. Retrieved from http://www.ieso.ca/imoweb/pubs/marketReports/18MonthOutlook_2012sep.pdf

Independent Electricity System Operator (IESO). (2012c). Demand overview. Retrieved from http://www.ieso.ca/imoweb/media/md_demand.asp

International Renewable Energy Agency (IREA). (2012). Renewable energy technologies: Cost analysis series. (Working paper Volume 1: Power Sector). Retrieved from http://www.irena.org/DocumentDownloads/Publications/RE_Technologies_Cost_Analysis-SOLAR_PV.pdf

Intergovernmental Panel on Climate Change (IPPC). (2007). Climate Change 2007 : An Assessment of the Intergovernmental Panel on Climate Change, (November), 12-17.

Janke, J.R. (2010). Multicriteria GIS modeling of wind and solar farms in Colorado. *Renewable Energy*, 35, 2228-2234.

Jochem, A., Wichmann, V. and Hofle, B. (2009). Large area point cloud based solar radiation modeling. *Hamburg Contributions to Physical Geography and Landscape Ecology*, 20, 1-9.

Kahraman, C. and Kaya, I. (2010). A fuzzy multicriteria methodology for selection among energy alternatives. *Expert Systems with Applications*, 37, 6270-6281.

Kahraman, C., Kaya, I. and Cebi, S. (2009). A comparative analysis for multiattribute selection among renewable energy alternatives using fuzzy axiomatic design and fuzzy analytic hierarchy process. *Energy*, 34(10), 1603-1616.

Kalogirou, S. A. (2009). *Solar energy engineering: Processes and systems*. San Diego, CA: Elsevier.

Kryza, M., Szymanowski, M., Migala, K. and Pietras, M. (2010). Spatial information on total solar radiation: Application and evaluation of the r.sun model for the Wedel Jarlsberg Land. *Polish Polar Research*, 31(1), 17-32.

Latif, Z.A., Zaki, N.A.M. and Salleh, S.A. (2012). GIS-based estimation of rooftop solar photovoltaic potential using LiDAR. *IEEE 8th International Colloquium on Signal Processing and its Applications*, 38-392.

Lehman, R.G. (2011). Concentrated solar thermal facilities: A GIS approach for land planning: a thesis presented to the Faculty of the USC Graduate School, University of South California, in partial fulfillment of the requirements for the degree of Master of Science. Retrieved from http://spatial.usc.edu/wp-content/uploads/2012/05/Lehman.pdf

Liddell, R.M. and Bishop, J.A. (2011). Estimating rooftop solar electricity potential in Seattle from LiDAR data. Retrieved from http://www.nwgis.org/sessions/estimating-rooftop-solar-electricity-potential-seattle-lidar-data

Mala, K., Schläpfer, A. and Pryor, T. (2009). Better or worse? The role of solar photovoltaic (PV) systems in sustainable development: Case studies of remote atoll communities in Kiribati. *Renewable Energy*, 34, 358-361.

Morcos, V.H. (1994). Optimum tilt angle and orientation for solar collectors in Assiut, Egypt. *Renewable Energy*, 4(3), 291-298.

Mulherin, A. (2011). A spatial approach to determine solar PV potential for Durham homeowners. Retrieved from http://dukespace.lib.duke.edu/dspace/handle/10161/3685

Navigant Consulting Inc. (2012). Sector profile for solar photovoltaics in Canada, report # 2012-063 (RP-TEC), CanmetENERGY, Natural Resources Canada. Retrieved from http://canmetenergy.nrcan.gc.ca/sites/canmetenergy.nrcan.gc.ca/files/files/pubs/2012-063-eng.pdf

Nijcamp, P. and Volwahsen, A. (1990). New directions in integrated energy planning. *Energy Policy*, 18(8): 76-73.

Nguyen, H.T., Pearce, J.M. (2010). Estimating potential photovoltaic yield with r.sun and the open source Geographical Resources Analysis Support System. *Solar Energy*, 84(5), 831-843.

Ontario Ministry of Energy (2000). Ontario's System-Wide Electricity Supply Mix: 2000 Data. Retrieved from http://www.ontarioenergyboard.ca/documents/electricity_mix.pdf

Ontario Ministry of Energy (2005). Meeting Ontario's Electricity Needs. Retrieved from http://media.cns-snc.ca/uploads/branch_data/branches/ChalkRiver/Symposium/seminar-1-garry-mckeever-final-adobe.pdf

Ontario Ministry of Energy (2010). Ontario's Long-Term Energy Plan. Retrieved from http://www.energy.gov.on.ca/en/ltep/supply/

Ontario Power Authority (OPA). (2012). Ontario electricity demand – 2012 annual long term outlook. Retrieved from http://www.powerauthority.on.ca/sites/default/files/news/Q2-2012LoadForecast.pdf

Ontario Power Authority (OPA). (2013a). Bi-weekly FIT and microFIT reports. Retrieved from http://microfit.powerauthority.on.ca/microfit-program-resources/version-2-program-updates/bi-weekly-reports

Ontario Power Authority (OPA). (2013b). FIT Program Quarterly Report: March 31, 2013. Retrieved from http://fit.powerauthority.on.ca/sites/default/files/page/March%2031%2C%202013%20FIT%20Program%20quarterly%20report.pdf

Ontario Power Generation. (2010). How it works: Electricity generation. Retrieved from http://www.opg.com/education/kits/grade9student.pdf

Pavlović, T., Pavlović, Z., Pantić, L. and Kostić, Lj. (2010). Determining optimum tilt angles and orientations of photovoltaic panels in Nis, Serbia. *Contemporary Materials* I-2.151-156.

Pletka, R., Block, S., Cummer, K., Gilton, K., R., O., Roush, B., Stoddard, L., Tilley, S., Woodward, D. and Hunsaker, M. (2007). Arizona renewable energy assessment. Black & Veatch Corporation, Overland Park, Kansas.

Pohekar, S.D. and Ramachandran, M. (2004). Application of multi-criteria decision making to sustainable energy planning—A review. *Renewable and Sustainable Energy Reviews*, 8, 365-381.

Powers, L., Newmiller, J. and Townsend, T. (2010). Measuring and modeling the effect of snow on photovoltaic system performance. *Photovoltaic Specialists Conference (PVSC), 2010 35th IEEE*, On page(s): 000973 - 000978

Redweik, P., Catita, C. and Brito, M.C. (2011). 3D local scale solar radiation model based on urban LiDAR data. Retrieved from http://www.ipi.uni-hannover.de/fileadmin/institut/pdf/ISPRS-Hannover2011/contribution169.pdf

REEP. (2013). Renewable energy – A primer. Retrieved from http://www.reepwaterlooregion.ca/info_renewable.php

Region of Waterloo. (2012). Construction of Waterloo landfill North Expansion Area Cell Four (NE-4), leachate and landfill gas collection systems. Retrieved from http://www.regionofwaterloo.ca/en/aboutTheEnvironment/resources/waterlooland fillcommunication.pdf

Rehman, S. and Ghori, S.G. (2000). Spatial Estimation of Global Solar Radiation Using Geostatistics. *Renewable Energy*. 21, 583-605.

Reijenga, T. and Ruoss, D. (2005). *Technologies and integration concepts*. In: D. Prasad and M. Snow (Eds.). Designing with solar power – A source book for Building Integrated Photovoltaics (BiPV). Victoria, Australia: The Images Publishing Group Pty Ltd.

Rich, P, M., Dubayah, R., Hetrick, W. A. and Saving. S. C. (1994). Using viewshed models to calculate intercepted solar radiation: Applications in ecology. *American Society for Photogrammetry and Remote Sensing Technical Papers*, 524-529.

Rich, P. M. and Fu, P. (2000). Topoclimatic habitat models. Proceedings of the Fourth International Conference on Integrating GIS and Environmental Modeling.

Roberst, M. (2010). Solar fills: The future? *Waste Management World*, 11(6). Retrieved from http://www.waste-management-world.com/articles/print/volume-11/issue-6/features/solar-landfills-the-future.html

Rowlands, I.H., Kemery, B.P. and Beausoleil-Morrison, I. (2011). Optimal solar-PV tilt angle and azimuth: An Ontario (Canada) case-study. *Energy Policy*, 39, 1397-409.

Roy. B. (1996). *Multicriteria methodology for decision aiding*. London: Springer-Verlag.

Rupp, W. (2013). Installation of solar panels at old Forbes Street Landfill to Start in June. Retrieved from http://eastprovidence.patch.com/groups/politics-and-elections/p/installation-of-solar-panels-at-old-forbes-street-lan099e340d57

Saaty, T.L. (1980). The Analytic Hierarchy Process. New York: McGraw-Hill.

Saaty, T.L. (2003). Decision-making with the AHP: Why is the principal eigenvector necessary. *European Journal of Operational Research*, 145, 85-91.

Sambo, A.S. (2008). Matching electricity supply with demand in Nigeria. *International Association for Energy Economics*, Fourth Quarter, 32-36.

San Cristóbal Mateo, J.R. (2012). *Multi criteria analysis in the renewable energy industry*. London: Springer-Verlag.

Sen, Z. (2008). *Solar energy fundamentals and modeling techniques – Atmosphere, environment, climate change and renewable energy*. London: Springer-Verlag.

Sen, Z. and Sahin, A.D. (2001). Spatial Interpolation and Estimation of Solar Irradiation by Cumulative Semivariograms. *Solar Energy*. 71(1), 11-21.

Sfetsos, A. and Coonick, A.H. (2000). Univariate and Multivariate Forecasting of Hourly Solar Radiation with Artificial Intelligence Techniques. *Solar Energy*. 68(2), 169-178.

Siraki, A.G. and Pillary, P. (2012). Study of optimum tilt angles for solar panels in different latitudes for urban applications. *Solar Energy*, 86, 1920-1928.

Snedden, N. (2011). Solar landfill provides a shining example. *CNN*, Retrieved from http://www.cnn.com/2011/11/30/us/landfill-atlanta-solar

Solangi, K. H., Islam, M. R., Saidur, R., Rahim, N. A. and Fayaz, H. (2011). A review on global solar energy policy. *Renewable and Sustainable Energy Reviews*, 15(4), 2149-2163.

Sorensen, B. (2001). GIS Management of Solar Resource Data. *Solar Energy Materials and Solar Cells*, 67, 503-509.

STEP (Sustainable Technology Education Project). (2013). FED Hall solar photovoltaic (PV) installation. Retrieved from http://www.step.uwaterloo.ca/projects.php

Stoffel, T. (2005). 20 Years of Solar Measurements: The Solar Radiation Research Laboratory (SRRL) at NREL. Retrieved from http://www.nrel.gov/solar_radiation/pdfs/history.pdf

Strauch, J., Moore, L. and Coolins, E. (2010). Solar cell systems: Definition, performance, and reliability. In Fraas, L. and Partain, L. (Eds.). *Solar cells and their applications*. (pp. 219 - 249). Hoboken, New Jersey: John Wiley and Sons, Inc.

Svantesson, J. and Linder, E. (2012). Solar electricity for rural households at the Fiji islands: a thesis presented in fulfilment of the requirements for the degree of Bachelor of Science in KTH School of Industrial Engineering and Management, Stockholm, Sweden. Retrieved from kth.diva-portal.org/smash/get/diva2:540264/FULLTEXT01

Tang, R. and Wu, T. (2004). Optimal tilt-angles for solar collectors used in China. *Applied Energy*, 79, 239-248.

The German Solar Society. (2005). *Planning and installing solar thermal systems: A guide for installers, architects and engineers*. London: Earthscan.

The Hayter Group. (2013). Survey response of solar panel installation questionniare.

The U.S. Environmental Protection Agency (EPA) and the National Renewable Energy Laboratory (NREL). (2013). Best practices for siting solar photovoltaics on municipal solid waste landfills. Retrieved from http://icma.org/en/icma/knowledge_network/documents/kn/Document/304833/Best_Practices_for_Siting_Solar_Photovoltaics_on_Municipal_Solid_Waste_Landfills

Thevenard, D. and Pelland, S. (2013). Estimating the uncertainty in long-term photovoltaic yield predictions. *Solar Energy*, 91, 432-445.

Tiris, M. and Tiris, C. (1998). Optimum collector slope and model evaluation: case study for Gebze, Turkey. *Energy Conversion and Management*, 39(3/4), 167-72.

Trieb, F., Langnib, O. and Klaib, H. (1997). Solar electricity generation – A comparative view of technologies, costs and environmental impact. *Solar Energy*, 59, 88-99.

Wang, J.-J., Jing, Y.-Y., Zhang, C.-F. and Zhao, J.-H. (2009). Review on multi-criteria decision analysis aid in sustainable energy decision-making. *Renewable and Sustainable Energy Reviews*, 13(9), 2263–2278. doi:10.1016/j.rser.2009.06.021

Wehr, A. and Lohr, U. (1999). Airborne laser scanning- an introduction and overview. *ISPRS Journal of Photogrammetry and Remote Sensing*, 54, 68-82.

Wiginton, L. K., Nguyen, H. T., and Pearce, J. M. (2010). Quantifying Rooftop Solar Photovoltaic Potential for Regional Renewable Energy Policy. *Computers, Environment and Urban Systems,* 34(4), 345-357.

Vector Magic, Inc. (n.d.). Average weather for Regional Municipality of Waterloo, Ontario, Canada. Retrieved from http://weatherspark.com/averages/28280/Regional-Municipality-of-Waterloo-Ontario-Canada

Voegtle, T. Steinle, E. Tóvári D. (2005). Airborne laser scanning data for determination of suitable areas for photovoltaic. ISPRS WG III/3, III/4, V/3 Workshop "Laser scanning 2005". Enschede, the Netherlands, September 12-14, 2005.

Yimprayoon, C. and Navvab, M. (2010). Quantification of available solar irradiation on rooftops using orthophotograph and LiDAR Data. Fourth National Conference of IBPSA-USA, New York City, New York, pp. 238-243.

Appendix A – Digital Elevation Model of the City of Waterloo

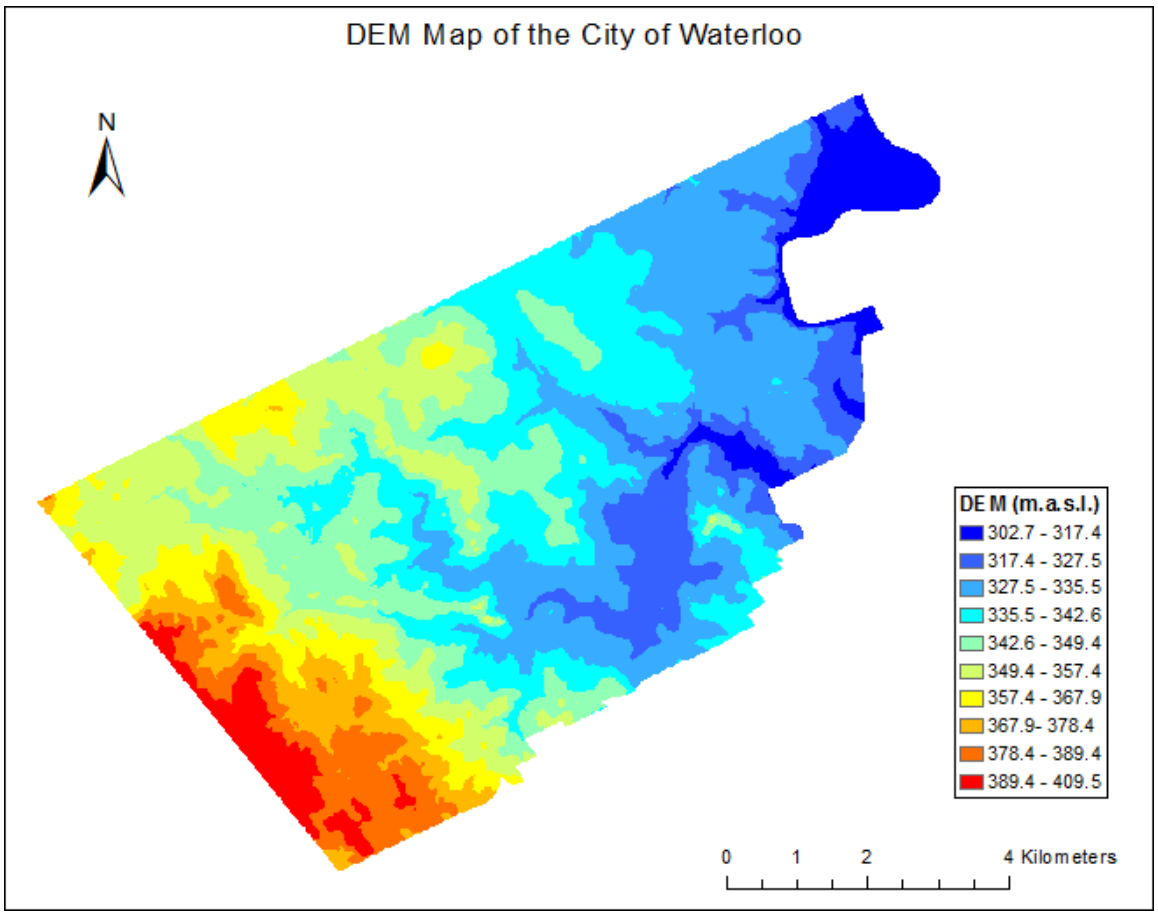

Appendix B – Solar radiation results by different combinations of transmissivity and diffuse proportion values (WH/m^2)

		Diffuse Proportion								
		0.1	**0.2**	**0.3**	**0.4**	**0.5**	**0.6**	**0.7**	**0.8**	**0.9**
Transmissivity	**0.1**	N/A	N/A	N/A	N/A	N/A	N/A	650.02 - 260886	1114.32 - 368331	2507.22 - 694847
	0.2	N/A	N/A	N/A	N/A	N/A	1071.48 - 520962	3716.17 - 639188	2738.2 - 893143	6428.87 - 1769340
	0.3	N/A	N/A	N/A	N/A	1285.62 - 777317	1928.48 - 921779	2999.85 - 1167510	5142.6 - 1662760	N/A
	0.4	N/A	N/A	N/A	N/A	2001.1 - 1188530	3001.64 - 1412950	4669.22 - 1794350	N/A	
	0.5	N/A	N/A	1356.88 - 1306680	1920.56 - 1465060	2880.83 - 1680410	4321.25 - 2003440	6721.94 - 2550750	N/A	N/A
	0.6	N/A	967.521 - 1568720	1696.55 - 1762810	2639.08 - 1968850	3958.62 - 2264730	5937.93 - 2708540	N/A	N/A	N/A
	0.7	587.828 - 1926460	1299.13 - 2042250	2267.34 - 2291650	3526.97 - 2566180	5290.45 - 296060	N/A	N/A	N/A	N/A
	0.8	775.248 - 2441250	1744.31 - 2648190	2990.24 - 2919700	4651.49 - 3281700	N/A	N/A	N/A	N/A	N/A
	0.9	1026.62 - 3055190	2309.9 - 3324080	3959.82 - 3683570	N/A	N/A	N/A	N/A	N/A	N/A

Appendix C – Models for creating the MCA criteria layers

C1: Slope

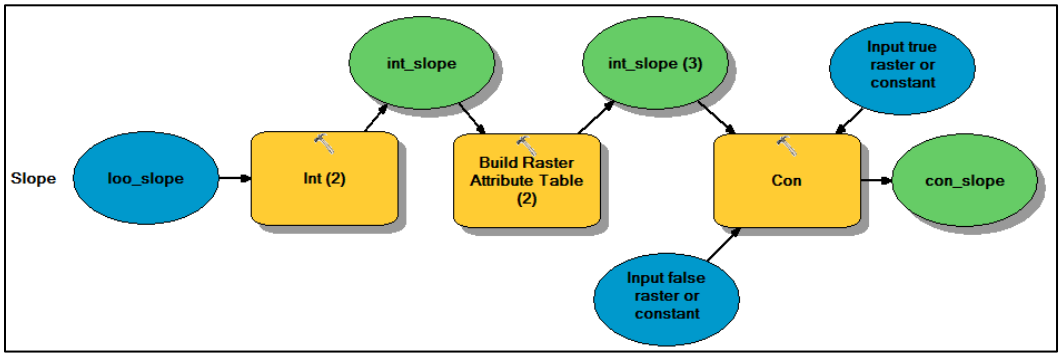

C2: Aspect

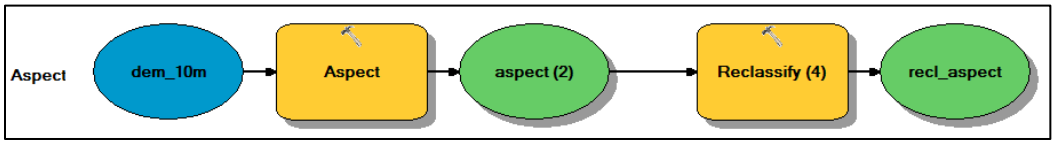

C3: Solar Radiation

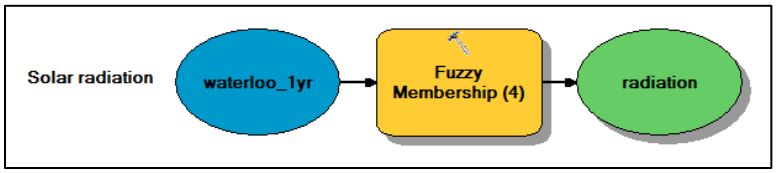

C4: Water Sources

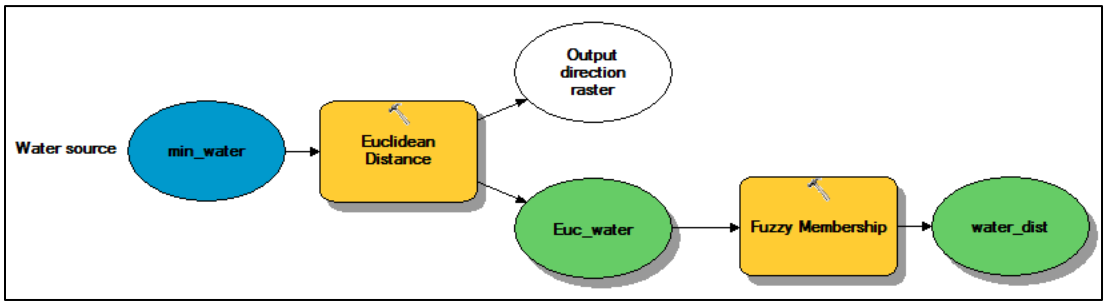

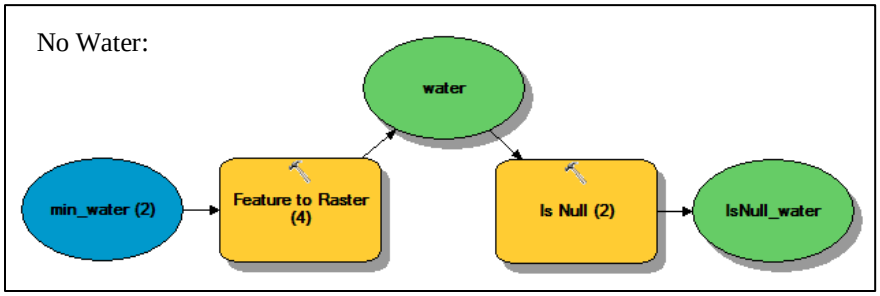

C5: Road Network

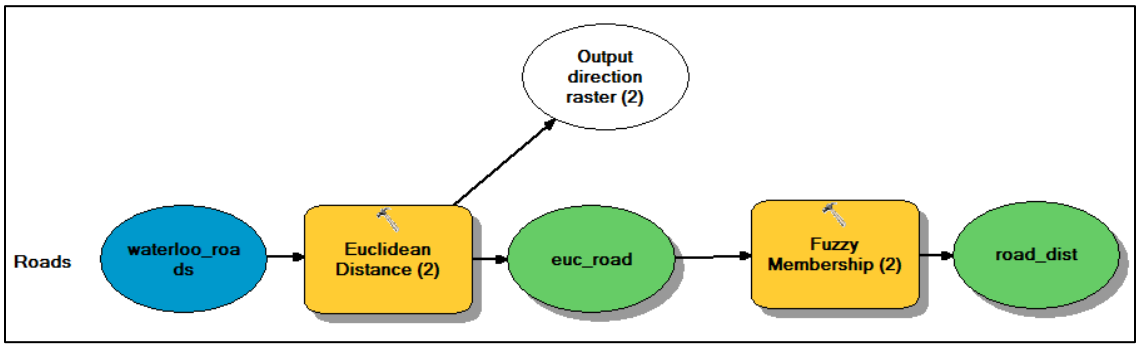

C6: Transmission Lines

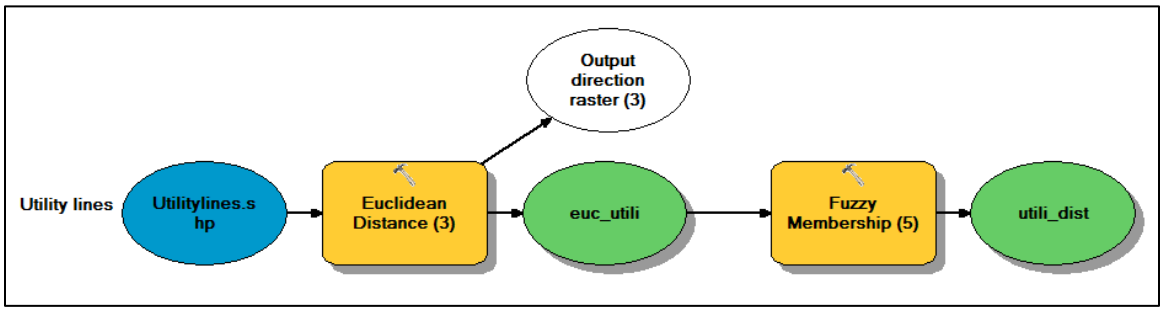

C7: ESA

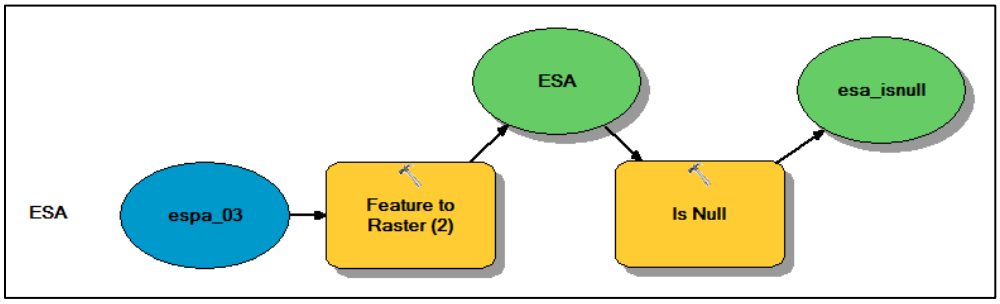

C8: Pit and Quarry Sites

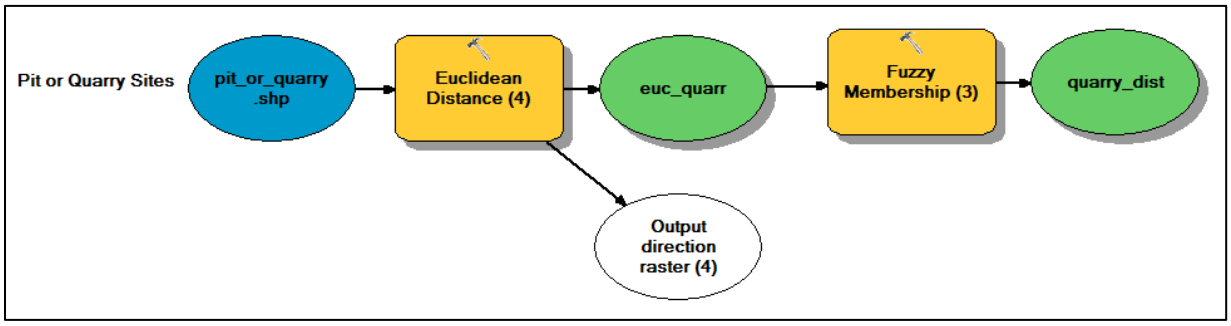

C9: Sand Content

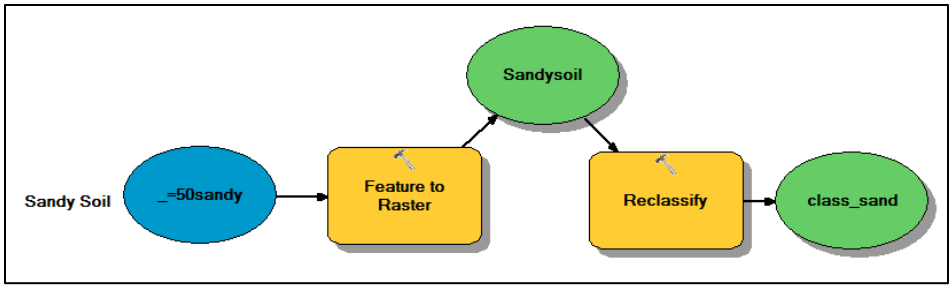

C10: Land Suitability

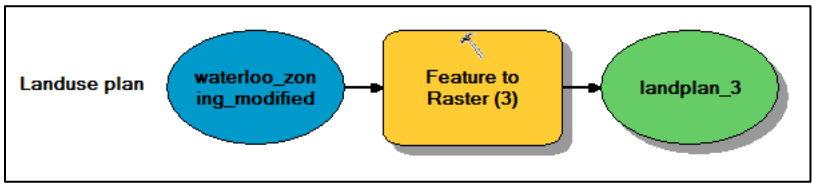

C11: Residential Area

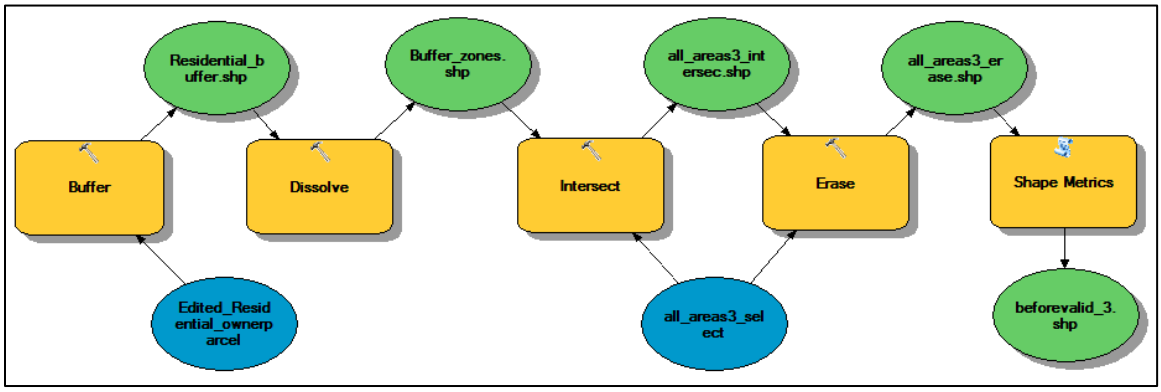

Site Selection Using Weighted Criteria:

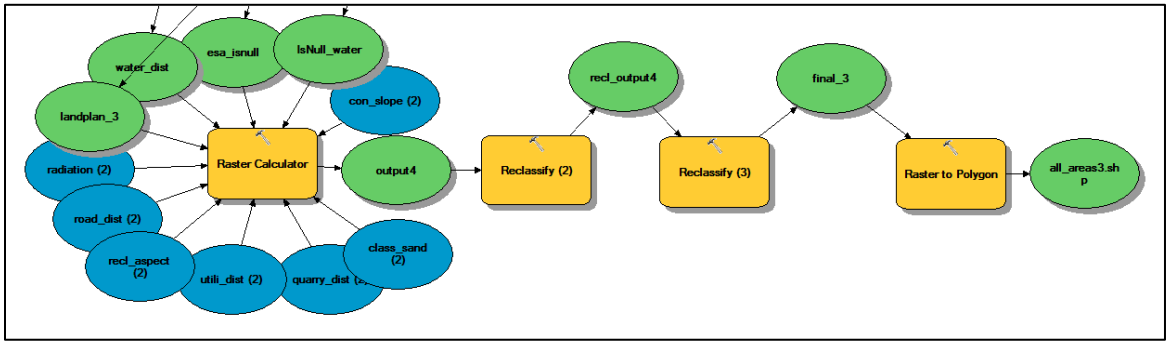

Appendix D – Questionnaire

January 30, 2013

Dear Sir/Madam,

Thank you in advance for participating in this survey on solar panel installation. The main purpose of this study is to determine the optimal sites for solar panel installation at both micro and macro scales of analysis. Micro scale analysis refers to solar panel installation on flat/pitched rooftop among several buildings, whereas macro scale installation refers to a large region involving rooftop and ground-mounted types.

In order to obtain information to improve solar panel installation practices in industry, I would like to conduct a survey to explore and summarize the commonly used approaches and datasets applied by solar companies in Ontario. After collecting the information from participants, differences among the current techniques and methods used in this study will be compared. In addition, this study will tackle some problems existing in current site selection methods regarding solar energy efficacy improvement.

Sincerely,

Dongrong Li
Department of Geography & Environmental Management
Faculty of Environment
University of Waterloo
Email: d59li@uwaterloo.ca
Tel: 1-519-590-5067

Dr. Su-yin Tan

Department of Geography & Environmental Management
Faculty of Environment
University of Waterloo
Email: su-yin.tan@uwaterloo.ca
Tel: 1-519-888-4567 ext.38772

1. Approximately *how many customers* does your company service on average per month? What *types of customers* (e.g., commercial, residential) do you usually work with?

2. How do you evaluate *suitable sites* on urban infrastructure and buildings for solar panel installation? What *location or physical factors* (e.g., shadow effects, height, building dimensions) are usually considered when determining where panels should be installed?

3. What kind of *data or information sources* does your company usually use when assessing where solar panels should be placed or installed (e.g., Google maps, building survey plans, LiDAR data)?

4. How do considerations change for building rooftop solar panel installation or placement compared to ground-mounted installation?

5. After completion of an installation project, what kind of maintenance does your company usually provide to the client? *How many years* does the maintenance last or is provided?

6. What are the most significant challenges encountered when installing solar panels correctly? What countermeasures can be taken to avoid these problems or how are they usually dealt with after completing an installation?

7. Between a grid-connected solar system and a stand-alone system, which is more popular with your customers? For the grid-connected solar system, what extra factors do you need to consider (e.g., distance to the transmission lines)?

Thank you for completing this survey!

Appendix E – Sensitivity Analysis Results

Table E1. Final weights of sub-criteria under seven scenarios*.

Scenarios	**A**	**B**	**C**	**D**	**E**	**F**	**G**
Slope	11%	12.9%	13.76%	10.8%	9.3%	12.9%	12.9%
Aspect	21.3%	24%	25.6%	24.3%	25.5%	24%	24%
Solar	22.2%	24.9%	26.6%	27.0%	25.0%	24.9%	24.9%
Water	2.53%	2.85%	3.04%	2.7%	2.3%	2.85%	2.85%
Quarry	4.57%	5.1%	5.48%	4.8%	4.1%	5.1%	5.1%
Sandy	4.57%	5.1%	5.48%	4.8%	4.1%	5.1%	5.1%
Transmission	28.90%	21.5%	17.20%	21.5%	21.5%	20%	16.7%
Roads	4.70%	3.57%	2.80%	3.5%	3.5%	5%	8.3%

***Note:**

Scenario A: Efficiency/Economic = 4/1;
Scenario B (Base run of this study): Efficiency/Economic = 3/1, Slope/Aspect and Slope/Solar Radiation = 1/2, and Transmission Lines/ Roads = 1/6;
Scenario C: Efficiency/Economic = 2/1;
Scenario D: When Efficiency/Economic = 3/1, Slope/Aspect and Slope/Solar Radiation = 1/4;
Scenario E: When Efficiency/Economic = 3/1, Slope/Aspect and Slope/Solar Radiation = 1/6;
Scenario F: When Efficiency/Economic = 3/1, Transmission Lines/ Roads = 1/4;
Scenario G: When Efficiency/Economic = 3/1, Transmission Lines/ Roads = 1/2.

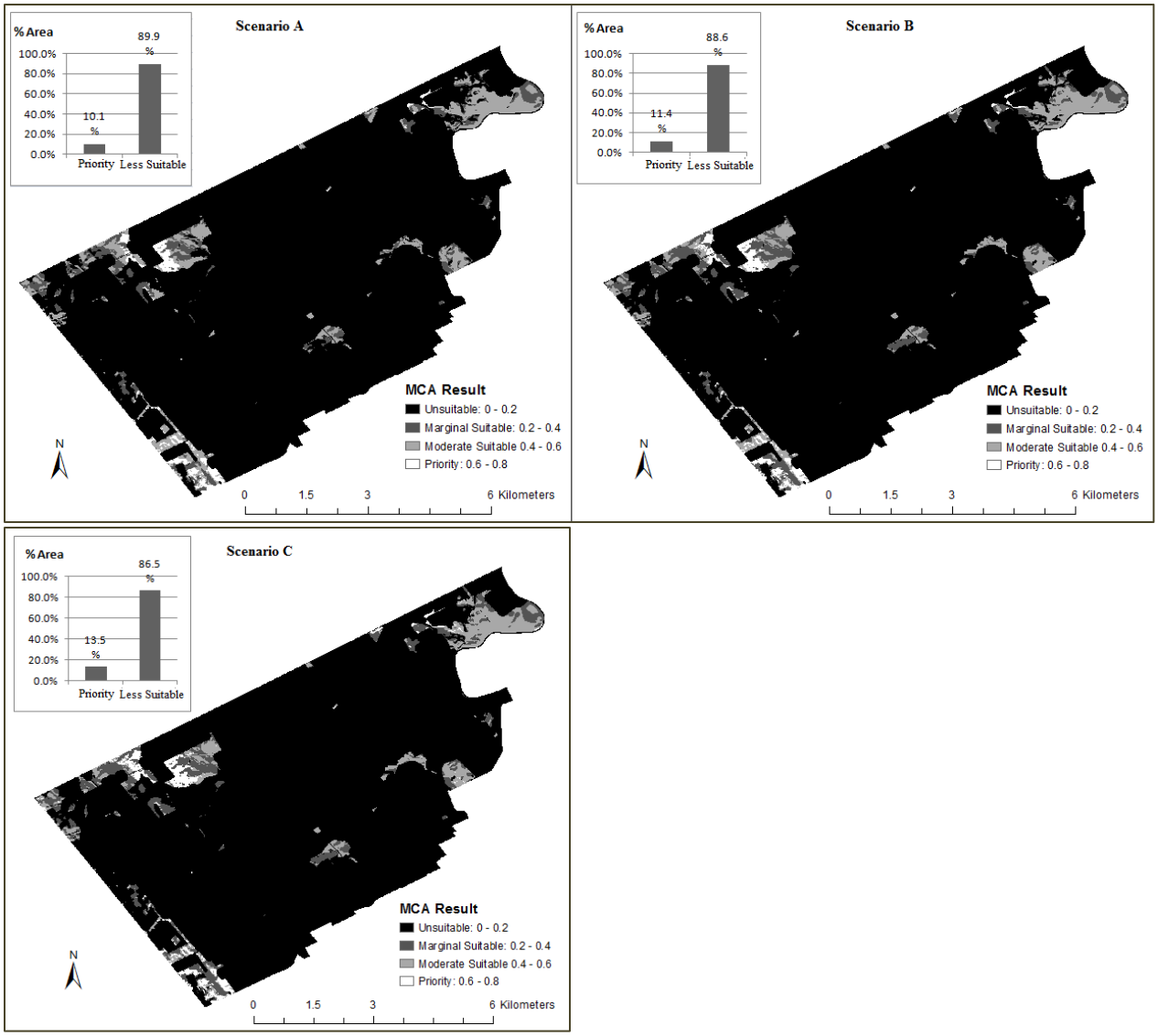

Figure E1. Solar panel installation suitability maps of three simulation runs for the selected criteria of Efficiency/Economic. (A) Efficiency/Economic = 4/1; (B) Efficiency/Economic = 3/1; (C) Efficiency/Economic = 2/1

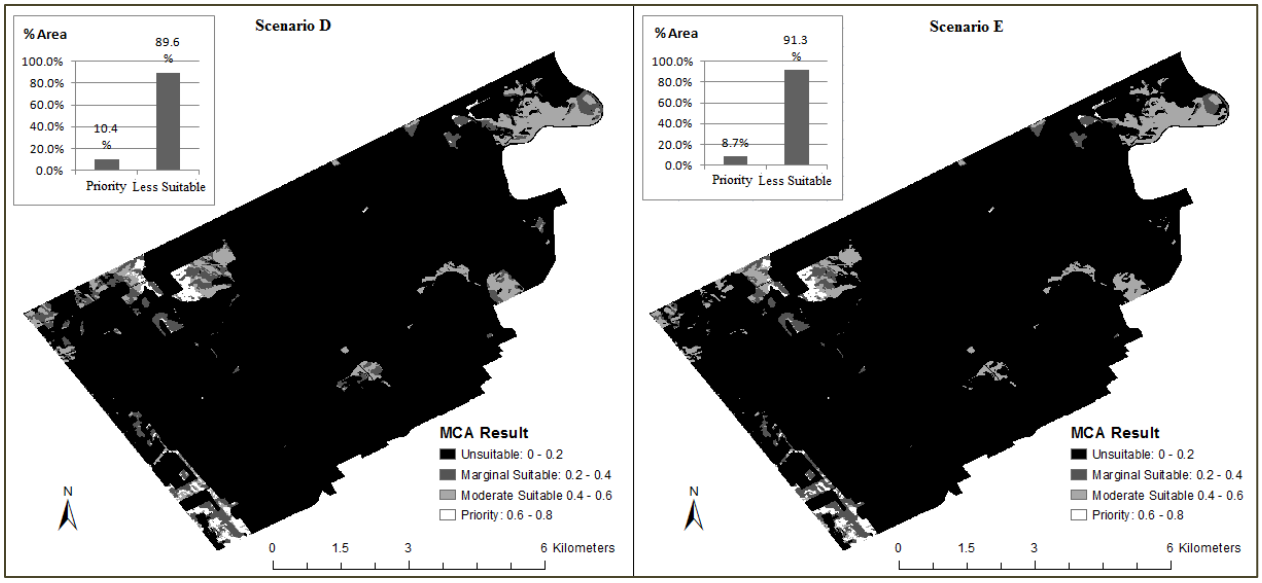

Figure E2. Solar panel installation suitability maps of two simulation runs for the selected criteria of Slope/Aspect and Slope/Solar Radiation. (A) Slope/Aspect and Slope/Solar Radiation = 1/4; (B) Slope/Aspect and Slope/Solar Radiation = 1/6.

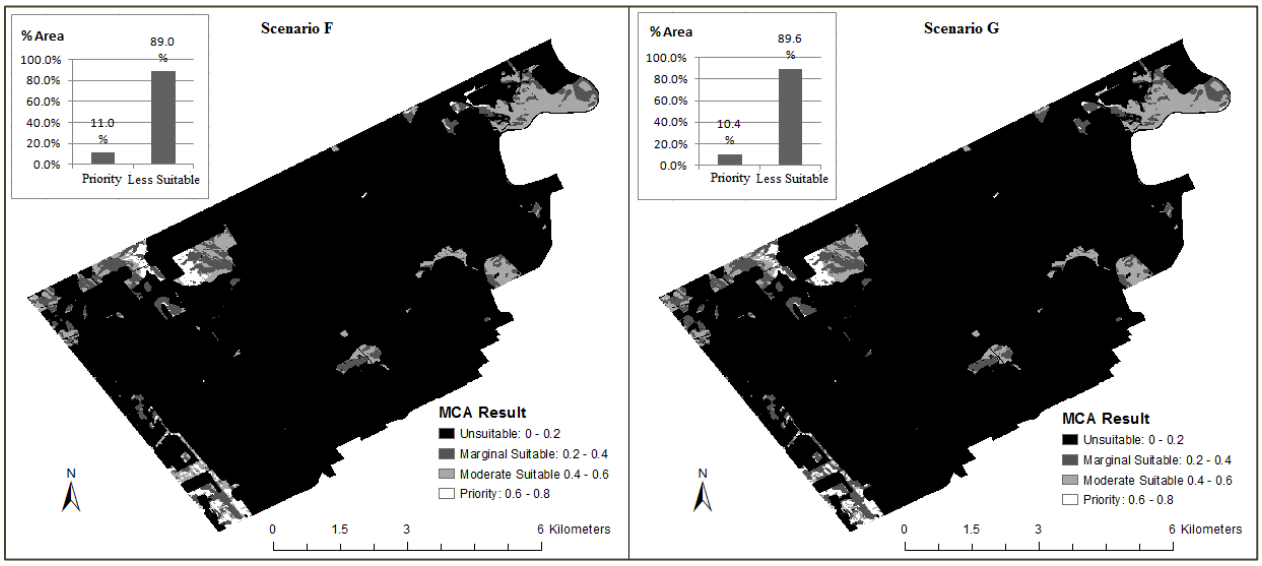

Figure E3. Solar panel installation suitability maps of two simulation runs for the selected criteria of Transmission Lines/ Roads. (A) Transmission Lines/ Roads = 1/4; (B) Transmission Lines/ Roads = 1/2.